Metabolic diversity and synthesis of medium chain length polyhydroxyalkanoates by *Pseudomonas putida* LS46 cultured with biodiesel-derived by-products

by

Jilagamazhi Fu

A Thesis submitted to the Faculty of Graduate Studies of

The University of Manitoba

in partial fulfilment of requirements of the degree of

DOCTOR OF PHILOSOPHY

Department of Biosystem Engineering

University of Manitoba

Winnipeg

Supervisory Committee

Dr. David B. Levin (Department of Biosystem Engineering, University of Manitoba)

Supervisor

Dr. Nazim Cicek (Department of Biosystem Engineering, University of Manitoba)

Departmental Member

Dr. Silvia Cardona (Department of Microbiology, University of Manitoba)

Departmental Member

Dr. Juliana A. Ramsay (Department of Chemical Engineering, Queen's University)

External Examiner

Abstract

The metabolism and physiology of *Pseudomonas putida* strain LS46 was investigated using biodiesel-derived waste streams as potential low cost substrates for production of medium chain length polyhydroxyalkanoates (mcl-PHA). Proteomic and trranscriptomic analyses were used to correlate specific gene and gene product expression patterns with differences in phenotypes of mcl-PHA biosynthesis by *P. putida* LS46. Growth and mcl-PHA content of *P. putida* LS46 were similar in cultures containing biodiesel-derived waste glycerol versus pure glycerol, and mcl-PHA synthesis occurred during stationary phase after nitrogen concentrations in the medium were exhausted. Waste glycerol cultures contained elevated concentrations of heavy metal ions, such as copper, which induced significant changes in gene expression levels related to heavy metal resistance. Several membrane-bound proteins, such as CusABC efflux and CopAB were identified and putatively play a role in regulating cellular copper concentrations. Cultures containing waste free fatty acids synthesized mcl-PHA throughout the exponential growth phase. Protein expression levels of two mcl-PHA synthases were suppressed during exponential phase growth in waste glycerol cultures, putatively via post-transcriptional regulation. Culture specific expression of monomer supplying proteins (PhaJ1 and PhaG), and sets of fatty acid oxidation enzymes were observed, and may have contributed to differences in the composition of polymers synthesized by *P. putida* LS46 cultured on the two substrates. Expression levels of the majority of mcl-PHA biosynthesis pathway genes were stable during active polymer synthesis in waste glycerol cultures. However, variations in protein expression levels, and in some cases their corresponding mRNAs, were observed in a number of other metabolic patheays, such as glycerol transportation, partial glycolysis, pyruvate metabolism, the TCA cycle, and fatty acid biosynthesis. These data suggest potential regulatory points that may determine carbon flux during mcl-PHA

biosynthesis. Evaluation of identified genetic targets in *P. putida* LS46 that putatively influence mcl-PHA biosynthesis and monomer composition merit further studies.

Acknowledgments

I take this opportunity to express gratitude to all of the individuals for their kind helps and supports. Firstly, I wish to express my sincere thanks to my supervisor, Dr. David Levin, for providing me the opportunity to study and pursue the research in University of Manitoba. His expertise, patience, and understanding added considerably to my graduate life. I appreciate his knowledge and guidance in developing my skills in technical and scientific thinking and writing, which truly made a different in my life. I would like to thank the other members of my supervisory committee members, Dr. Nazim Cicek, Dr. Silvia Cardona, and Dr. Juliana A Ramsay for their assistance in supporting and mentoring my study at all level of the research project. I would like to thank Dr. Richard Sparling at Department of Microbiology and Dr. John Sorensen at Department of Chemistry for their time and technical supports on my research. I would like to thank all the members from Dr. John Willkins and Dr. Oleg Krokhin's Lab at Manitoba Center for Proteomics and System Biology for the host and technical assistances.

A very special thanks goes to Dr. Parveen Sharma. He provided me with direction, technical support during all these years of my studies, and became more of a mentor and friend. My sincerely thanks to Victor Spicer and XiangLi Zhang (Justin) whose technical supports on 'Omics analyses definitely the key to my research. I would like to thanks all members of our lab. Spending time with them either in the lab or off campus make me feel supportive and relax. My thanks to Evelyn Fehr and Debby Watson at Biosystem Engineering office for all the administrative helps.

This research would not have been possible without the financial assistance of Natural Sciences and Engineering Research Council of Canada (NSERC), through a Strategic Programs grant (STPGP 306944-04), by Genome Canada, through the Applied

Genomics Research in Bioproducts or Crops (ABC) program for the grant titled, “Microbial Genomics for Biofuels and Co-Products from Biorefining Processes”, and by the government of the Province of Manitoba through the Manitoba Research Innovation Fund (MRIF) and the Manitoba Rural Adaptation Council (MRAC).

Finally, I would also like to thank my family numbers, my parents, my wife and my sister, for the consistent support they provided me through my entire life.

Dedication

I wish to dedicate this work to my parents, Yubao Lin and Buhe Fu, for they gave me the chance to explore, enjoy and learn much from this world, and always being supportive. Thank you!

Table of Contents

List of Abbreviations

Mcl-PHA: Medium chain length polyhydroxyalkanoates

WG: waste glycerol; WFA: waste fatty acids

C6: 3-hydroxyhexnoic acid

C7: 3-hydroxyheptanoic acid

C8: 3-hydroxyoctanoic acid

C9: 3-hydroxynonanoic acid

C10: 3-hydroxydecanoic acid

C12: 3-hydroxydodecanoic acid

C12:1: 3-hydroxydodecenoic acid

C14: 3-hydroxytetradecanoic acid

C14:1: 3-hydroxytetradecenoic acid

RNAseq: RNA sequencing

HPLC: High Performance Liquid Chromatography

GC: Gas Chromatography

1D-LC-MS/MS: 1 Dimensional Liquid Chromatography tandem Mass Spectrometry

cdw: cell dry weight

wt %: percentage of cell dry weight

NAD(P)H: Nicotinamide adenine dinucleotide (phosphate)

FAD: Flavin Adenine Dinucleotide

C/N: Carbon to Nitrogen ratio

COG: Clusters of Orthologous Groups

pi: Post inoculation.

List of Tables

List of Figures

List of Copyrighted Material for which Permission was obtained

License agreement for reusing of previously published works in Chapter 3 of the Thesis was obtained between Jilagamazhi Fu and NRC Research Press provided by Copyright Clearance Center, Inc. Found in: Jilagamazhi Fu, Umesh Sharma, Richard Sparling, Nazim Cicek, and David B. Levin. 2014. Evaluation of medium chain length polyhydroxyalkanoate production by *Pseudomonas putida* LS46 using biodiesel byproductm streams. 60: 461-467.

License agreement for reusing of previously published works in Chapter 4 of the Thesis was obtained between Jilagamazhi Fu and Applied Microbiology and Biotechnology provided by Copyright Clearance Center, Inc. Found in: Jilagamazhi Fu, Parveen Sharma, Vic Spicer, Oleg V. Krokhin, Xiangli Zhang, Brian Fristensky, John A. Wilkins, Nazim Cicek, Richard Sparling, David. B. Levin. 2015. Effects of impurities in biodieselderived glycerol on growth and expression of heavy metal ion homeostasis genes and gene products in *Pseudomonas putida* LS46. 99(13): 5583-5592.

List of Supplementary Materials

Chapter 1

Literature Review

1.1 Short review on bio-plastics

Plastics made from synthetic polymers (petroleum based) are often non-degradable and accumulate in the environment when discarded. Although they have good mechanical integrity and excellent durability, they have deleterious effects on wildlife and on the aesthetic qualities of cities and forests (Chanprateep, 2010). Moreover, the increased cost for plastic waste disposal, as well as toxic hazards generated by incineration (such as air emission of dioxin, hydrogen chloride and hydrogen cyanide) cause waste management problems (Ojumu et al., 2004; Johnstone, 1990). Recycling offers the possibility of waste re- utilization, but it is can be difficult and costly to sort and separate the wide variety of plastics that are sent to recycling centres. Moreover, physical changes in the plastic material can limit their reuse (Johnstone, 1990). Making eco-friendly products such as bioplastics using biodegradable biopolymers can help to overcome the problems caused by non-degradable plastics, and, thus, though hard to completely replace conventional plastics, increasing proportion of biodegradable plastics usage over non-degradable plastics is of major interest to the plastics industry, consumers, and decision-makers (Song et al., 1999).

Bioplastics have physical and chemical properties very similar (if not identical) to plastics made from non-biodegradable synthetic plastics derived from petroleum. Various types of bio-based polymers have been studied and can be categorized into three platforms: 1) natural polymers, such as cellulose and starch; 2) polymers

produced by microbial fermentation plus chemical conversion process, such as polylactatic acid (PLA); and 3) polymers synthesized directly by microbial fermentation, such as polyhydroxyalkanaote (Nopharatana et al., 2007; Babu et al., 2013).

Cellulose-based polymers are currently produced at industrial scale, and can be chemically treated or modified and used to manufacture fibers for textiles, bedding, and filters (Roy et al., 2009). Starch-based polymers are also produced at industrial scale, and are often blended with other biodegradable polymers, such as PLA to create fully biodegradable polymers with physical properties that are better than the starch-based polymer alone (Marques et al., 2002). Over 140,000 tonnes of PLA is produced each year, and PLA represents a large portion of biodegradable polymers used to make biodegradable plastic products. Two factors driving the increased use of PLA polymers for production of plastic products are: 1) the increased availability (and thus decreasing price) of PLA; and 2) the fluctuating cost of petroleum, which has enabled PLA to be competitive with petroleum-based plastics, depending on the price of oil (Mukherjee and Kao, 2011).

The scale of polyhydroxyalkanoates (PHA) production is quite small compared to cellulose and PLA-based polymers (Kosior et al., 2006). In 2013, PLA polymers accounted for approximately 11.4% of global bioplastics production, while PHA polymers accounted for only 2.1% (European Bioplastics, Institute for Bioplastics and Biocomposites, Nova-Institute, 2014). However, PHAs have gained attention by both scientists and industry because it is fully biodegradable and its production can use renewable feedstock. Furthermore, various bacterial PHA producing platforms offer the potential to screen and produce novel polymers that may be tailored into various applications. The focus of this thesis is the synthesis of medium chain length PHA

using low cost feedstock, which may contribute to lower costs of overall production. Details about PHA as biodegradable polymer will be reviewed in this chapter.

1.2 PHA in general

Polyhydroxyalkanoates (PHA) are a family of bacterial polyesters synthesized as intra-cellular storage materials for cellular survival under nutritional stress conditions (Nopharatana et al., 2007). PHA were discovered in 1926 when poly-3-hydroxybutyrate (PHB) was first observed as intra-cellular lipid-like granules in *Bacillus megaterium* (Steinbüchel and Valentin, 1995). In 1983, studies of *Pseudomonas oleovorans* revealed another type of PHA granules rather than PHB, which consisted primarily of 3-hydroxyoctanoate (3HO), plus smaller amounts of other 3-hydroxyacids (3-HAs) shorter than C8 (de Smet et al., 1983). To date, over 150 types of PHA monomer have been identified, which endows PHA polymers with a wide range of properties that may be tailored into various potential applications (Sudesh et al., 2000). These PHA monomers, can be generally divided into two groups according to the numbers of carbon atoms in their side chains. Short chain length polyhydroxyalkanoates (scl-PHA) contain 3-5 carbon atoms. For example, PHB monomer contains four carbon atoms. Medium chain-length PHA (mcl-PHA) contain 3-hydroxy acid subunits of six to fourteen carbon atoms, and are thus more structurally diverse than scl-PHA (Reddy et al., 2003). The chemical structure of PHA is showed in **Figure 1-1**. Because of the native structure, mcl-PHA, in general, have the following properties: low crystallinity, low glass-transition temperature, low tensile-strength, and high elongation-to-break, which means they are more elastomeric polymers compare to scl-PHA, thus may be preferred where more structurally flexible biomaterials are required, such as in the biomedical field, or as resins in composite materials (Rai et al., 2011a).

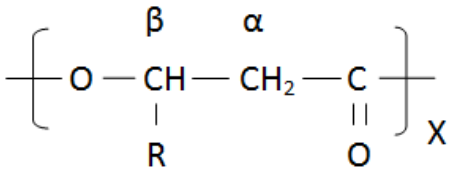

Figure 1-1. Chemical structure of poly-3-hydroxyalkanoates (PHA). PHA are also referred to as poly-β-hydroxyalkanoates, since the hydroxyl group is on the β carbon. The "R"- group varies from C1 to C13, therefore, the corresponding polymers will be named as from poly-β-hydroxybutyrates to poly-β-hydroxyhexadecanoates.

Although PHA have many advantages, the production scale and the price of mcl-PHA is still non-competitive with petroleum-based plastics, due primarily to the high cost of the feedstocks (carbon sources) used for PHA production. It was estimated that the cost of PHA products is determined to a great extent (up to 50 % of the total production costs) by the cost of the raw materials (Chanprateep, 2010). **Table 1-1** summarizes the cost of different bio-polymers and their price compared with low density polyethylene, a conventional petroleum based plastic.

The cost of PHA production could be reduced by using low cost feedstocks derived from "waste" and surplus materials to support growth of microorganisms that synthesize PHA polymers. A variety of low cost materials from agricultural and agriculture related industrial wastes have been tested for PHA production, including molasses, soluble starch, cellulose hydrolysate, glycerol, and wastewater (Braunegg et al., 1998; Shrivastav et al., 2010).

Table 1-1. Production scale and pricing of different types of bioplastics manufactured by industry.

Polymers	Producer	Capacity in 2013 (kt)	Price ($/kg) [a]
PHB copolymer [b]	Meredian(US)	272	3.4-6.8
PHB	Telles (US)	50	2.04
PLA	NatureWorks (US)	300	1.98-2.2
Starch plastics	Cereplast (US)	225	--
LDPE [c]			1.64

[a] Reflects the product price in 2010, expect for price for LDPE.
[b] Co-polymers of PHB with other PHA units, such as PHV, PHH.
[c] Low density polyethylene for comparison.

1.3 PHA producing bacterial species

The accumulation of storage molecules in microorganisms as carbon and energy sources is a common phenomenon. Microbial storage molecules can be in the form of lipids, starch, cellulose, or PHA. A wide range of eubacteria, archaea, and even eukaryota, such as some yeast species, are known to produce PHA (Desuoky et al., 2007), but the majority of microorganisms that synthesize PHA are found in the eubacteria. Although PHA have a wide distribution of monomer composition, bacteria tend to produce PHA with specific monomer combinations, such as those with primarily C4 (PHB) or C5 (PHV) from scl-PHA producers, or those with C6 to C14 from mcl-PHA producers. And some bacteria can synthesize PHA polymers with an even broader carbon chain length distribution (from C4 to C12). The type of PHA polymer and its monomer composition are key factors to determine the final physical property of the polymers and in turn their potential applications (Akaraonye et al., 2010). The monomer composition could be greatly different in the bacteria harboring different types of PHA synthase (encoded by *pha*C) that carries out the polymerization reaction (Steinbüchel and Valentin, 1995).

Attempts have been made to correlate various bacteria taxonomies with their genome contents associated with PHA biosynthesis, although sequences of different PHA synthases showed various degrees of similarity. Using the amino acid sequence of the scl-PHA synthase as reference to search against sequence databases using HMMER (profile Hidden Markov Models) identified 2362 sequences across various taxonomies with protein domain architectures consisting common PhaC domain and α/β hydrolase domain. The majority of these "hits" fell in the Phyla of *Proteobacteria, Actinobacteria*, and *Firmicutes*.

The further classification of these PhaC enzymes with respect to amino acid sequence, deduced secondary structures, substrate specificity, subunit composition, and genetic arrangement of the genes that encode them, fall into four classes: Class I, for which *Cupriavidus necator* is the type species (Qi and Rehm, 2001); Class II with *Pseudomonas* species as most well-known mcl-PHA producer (Witholt and Kessler, 1999); Class III, with *Allochromatium vinosum* as the type species (Yuan et al., 2001), and Class IV, with *Bacillus megaterium* as the type species (McCool and Cannon, 2001).

1.3.1 scl-mcl-copolymer producers

The motivation for exploring co-polymer production lies in their enhanced physical properties. Mcl-PHA containing medium length alkyl side chains make them tacky and unsuitable for structural or fiber application. Scl-PHA on the other hand are brittle, whereas scl-mcl copolymers composed of mostly C4 monomer and small amount of C6 monomer have been shown to have properties most similar to polypropylene (Nomura et al., 2004). Therefore, it might be necessary to provide strategies by which scl-co-mcl-PHA can be synthesized in order to produce the material that is strong, yet ductile, for certain applications (Ashby et al., 2002). The PHA synthases derived from co-polymer producing strains, such as *Pseudomonas* sp. 61-3 and *Thiocapsa pfennigii*, have significant amino acid sequence similarities and highly conserved amino acid residues with the Class I to IV PHA synthases (Matsusaki et al., 2000; Liebergesell et al., 2000).

1.3.2 Short chain length PHA (scl-PHA) producing bacteria

Cupriavidus necator, formally also known as *Alcaligenes eutrophus* or *Ralstonia eutropha* H16, is the most well studied scl-PHA producing bacterium so far (Abedi et al., 2006). *C. necator* is well known to synthesize large quantities of intracellular PHB,

which accumulates to as much as 72% - 76% of the cell dry weight (cdw) from soybean oil containing culture medium of *Cupriavidus necator* (Kahar et al., 2004). *C. necator* can also synthesize and accumulate up to 75% cdw of polyhydroxybutyrate-co-polyhydroxyvalerate (PHB-co-PHV) copolymers when grown in cultures containing glucose and propionate (Chen, 2009). The lower crystallinity and melting temperature (well below its thermal decomposition temperature) of PHB-co-PHV copolymers make them easier to process, and offer greater ductility and toughness, which are required for many practical applications. In comparison, polymers of pure PHB are very brittle, which limits the range of products it can be used in (Noda et al., 2005).

Alcaligenes latus, unlike *C. necator*, does not require nutrient-limitation to stimulate synthesis of PHB from various sugars (Hrabak, 1992). However, increased PHB accumulation was observed under nitrogen-limitating conditions, resulting in an increase in accumulation of PHB from 50% to 78% cdw (Wang and Lee, 1997). This property may be useful in evaluating the balance between the polymer production and productivity from an industrial perspective.

Gram-positive bacteria, notably *Bacillus*, are able to produce natural PHB-co-PHV copolymers from simple carbon sources without co-feeding a secondary carbon source, such as valeric or propionic acid. *Bacillus cereus* SPV, was able to synthesize PHA containing 3-hydroxybutyrate (3HB), 3-hydroxyvalerate (3HV), and 4-hydroxybutyrate (4HB)-like monomer units from structurally unrelated carbon sources, such as fructose, sucrose, and gluconate (Valappil et al., 2007b). Furthermore, no lipopolysaccharides (LPSs) synthesized by gram-positive bacteria also provide medical/pharmacological applications benefit, as LPSs can induce fever (pyrogens) in humans exposed to them, are also known to co-purify with the PHA during extraction. This can be an advantage

in some medical/pharmacological applications (Valappil et al., 2007a).

1.3.3 Medium chain length PHA (mcl-PHA) producing bacteria

Bacteria that synthesize mcl-PHA express Class II PHA synthase enzymes, which mostly have been identified in various *Pseudomonas* species. Using the amino acid sequence of the *P. putida* KT2440 PhaC protein to search against the annotated genome sequence databases revealed 2362 candidate enzymes containing conserved domains for PhaC. However, these sequences may overlap with PhbC of scl-PHA producing bacteria due to sequence similarity between two classes of PHA synthase. An extensive comparison of the 59 PHA synthases of different groups revealed that these proteins share amino acid sequence identities that range from 8% to 96% (Rehm, 2003). The most unique genetic feature for mcl-PHA synthesizing bacteria is presence of the mcl-PHA biosynthesis cluster genes (De Eugenio et al., 2010b). The genetics of mcl-PHA biosynthesis cluster and pathway will be reviewed in later section of the Chapter 1 (see **section 1.6**).

To date, *Pseudomonas* species have been extensively investigated for their ability to synthesize mcl-PHA (see **Table 1-2**). Species tested include: *P. aeruginosa*, *P. entomophila*, *P. fluorescens*, *P. oleovorance*, *P. putida*, and *P. stutzer* (PHB producer). *Pseudomonas* species can utilize a wide range of carbon sources for synthesizing mcl-PHA containing versatile functional groups in their side chains, such as branched alkyls groups (Lenz et al., 1992), halogens (Kim et al., 2000), epoxy moieties (Imamura et al., 2001), alkyl esters (Scholz et al., 1994), unsaturated aliphatic groups (Kim et al., 2001), and aromatic groups (Abraham et al., 2001). These functional groups can greatly change the physical properties of the mcl-PHA polymers containing them, imparting excellent

modification for different applications.

The carbon source used to grow the bacterial species that synthesize mcl-PHA has a significant effect on the monomer composition of the polymer produced (**Table 1-2**). 3-hydroxyoctanoate (C8) is the most dominate monomer of mcl-PHA when the bacteria are grown on fatty acid based carbon sources, while a greater mol % of 3-hydroxydecanoate (C10) is incorporated into the mcl-PHA polymer when the bacteria are cultured on carbon sources such as glucose or glycerol. Species such as *P. chlororaphis*, *P. fluorescens*, and *P. fulva*synthesize mcl-PHA with "uncommon" monomer compositions, such as significant amounts of unsaturated or longer chain length PHA. *P. mendocina* CH50 is the only wild type strain producing C8 homo-polymer from octanoate reported to date (Rai et al., 2011b). In short, there is great potential for synthesis of mcl-PHA with tailored properties that could have a wide range of applications.

Table 1-2. Summary of mcl-PHA production and monomer composition profile from different carbon sources by various *Pseudomonas* species based on information from published papers.

Strain	**Culture conditions**			**PHA (wt%)**	**Monomer composition (mol%)**						**Other reported metabolites**	**References**
	Substrate	Concentration (g/L)	C/N ratio [a]		C6	C8	C10	C12	C12:1	C14		
***P. putida* LS46**	Glucose	10	22.4	22	2.2	15.7	76.1	5.6	-	-	-	Sharma et al., 2012
	Octanoic acid	3.2	11.7	56	6.9	89.3	3.4	-	-	-	-	This study
	Decanoic acid	2.8	10.7	34	4.6	47.5	46.6	1.3	-	-	-	This study
***P. putida* KT2440**	Sodium octanoate	12	39	52	18.8	81.2	-	-	-	-	-	Ouyang et al., 2007
	Sodium octanoate	2.2	40	70	8	92	-	-	-	-	3-HA acid [b]	De Eugenio et al., 2010a
	Glucose	18.5	41	25	5	11.8	70.3	4.7	9.4	0.8	Gluconate; 2-ketogluconate	Poblete-Castro *et al.*, 2013
	Glycerol	3.7	40	19	-	-	-	-	-	-	-	Escapa et al., 2013
***P. entomophila* L48**	Dodecanoic Acid	15	-	50.4	6.4	44.5	38.6	10.6	-	-	-	Chung et al., 2011
***P. putida* CA-3**	Phenylaceti c acid	2	24	28	-	-	-	-	-	-	Polyphosphate	Tobin et al., 2007
***P. aeruginosa* PAO1**	Sodium gluconate	15	48	20	14	21	61	4	-	-	Alginate Rhmnolipid	Pham et al., 2004
***P. aeruginosa* L2-1**	Waste fryer oil	2	-	43	-	37.5	42.1	13.2	2.2	2.1	Rhamnolipids	Costa et al., 2009
***P. aeruginosa* IFO3924**	Palm oil	7	27	36	4	38	43	12	-	-	Rhamnolipids	Marsudi et al., 2008

***P. aeruginosa* PA14**	Decanoic acid	5.2	30	16.9	8.2	55	36.8	-	-	-	Rhamnolipids	Choi et al., 2011
P. mendocina	Gluconate	15	54	13	3	15	68	13.8	-	-	-	Lee et al., 1995a
	Octanoic acid	10	65	30	9.1	90.9	-	-	-	-	-	
***P. mendocina* 0806**	Glucose	20	89	32	5	17	71	1	5	-	-	Tian et al., 2000
***P. mendocina* NK-01**	Glucose	20	--	20	-	-	-	-	-	-	Alginate	Guo et al., 2011
***P. mendocina* CH50**	Sodium octanoate	3.3	27	31.4	-	100	-	-	-	-	-	Rai et al., 2011b
***P. fulva* TY16**	Glucose	10	39	27	2.1	17.7	60.1	8.5	11.7	-	-	Ni et al., 2010
	Gluconic acid	10	36	34	2.4	20.5	63.5	7.1	6.5	-	-	
	Octanoic acid	4	26	55	9.6	79.1	11.3	3.7	-	-	-	
***P. chlororaphis* NRRL B-30761**	Glucose	10		-	-	25	46	29	-	-	Rhamnolipids	Solaiman et al., 2013
	Gluconate	10		-	-	5	39	52	-	1		
	Octanoic acid	10		-	16	78	6	-	-	-		
***P. fluorescens* GK13**	Glucose	15	58	38	1.6	9.4	68.5	19.3	-	-	-	Lee et al., 1995a
	Octanoic acid	10	65	31	4.2	95.8	-	-	-	-	-	
***P.fluorescens* BM07**	Glucose	12.6	42	8.2	-	5.2	35.5	19.3	32.5	7.4 [c]	-	Lee et al., 2001
	Octanoate	5.8	32	23.3	11.8	84.4	1.8	0.4	0.4	0.4	-	
***P. stutzeri* 13176**	Glucose	10	45	58 [d]	2.4	21.3	63.2	4.2	6.1	1	-	He et al.,1998
	Soybean oil	10	-	63 [d]	-	8.2	63.4 [e]	2.6	-	-	-	

a: Carbon to nitrogen ratio
b Extracellular 3-hydroxyalkanoic acid;
c Among total 7.4 mol% of C14 monomer**,** 4.6 mol% was made up with C14:1 unsaturated monomer;
d PHA was measured gravimetrically; and numbers refer to PHB production;
e made up with 3,6-epoxy-7-cis/trans nonene-1,9-dioic acid;

1.4 Sustainable mcl-PHA production

As mentioned earlier, raw feedstock prices account for a large portion of PHA production costs. Therefore, there is considerable interest in the use of low costs agro-industrial waste streams to support growth of PHA synthesizing bacteria. As the focus of this thesis is mcl-PHA production by *Pseudomonas putida*, waste sources that have been used for mcl-PHA synthesis by *P. putida* will be reviewed. Common carbon sources that *P. putida* can utilize for mcl-PHA synthesis include simple sugars, such as glucose and fructose, polyol, and free fatty acids.

mcl-PHA production by *Pseudomonas putida* IPT 046 growing on glucose or fructose as sole carbon source resulted in 50 % cdw accumulation of mcl-PHA (Sánchez et al., 2003). An inexpensive feedstock that could represent these two simple sugars is sugarcane hydrolyzed carbohydrates, which has been used for mcl-PHA production by *P. putida* IPT046 (Diniz et al., 2004). However, recent studies have focused on using sugarcane bagasse and sugarcane molasses for PHA production to avoid the food versus energy debate (Albuquerque et al., 2007; Silva et al., 2004).

Sugarcane bagasse is a renewable, cheap, and widely available waste. Xylose from sugarcane bagasse hydrolytes could be used as carbon source for PHA production. However, there are two important issues: first, an additional hydrolysis step is often required to release the sugars, and the second problem is that *P. putida* is not able to metabolize xylose, which eliminates use of this waste carbon source for mcl-PHA production. The later problem, however, can be overcome by heterologous expression of *xylA* (encoding xylose isomerase) and *xylB* (encoding xylulokinase) from *E. coli* (Le Meur et al., 2012). Sugar cane molasses is a by-product of the sugar refinery industry with high sugar content and over 50 % dry mass (Albuquerque et al., 2007). The price

for sugarcane molasses in 2008 was less than $ 0.50 per kg. Therefore sugarcane molasses may be considered a viable substrate to reduce mcl-PHA production costs (Chan et al., 2012). Currently, fermented sugarcane molasses is being used for PHB production from mixed cultures (Bengtsson et al., 2010b; Bengtsson et al., 2010a).

Using glycerol to produce high-value compounds through microbial fermentation is promising. Glycerol is relatively inexpensive, abundant, and showed advantages for producing reduced chemicals, such as succinate and xylitol over sugars (da Silva et al., 2009). Waste glycerol is unprofitable and detrimental to use as feedstock for other downstream purposes, such as use for cosmetic products and animal feeds (Yazdani and Gonzalez, 2007; Yang et al., 2012). Instead, several studies have demonstrated scl- and/or mcl-PHA production from biodiesel derived glycerol by several *Pseudomonas* species, including *P. oleovorans*, *P. corrugate* (Ashby et al., 2005), and *P. putida* (Kenny et al., 2012). But waste glycerol used in these studies contains high amount of fatty acids (10 % to 34 %) and methanol as common "contaminants", which would not be expected as "standard waste" with efficiency on fatty acids recycling during glycerol refining improving.

Another type of low cost carbon source for mcl-PHA production are fatty acid-based wastes, including waste vegetable fryer oils and biodiesel-derived free fatty acids. Waste fryer oil is available in large amounts in North America but its recycle is limited due to harmful compounds generated from the oxidation of triacylglycerides during frying. In addition, disposal of waste fryer oil creates environmental problems to local ecosystems and disposal of waste fryer oil into municipal sewage systems is prohibited in many jurisdictions (Kulkarni and Dalai, 2006).

Waste fryer oil could be used as a low cost carbon source for mcl-PHA production

by various *Pseudomonas* species (Song et al., 2008; Tan et al., 1997; Marsudi et al., 2008). The monomer composition of mcl-PHA polymers can vary depending on the type of vegetable oil used. Using 10 g/L of hydrolyzed corn oil as the sole carbon source (which contains over 90% of unsaturated fatty acids), mcl-PHA production by *P. putida* was 20% of cell dry weight (dcw), and contained up to 25 mol % unsaturated side chains (Shang et al., 2008). In contrast, palm oil is one of the few vegetable oils that contains a relatively high percentage of saturated fatty acids (over 45%). Using $7\,g/L$ palm oil as the sole carbon source, mcl-PHA production by *P. aeruginosa* was 36% dcw and contained about 1.7 mole % of unsaturated mcl-PHA monomers (Marsudi et al., 2008). Although C8 and C10 were the dominant mcl-PHA monomers found in both the studies, differences in monomer saturation level would produce mcl-PHA polymers with very different physical and thermal properties.

Biodiesel-derived free fatty acids are residual free fatty acids removed from crude glycerol generated by transesterification of vegetable oils in the process of biodiesel production. Biodiesel-derived free fatty acids can be recycled or used, for example, for mcl-PHA production without further purification, which has not been explored yet. Characterization of cell growth and mcl-PHA production using biodiesel derived free fatty acids are discussed at Chapter 2 and 4.

1.5 Impurities from industrial waste carbon sources

While the use of inexpensive carbon sources derived from industrial waste streams is attractive, it may be problematic because impurities derived from the waste may affect cell growth. For example, accumulated effect of potential impurities from waste glycerol culture has showed negative effect on the growth of *E. coli* cell at high cell density (Verhoef et al., 2013).

In general, while the components of crude biodiesel derived glycerol may vary from plant to plant, the two major impurities are residual methanol and sodium or potassium soaps derived from the catalysts used to synthesize biodiesel. In addition, biodiesel derived glycerol may contain residual free fatty acids, non-reacted mono-, di- and triacylglycerides, and residual fatty acid methyl esters (Chatzifragkou and Papanikolaou 2012). Various elements such as calcium, potassium, phosphorus, magnesium, sulfur may also be present in the waste glycerol, and although the biodiesel production process does not include any heavy metals, the oil feedstock used may contain heavy metals in various amounts (Pyle et al., 2008; Thompson and He 2006; Verhoef et al., 2013). Impurities in biodiesel-derived glycerol, such as heavy metals, may be toxic to cells, or toxic at concentrations above a certain concentration. The problem may be exacerbated by the greater substrate loading and high-cell density required for large-scale industrial production of mcl-PHA. Microorganisms develop various strategies to finely regulate the heavy metal concentration intra-cellularly. Concentrations of copper ions are tightly regulated within bacterial cells through a variety of mechanisms that include efflux, segregation, and reduction (Nies 1999; Zhang et al., 2012). *P. putida* is well known for resistance to heavy metals, solvents, and antibiotics (Cánovas et al., 2003; Wu et al., 2011). A comparative genomics analysis of *P. putida* LS46 revealed many genes that are putatively involved in resistance of various toxic materials, such as aromatic compounds and heavy metals (Sharma et al., 2014), whose expression may therefore confer the strain potential of adaptability when culturing with industrial waste streams.

1.6 Genetics of mcl-PHA metabolism pathway

1.6.1 Mcl-PHA synthase and mcl-PHA depolymerase

Before reviewing mcl-PHA biosynthesis pathways, the enzymes that play an essential role in PHA polymer synthesis, recycling, and help to maintain the inter-cellular energy and carbon flux balance of the bacteria need to be reviewed. Biochemically, PHA synthase catalyses the stereo-selective conversion of (R)-3-hydroxyacyl-CoA substrates to PHA with the concomitant release of CoA. Recognition of the (R)-3-hydroxyacyl-CoA intermediate is highly dependent on the substrate specificity of the PHA synthase itself. Mcl-PHA synthases are preferentially active towards CoA thioester of various mcl-3-HA comprising 6 to 14 carbon atoms (Rehm and Steinbüchel, 1999).

The catalytic mechanism of PHA synthase employed by α/β hydrolases is a conserved domain in both scl-PHA and mcl-PHA synthase. In short, the active PHA synthase involves two subunits forming a homo-dimer. Two thiol groups from each subunit are active in the catalysis process, including substrate loading, priming, and elongation (Amara and Rehm, 2003). With increasing substrate availability and covalent synthesis of the hydrophobic polyester chain, PHA granules are formed with the hydrophobic PHA in the core and the active water soluble PHA synthases at the surface (Rehm, 2003). More recent findings suggested that the PHA granule is not randomly distributed in the cell, but is attached to a scaffold, most likely the nucleoid (the so-called scaffold model; see (Jendrossek and Pfeiffer, 2014). The key linker between the granule and the scaffold is the granule-associated protein, PhaM for scl-PHA polymers and PhaF for mcl-PHA. PhaF is also appears to bind non-specifically to the nucleoid to facilitate polymer distribution during chromosome segregation (Pfeiffer et al., 2011; Galán et al., 2011). The scaffold model ensures equal distribution of PHA granule into every daughter cell under simultaneous growth and PHA synthesis condition.

Bacteria that synthesize mcl-PHA usually contain two PHA synthases, namely PhaC1 and PhaC2. This is one of the most unique genetic features that distinguishes mcl- PHA synthesizing bacteria from scl-PHA producing species. The role of genetic redundancy of having two mcl-PHA synthases have been studied in several *Pseudomonas* species. The first study of purified Class II PHA synthases, PhaC1 and PhaC2, was conducted with *P. aeruginosa,* and the specific activity of both the PhaC1 and PhaC2 enzymes towards R/S-3HD-CoA were similar, indicating the two enzymes are able to incorporate R-3-hydroxy-CoA into mcl-PHA (Qi et al., 2000). However, the substrate specificity preference of the two enzymes may not be identical. For example, a mutant strain of *P. putida* U in which the *pha*C1 gene was delected (Δ*phaC1*) resulting PhaC2 was the only expressed synthase. In this mutant, mcl-PHA was synthesized in poor quality and with altered monomer distribution compared to the wild-type strain. The Δ*phaC1* (PhaC2 expressing) strain also failed to incorporate various aromatic monomers for aromatic PHA production (Arias et al., 2008), and was not able to convert R-3-hydroxyoctanoyl-CoA (Ren et al., 2010). A Δ*phaC1* strain of *P. putida* KT2440 also was unable to utilize octanoic acid as a substrate for mcl-PHA synthesis (Escapa et al., 2012). Therefore, it is likely that PhaC1 is the major synthase in mcl-PHA biosynthesis. However, it may also be stated that PhaC2 has substrate specificity for different carbon sources, as PhaC2 expressing strains were able to incorporate more 3HA-hexanoic acid into mcl-PHA polymers compare to PhaC1 (Arias et al., 2008).

The primary structure of the two proteins share over 55% amino acid sequence identity. In addition, two synthases contain conserved α/β hydrolase domains (amino acid 190 to amino acid 480) and a putative catalytic triad within this region: Cys296-His479- Asp451 (PhaC1) or Cys296-His480-Asp452 (PhaC2) in *P. putida* U.

This active site, or at least the α/β hydrolase core, is therefore most likely not responsible for the observed differences in substrate specificity of these enzymes. So, it was proposed that sequence variation outside the α/β hydrolase core could be responsible for the differences (Rehm, 2003).

An intracellular PHA depolymerase (PhaZ) hydrolyzes mcl-PHA polymers into R-3HA acids, which in turn are mobilized into fatty acid metabolism, or are recycled back to mcl-PHA biosynthesis, by PhaC1/C2 (De Eugenio et al., 2010a). This cycle seems futile, but it suggests a fundamental role for PHA in balancing stored carbon in the bacterial with cell growth in anticipation of carbon-limiting conditions, and allows cells to adapt the flux of hydroxyacyl-CoAs to cellular demand. Therefore, PhaZ was expressed concomitantly with PHA synthesis, and not independent of it (Ren et al., 2010). Mutant strains of *P. putida* KT2442 in which the *phaZ* gene had been knocked-out (Δ*phaZ*) resulted in mcl-PHA overproduction (Cai et al., 2009), and no extracellular R- hydroxyalkanoic acids compare to the wild strain (De Eugenio et al., 2010a). These results confirmed the essential role of PhaZ in mcl-PHA mobilization.

1.6.2 Phasins and in-cluster transcriptional regulator

PhaF and PhaI are two granule associated proteins (also known as Phasins) of the mcl-PHA biosynthesis cluster. Earlier study of *P. putida* GPo1 showed the dual role of PhaF as both a phasin protein associated with PHA granule formation and as a transcriptional regulator (Prieto et al., 1999). A detailed study of the *P. putida* KT2440 PhaF revealed its role in granule localization within the cell (Galán et al., 2011). Although the function of PhaI is still unclear, sequence analysis has shown that the protein lacks the repeated AAKP motifs present at C-termini of the PhaF protein (Galán et al., 2011). The AAKP repeat motifs were showed to be required for DNA-

binding in many DNA-binding proteins from *Pseudomonas* species (Deretic and Konyecsni, 1990; Deretic et al., 1992), suggesting PhaI, unlike PhaF, does not bind to nucleoid DNA.

In *P. putida* KT2440, the mcl-PHA biosynthesis cluster putatively forms two putative transcriptional units: *pha*C1-*pha*Z-*pha*C2-*pha*D and *pha*F-*pha*I, which under the regulation of an in-cluster transcriptional regulator, PhaD (De Eugenio et al., 2010b). The regulator was proposed be activated by an intermediate from fatty acid oxidation pathway resulting in higher transcriptional level of mcl-PHA cluster genes when the cell grown on octanoic acid vs glucose (De Eugenio et al., 2010b). Transcription of the mcl-PHA cluster genes thus potentially created the first level of regulatory variation giving rise to substrate-dependent mcl-PHA biosynthesis patterns of *P. putida*.

1.6.3 Substrate-specific mcl-PHA biosynthesis pathways

Mcl-PHA production from *Pseudomonas* species is highly dependent on the choice of substrates. Except regulatory differences on mcl-PHA cluster genes expression mentioned above (**section 1.6.2**), *P. putida* synthesizes mcl-PHA through a fatty acid *de novo* synthesis route (anabolic pathway) or through a fatty acid β-oxidation route (catabolic pathway) (Reddy et al., 2003). The proposed mcl-PHA metabolic pathways on different carbon sources has been depicted in **Figure 1-2**.

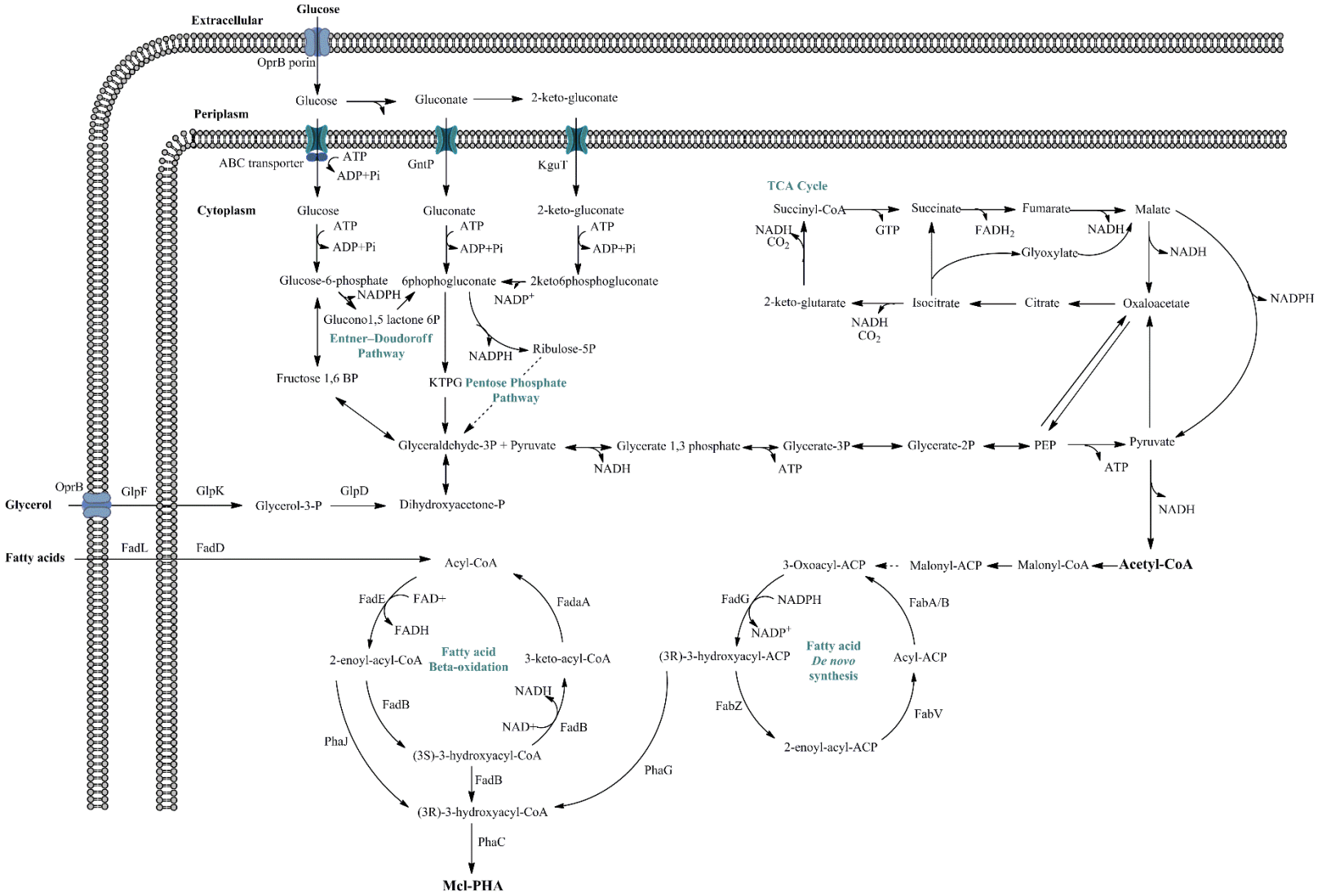

Figure 1-2. Proposed metabolic pathways for mcl-PHA biosynthesis in *P. putida* LS46.

The fatty acid *de novo* route for mcl-PHA biosynthesis of *P. putida* refers to mcl-PHA synthesis from sugar, glycerol, or carbon sources that shares fatty acid *de novo* synthesis as the primary route to provide mcl-PHA intermediates: R-3HA-ACP, the pathway intermediate for mcl-PHA synthase. However, the mechanisms on initial carbon uptake and metabolism (such as, glucose vs glycerol) are greatly different (see **Figure 1-2**). A glycerol uptake cluster is specifically required for glycerol metabolysis in *Pseudomonas* (Schweizer et al., 1997), while transportation of glucose into cytoplasm requires an ABC-type glucose transporter. Simultaneously, enzymes, such as glucose dehydrogenase and gluconate dehydrogenase carry out series oxidation reactions in the periplasmic space, converting glucose into gluconate and keto-gluconate, respectively (Castillo et al., 2007). These variations suggested that mcl-PHA biosynthesis of *P. putida* is regulated at the initial substrates transportation step. For example, a repressor protein (coded by *glp*R) located in glycerol uptake cluster was knockedout to reduce the lag phase of *P. putida* KT2440 grown on glycerol (Escapa et al., 2013). On the other hand, the glucose uptake pathway has been modified by knocking out glucose dehydrogenase in *P. putida* KT2440, leading to a increased mcl-PHA production from glucose (Poblete-Castro et al., 2013).

As the next step, carbons were converted into acetyl-CoA via partial glycolysis through the Entner-Doudoroff (ED) pathway, which is then fluxed to fatty acid biosynthesis metabolism. While, (R)-3-hydroxyalkanoates-acyl carrier proteins are used as the intermediate for mcl-PHA biosynthesis. However, (R)-3-hydroxyalkanoates-acyl carrier proteins must to be converted into their CoA derivatives, which is carried out by PhaG, a 3-hydroxyacyl-ACP-CoA transacylase. PhaG (also known as mcl-PHA monomer supplying protein) is identified biochemically as a unique protein that is

required for mcl- PHA synthesis from fatty acid *de novo* synthesis in *Pseudomonas*, and its expression was highly up-regulated in *P. putida* grown in either glycerol or glucose cultures under mcl- PHA producing condition (Hoffmann et al., 2002).

The fatty acid β-oxidation route is used for mcl-PHA biosynthesis when fatty acids are used as sole carbon source. The key precursor for mcl-PHA synthase, (R)-3HA-CoA, is converted from trans-2-enoyl-CoA, the intermediate of fatty acid β-oxidation. The key enzyme that carries out this reaction is an R-specific enoyl-CoA hydratase coded by *pha*J in *Pseudomonas* species. There are four *pha*J homogs identified in *P. aeruginosa*, and their gene products expressed in recombinant *E. coli* were demonstrated to provide monomer for mcl-PHA biosynthesis from fatty acids (Tsuge et al., 2003). When expressed in *E. coli*, PhaJ1 of *P. aeruginosa* showed a substrate specificity toward enoyl-CoAs with acyl chain lengths from C4 to C6 (short to medium chain length), while PhaJ2, PhaJ3, and PhaJ4 exhibited substrate specificities toward enoyl-CoAs with acyl chain lengths from C6 to C12 (medium chain length). Only 2 *pha*J genes (*pha*J1 and *pha*J4, based on the sequence similarity to those of *P. aeruginosa*) are present in in *P. putida*, and the product of *pha*J4 ortholog was shown to act as the primary mcl-PHA monomer supplying enzyme in *P. putida* (Sato et al., 2011). Another putative monomer supplying enzyme for mcl-PHA synthesis from fatty acid β-oxidation is a 3-ketoacyl-CoA reductase, coded by *fab*G. This enzyme is an NADPH-dependent 3-ketoacyl reductase, and identified in *P. aeruginosa* as a mcl-PHA monomer supplying protein by reducing mcl-3-ketoacyl-CoAs to mcl-3-hydroxyacyl- CoA from fatty acid β-oxidation (Ren et al., 2000). Yet, no evidence has showed that the protein (FadG) played a role as monomer supplying enzyme for mcl-PHA biosynthesis from fatty acid β-oxidation in *P. putida*.

The biosynthesis of the polymer can be regulated at various steps due to metabolic and regulatory versatility of the *P. putida* genome: it is possible that putative competing pathways, redundancy in pathway genes, and regulatory mechanisms of mcl-PHA biosynthesis genes are all potential driving forces for determining the final mcl-PHA profile from different carbon sources. Therefore, to achieve a better understanding of cell metabolism in term of mcl-PHA biosynthesis, the technologies reviewed below offer a systematic and informative analyses helping to explore, but not limited to, i) identification of pathway genes that are actively involved in metabolic processes; ii) differentiation of active genes from redundantly encoded genes in the genome; iii) prediction of carbon and electron flow, which influence metabolic flux, and therefore determine end-product synthesis patterns; and iv) insight into mechanisms of gene regulation and regulatory variation at transcriptional or translational level.

1.7 'Omics technologies

The term "'Omics" has been used in many fields of studies, which in general include, genomics for quantitative study of protein coding/non-coding genes, and regulatory elements; transcriptomics for RNA and gene expression; proteomics focusing on protein expression levels; and metabolomics which studies metabolites and metabolic networks (Schneider and Orchard, 2011). The cellular responses (mRNA, protein, and metabolite profiles) triggered under various physiological conditions, and their mutual relation can therefore be studied.

1.7.1 Genomics

High throughput microbial sequencing technologies can generate nucleotide sequences of entire bacterial genomes in a few hours, and genetic information encoded

by the genome can be elucidated by searching for homologous sequences in annotated genome databases. Thus, the genome structure is set up for many downstream analyses that are either predictive, like genomics, or evidence-based, like transcriptomics and proteomics.

The genome size of different *P. putida* strains deposited in IMG (Integrated Microbial Genomes) database ranged from about 3 Mbp (*P. putida* MR3) to 7 Mbp (*P. putida* S12), and some strains are predicted to contain plasmid DNAs of various sizes. BLASTn analyses of whole genome sequences of the ten *P. putida* strains revealed nucleotide sequence identities of 86.54% to 97.52% (Sharma et al., 2014). This comparative bioinformatics analyses revealed that central metabolism pathways and the mcl-PHA biosynthesis cluster are highly conserved in various *P. putida* isolates (Sharma et al., 2014). This study also revealed significant variation in genome content and the presence of a variety of accessory pathways that enable some *P. putida* strains to degrade toxic compounds, consume hydrocarbons, or tolerate heavy metals. Enrichment environments and different geographical locations are certainly important factors for such genome variation and enable *P. putida* strains to cope with the ever changing environments where they survive.

1.7.2 Transcriptomics and Proteomics

Transcriptomics and proteomics are usually applied under various physiological conditions or with mutant strains. These technologies are able to quantify the "abundance" of mRNA transcripts and peptides associated with specific proteins, respectively. However, the methods for detection and quantification of mRNAs and peptides (proteins) are fundamentally different.

Next-generation-sequencing (NGS) now allows for routine large-scale

quantification of RNA abundances in any organism. The technology, named RNAseq, has significant advantages over conventional cDNA microarray technology (Wang et al., 2009). After extraction, RNAs are sequenced directly by any high throughput sequencing platform, and the number of 'reads' per sequence (after accounting for sequence length) is used for quantification of mRNA abundance.

The recent technology for quantitative proteomics typically involves "shotgun" proteomics, where the quantification is achieved by measuring ion intensities in the mass spectrometer or by counting spectra that are derived from each peptide (Mallick and Kuster, 2010). Alternatively, one can incorporate isotopes (such as, isobaric tag for relative and absolute quantification: iTRAQ) to two or more biological samples, and quantification (relative abundance) of proteins can be determined by direct comparison of the labeled peptides in the mass spectra (Ross et al., 2004). Most label-based detection methods have potential limitations: complex sample preparation, incomplete labelling, and high sample concentration. Therefore, label-free quantification has recently evolved to address some of these limitations, while providing good protein coverage and fast processing time (both sample preparation and instrumental time) (Patel et al., 2009). Recent work using label-free LC-MS/MS based methods for fast and informative global profiling of protein mixtures from various biological samples has been reported (Verbeke et al., 2014).

While taking advantages of these two methods for fast and reliable gene and gene product expression profiling, it also important to notice the fundamental differences between mRNA and protein abundance measurements. Transcript abundances do not always reflect protein abundances. These are caused by the complexity of biological background, such as protein regulation, rather than experimental bias, such as

measurement errors (which could usually be counted out by comparing two biological replications) (Vogel and Marcotte, 2012). Therefore, integration of transcript and protein data even for steady-state cell (such as mid-log) transcript abundances only partially predict protein abundances, which indicates regulation of mRNA and protein must be invoked to explain how protein abundance levels are established.

1.7.3 Metabolomics

Unlike genes and proteins, the functions of which are subject to various regulations, post-translational modifications and protein degradation, metabolomics directly measures biochemical activity by monitoring substrates and products transformed during cellular metabolism. The technology could be used for profiling of these chemical transformations at a global level, which phenotypically is important in investigating the mechanisms of fundamental biological processes (Patti et al., 2012). However, compared with transcriptomics and proteomics, global metabolomics (untargeted metabolomics) is still facing many challenges. A complete database for all possible metabolites is required, and classical biochemical pathways may fail to explain any unknown biochemical perturbation detected by metabolomics (Baker, 2011).

1.7.4 Gene expression and mcl-PHA synthesis phenotypes

Physiologically, mcl-PHA production profiles (synthesis kinetics, cellular accumulation, and monomer composition) by *P. putida* vary with growth conditions, such as the type of carbon source used and nitrogen availability (see **Section 1.3.2**). Cultures of *P. putida* containing carbon sources metabolized via glycolysis, such as glucose or glycerol, require nutrient-limitation (nitrogen-limitation for example) to induce PHA synthesis and polymer accumulation, which take place during stationary phase. In

contrast, cultures containing fatty acids, which are metabolized via fatty acid β-oxidation, actively synthesize mcl-PHA during exponential growth in the presence of excess of nitrogen in the culture medium (Fu et al., 2014; Poblete-Castro et al., 2012). mcl-PHA synthesis, therefore, is not limited to conditions of stress when it is produced and accumulated in the cells as carbon and energy storage compound. There is increasing evidence that mcl-PHA biosynthesis is important for regulating carbon flux for optimal cell growth (Escapa et al., 2012).

Nonetheless, activation of mcl-PHA biosynthesis via up-regulation of mcl-PHA biosynthesis related genes (see **Section 1.6**) should be the first response of *P. putida* cells during polymer synthesis. In exploring the transcriptome of *P. putida* KT2440 in a decanoic acid cultures, transcription levels of the mcl-PHA cluster genes varied with different carbon to nitrogen ratios, resulting in different levels of mcl-PHA production (Poblete-Castro et al., 2012). However, discrepancies between gene expression levels and end-product accumulation were not observed in a mcl-PHA hyper-producing mutant of *P. putida* KT2440 grown on glucose (Poblete-Castro et al., 2013). These results suggested carbon-specific expression and regulation of the biosynthesis cluster gene, and support for this hypothesis was provided by studies that showed the effect of three specific regualtory elements (PhaD, Crc, and Csr) on mcl-PHA biosynthesis (De Eugenio et al., 2010b; La Rosa et al., 2014; Ryan et al., 2013). However, further evaluation of the expression profiles of mcl-PHA biosynthesis-related genes and gene products (encoded by PHA synthesis cluster and monomer supplying genes) under conditions of active polymer synthesis versus non-active PHA synthesis conditions are required to elucidate the nature and role of putative regulatory mechanisms that activate mcl-PHA biosynthesis.

During the mcl-PHA synthesis, metabolic flux to mcl-PHA biosynthesis depends heavily on the "enzyme capacity" that drives metabolic networks towards synthesizing specific precursor metabolite pools for polymer synthesis. According to the Michaelis-Menten equation, $Vo = [E] \times Kcat \times \frac{[S]}{Km+[S]}$ (where E is concentration of enzyme catalytic sites, Kcat is the turnover number, Km is the Michaelis-Menten constant, and S is the substrate concentration), changes in protein abundance (which can be determined by the level of transcription and/or translation) could be one of the most significant effectors that determines enzymatic reaction activity, and subsequently metabolic flux. Analyses of the transcriptome of *P. putida* KT2440 revealed specific metabolic changes with physiological differences in cells in response to different carbon sources, such as sugars, polyol, and carboxylic acids (Nikel et al., 2014; Sudarsan et al., 2014). These data suggested a strong correlation between metabolic shifts (leaded to phenotypic variations) and gene expression profiles. Similarly, we have previously shown that during mcl-PHA biosynthesis by *P. putida* LS46, the PHA production profile (intra-cellular accumulation and monomer composition) varies with different growth conditions (different carbon sources, different C/N ratios, etc…see **Section 1.3.2**) suggesting different growth conditions induce metabolic shifts that favors or repress mcl-PHA biosynthesis (Sharma et al., 2012; Fu et al., 2014).

Such shifts suggested by altered gene expression patterns were explored in the previous 'Omics studies using octanoic or decanoic acid as sole carbon source (Poblete-Castro et al., 2012; Escapa et al., 2012). So far, metabolic analyses conducted by multi-level 'Omics analyses pertinent to mcl-PHA biosynthesis of *P. putida* have not been carried-out with non-fatty acid carbon sources. Therefore, we selected the by-products from biodiesel industry (particularly, waste glycerol) for our 'Omics studies. We

expected the systematic analysis of gene (transcriptome) and gene product (proteome) expression would facilitate identification of potential "competing" or "facilitating" pathways as targets for further metabolic engineering to enhance mcl-PHA biosynthesis by *P. putida* LS46 using low cost substrates.

1.8 Structure and Objectives of Thesis

1.8.1 Objectives of the Thesis

The **long-term objective** of this research is to enhance and optimize production of medium chain-length polyhydroxyalkanoates (mcl-PHA) by *Pseudomonas putida* LS46 using inexpensive carbon sources. The mcl-PHA biopolymers of different monomer composition, derived from *P. putida* LS46 grown with different carbon sources, will be used alone, or blended with other biodegradable polymers, to make this type of bioplastic commercially acceptable. The specific **short-term objectives** of this thesis are to: 1) Characterize and compare of mcl-PHA production from reagent gradient glycerol and industrial waste carbon sources (waste glycerol and waste free fatty acid) by *P. putida* LS46; 2) Study industrial waste carbon induced major cellular responses of *P. putida* LS46 on transcriptional and translational level; 3) Use quantitative transcriptomics and proteomics to study the metabolic responses of *P. putida* LS46 under two different mcl-PHA inducing conditions (achieved under cross-substrate and cross-growing stage).

1.8.2 Hypotheses

Hypothesis 1: Because of the metabolic versatility of *P. putida* for mcl-PHA biosynthesis (as reviewed previously in **Section 1.5.3**), mcl-PHA production and producing profile by *P. putida* LS46 are expected to be different in fatty acid-based versus non-fatty acid based cultures of *P. putida* LS46. Also, industrial waste carbon

sources (biodiesel-derived waste glycerol and waste free fatty acids) containing mostly glycerol and free fatty acids could be used as an inexpensive alternative carbon source for mcl-PHA production by *P. putida* LS46.

Hypothesis 2: Previous study has indicated that impurities (heavy metals) in biodiesel-derived waste glycerol severely compromised growth of *E. coli*, but not *P. putida* S12 strain (Verhoef et al., 2013). Analysis of the *P. putida* genome revealed defence systems for various types of heavy metal "contamination". Therefore, we hypothesize that *P. putida* LS46 will activate the expression of heavy metal resistance genes and gene products, and/or regulatory elements when growing on biodiesel-derived waste glycerol which consists various impurities. Using relative quantitative transcriptomics and proteomics, a snapshot of the genome responses to impurities of waste glycerol culture could be revealed.

Hypothesis 3: Different mcl-PHA production profiles and metabolic shifts will be observed in *P. putida* LS46 growing under following physiological conditions: 1) fatty acid versus glycerol culture at exponential phase; and 2) glycerol culture at stationary vs exponential. Metabolic shifts pertinent to mcl-PHA biosynthesis will be observed either across-substrates (mcl-PHA produced via fatty acid beta-oxidation versus glycerol metabolism and fatty acid *de novo* synthesis) or across growth phases (log-phase versus stationary phase or cell proliferation versus mcl-PHA synthesis and storage).

1.8.3 Structure of the Thesis

Chapter 1 is a literature review on PHA production. The chapter starts with introducing bioplastics in general, and narrows down to PHA, including descriptions of their application, the bacterial species that synthesize them, and the use of inexpensive carbon sources that could improve the economically feasibility of polymer production.

The discussion about the genetic and biosynthesis pathways for PHA production has been focused on mcl-PHA synthesis, as this is the focus of this thesis. Finally, global gene expression profiles pertinent to mcl-PHA biosynthesis studied in *P. putida* by various recent 'Omics technologies has been reviewed.

Chapter 2 presents the characterization of mcl-PHA synthesis from reagent grade glycerol and industrial waste streams (waste glycerol, waste free fatty acid). The kinetics of mcl-PHA biosynthesis from waste glycerol and waste free fatty acid were also studied. Chapter 3 describes the molecular responses of *P. putida* LS46 and its adaption to biodiesel-derived waste glycerol, which was studied by transcriptomics and proteomics. Chapter 4 describes the transcriptomic and proteomic analyses on metabolic shifts under various mcl-PHA accumulating versus non-accumulating conditions: across substrates and across growth phases. Chapter 5 highlights the results of the research in the context of resolving the research hypotheses, summarizes the conclusions, and suggests some future research directions.

Chapter 2

Characterization mcl-PHA biosynthesis by *P. putida* LS46

This chapter is based on the publication titled, "Evaluation of Medium-Chain Length Polyhydroxyalkanoates production by *Pseudomonas putida* LS46 using biodiesel by-product streams", by Jilagamazhi Fu[1], Umesh Sharma, Richard Sparling, Nazim Cicek, David B. Levin published in the. Canadian Journal of Microbiology, 2014, 60(7): 461-468.

2.1 Abstract

The overall objective of the work in this chapter was to enhance our understanding of the sustainability and cost-effectiveness of a bacterial fermentation system in which industrial by-product ("waste") streams can be converted into value-added products, such as mcl-PHA. Medium-chain-length polyhydroxyalkanoate (mcl-PHA) production by *Pseudomonas putida* LS46 was analyzed in shake-flask-based batch culture reactions, using pure chemical grade glycerol (PG), biodiesel-derived "waste" glycerol (WG), and biodiesel-derived "waste" free fatty acids (WFA). Cell growth, substrate consumption mcl-PHA accumulation within the cells, and the monomer composition of the synthesized biopolymers were monitored. The patterns of mcl-PHA synthesis in *P. putida* LS46 cells grown on PG and WG were similar, but differed from the pattern of mcl-PHA synthesis in cells grown with WFA. Polymer accumulation in glycerol-based cultures was stimulated by nitrogen-limitation and plateaued after 48 hours in both PG and WG cultures, with a total accumulation of 17.9 % dry cell weight (cdw) and 16.3 % cdw, respectively. In contrast, mcl-PHA synthesis was independent of nitrogen

concentration in *P. putida* LS46 cells culture with WFA, which accumulated to 29 % cdw. In all cases, the mcl-PHA synthesized consisted primarily of 3- hydroxyoctanoate (C8) dominated in WFA culture, and 3-hydroxydecanoate (C10) dominated in WG culture. The results from current study suggest that biodiesel by-product streams could be used as low costs carbon sources for sustainable mcl-PHA production.

2.2 Introduction

The cost of PHA production is driven by three factors: the type of substrate, microbial fermentation, and extraction of the polymers, with substrate cost being a major contributor to the overall cost of production (Posada et al., 2011). By-products from industrial biodiesel production, such as "waste" biodiesel-derived glycerol (WG) and biodiesel-derived "waste" free fatty acids (WFA), are potential substrates for large- scale mcl-PHA production. WG is especially attractive as feedstock, as it is available in large quantities and at relative low cost (Yazdani and Gonzalez 2007; Ong et al., 2012). Moreover, WG is, in general, unprofitable to purify for use as a component in the food, pharmaceutical, or cosmetics industries (Chatzifragkou and Papanikolaou 2012). Several studies have demonstrated scl- and/or mcl-PHA production from WG by various *Pseudomonas* species, including *Pseudomonas oleovorans*, *Pseudomonas corrugate* (Ashby et al., 2004), and *Pseudomonas putida* (Kenny et al., 2012). The WG used in these studies contains various amount of fatty acids (10% - 34%) and methanol as common "contaminants", which may contribute to different mcl-PHA production profiles reported in those studies. With greater efficiency on fatty acids removal during glycerol refining, WG with less fatty acids content is expected to be used as "standard waste" for further downstream utilization. Correspondingly, a

larger proportion of WFA removed from the first step of glycerol refining can be recycled or used, for example, for PHA production without further purification. Yet, no studies to date have explored the use of WFA as potential carbon source for mcl-PHA production.

This study compares the use of pure, reagent-grade glycerol (PG) with WG and WFA extracted from the glycerol refining process as the primary carbon sources using a novel strain of *P. putida* (strain LS46, described by Sharma et al., 2012), with the aim to enhance our understanding of overall sustainability and to determine the cost- effectiveness in developing a bacterial fermentation system in which industrial by-product (waste) streams can be converted into value-added products, such as mcl-PHA.

2.3 Material and methods

2.3.1 Bacterial source, culture medium, and growing conditions

Pseudomonas putida LS46, isolated from a local wastewater treatment plant in Winnipeg, Manitoba, Canada (Sharma et al., 2012), was used in all experiments, as the mcl-PHA synthesizing bacterium. Ramsay's medium (Ramsay et al., 1990)) plus various carbon sources were used to support cell growth and mcl-PHA production. Reagent-grade glycerol was purchased from Sigma-Aldrich (Missouri, USA). WG and WFA were obtained from the Renewable Energy Group LLC (Danville, Illinois, USA). The medium components were (per liter): 6.7 g of Na_2HPO_4-$7H_2O$, 1.5 g of KH_2PO_4, 1.0 g of $(NH4)_2SO_4$, 0.2 g of MgSO4-$7H_2O$, 60 mg of ferrous ammonium citrate, 10 mg of $CaCl_2$-$2H_2O$, 1 mL of trace element solution. Each liter of trace-element solution contained: 0.3 g of H_3BO_3, 0.2 g of $CoCl_2$-$6H_2O$, 0.1 g of $ZnSO_4$-$7H_2O$, 30 mg of $MnCl_2$-$4H_2O$, 30 mg of $NaMoO_4$-$2H_2O$, 20 mg of $NiCl_2$-$6H_2O$, and 10 mg of $CuSO_4$-

$5H_20$. All the experiments were conducted in 500 mL shaking flasks with culture volumes of 150 mL at 30 ^oC and 150 rpm mixing. All experimental shake-flasks containing various carbon sources were sterilized by autoclaving for 40 minutes (min) at 121 ^oC.

Before inoculation of the experimental shake-flasks, a single colony of *P. putida* LS46 was picked up and inoculated in 20 g/L of LB (Luria Broth) medium and incubated overnight. Subsequently, 1% (v/v) of the overnight culture was transferred into sub-cultures containing 30 g/L pure reagent grade glycerol (PG) or waste biodiesel-derived glycerol (WG), or 1% v/v (at about 9 g/L) of waste biodiesel-derived free fatty acids (WFA), as the sole carbon source, respectively. The cultures were grown until mid-log phase, and then 5% (v/v) of the each resulting culture was used as inoculum for the actual cultures containing 30 g/L PG or WG or 9 g/L WFA.

2.3.2 Analysis of WG and WFA

The glycerol content within the WG was based on the Certificate of Analysis provided by Renewable Energy Group LLC, which showed that WG contained the following (in mass %): glycerine, 80.2 %; methanol, 0.02 %; water, 7.7 %; ash, 7.0 %; and total fatty acids, 0.08 %. The glycerol content was further confirmed in our laboratory using a WATERS HPLC system (Milford, Massachusetts, USA) equipped with a Model 1515 pump, Model 2707 auto-sampler, and a Model 2414 refractive index detector (Waters). A 300 mm $\times$ 7.8mmresin-based column was used for separation (Aminex HPX-87H, Bio-Rad Laboratories, Mississauga, Ontario). Sulfuric acid (5 mmol/L) was used as the mobile phase at a rate of 0.6 mL/min. Gas chromatography was used to quantify the composition of the total fatty acid in the WG as described in Braunegg et al (1978) with modifications: 5 mL of WG was mixed with 5 mL of water

and vortexed. A 5 mL volume of chloroform was then added to the mixture and shaken for 10 min at room temperature. After shaking, 1 mL of organic layer (chloroform) was taken for methylation. Briefly, another 1 mL of chloroform containing 1 mg/mL benzoic acid as internal standard was added. Methanol (2 mL) in 15 % (*v*/*v*) sulfuric acid was added to the mixture, boiled for 5 h, and then cooled to room temperature. Deionized water (1 mL) was added, and the organic layer was collected for gas chromatography (GC) analysis. Samples (1 µL) were injected into the Agilent 7890A GC coupled with a split-splitless injector and a flame ionization detector with a split ratio at 1:10. Separation of target chemicals was achieved using a DB-23 capillary column (30 m × 320 µm × 0.25 µm; Agilent, California, USA). Helium was used as carrier gas at a flow rate of 1.78 mL/min. The oven ramping program was set as follows: initial temperature at 75 °C for 4 min, then from 75 to 250 °C with incremental increases of 20 °C/min, and a final hold at 250 °C for 4 min. A Supelco 37 component FAME mix (Sigma-Aldrich) was used as standard for peak identification and calculation of response factors for different fatty acids. Fatty acid peaks were quantified by comparing the peak area of the internal standard (1 mg/mL benzoic acid), and corrected with its response factor. Total fatty acid content was achieved by adding the individual fatty acid concentrations together.

WFA are removed during first step in glycerol refining, and these extracted free fatty acids can be recycled. The composition of the WFA was determined by methylating the free fatty acids followed by GC analysis. Briefly, 100 µL of the waste free fatty acid sample was mixed with 1mL of chloroform and 1mL of methanol with 15% (*v*/*v*) sulfuric acid. The mixture was incubated in a boiling water bath for 3 h. Then 1 mL of deionized, distilled water was added, and the organic layer was collected for GC analysis using the

same program as mentioned above. A Supelco 37 component FAME mix (Sigma-Aldrich) was used as standard for peak identification.

2.3.3 Cell growth and residual medium glycerol and amino acid content analysis

Growth of *P. putida* LS46 in different concentrations of glycerol was measured by optical density (OD) at 600 nm using a BioMate3 Spectrophotometer (Thermo Scientific, Madison, Wisconsin, USA). Colony-forming units (CFU) were also measured via serial dilutions as an alternative method to confirm cell growth. Residual glycerol in medium was measured using a WATERS Breeze 2 HPLC system (model MO915P795A) with the same method described above. PG was used an external standard for quantification purposes. Residual ammonia concentrations in the medium were measured using the Quikchem method 10-107-06-1-I by flow injection analysis (Lachat Instrument, Colorado, USA) as described in Yang et al. (2003). This analysis is based on the Berthelot Reaction (Bolleter et al., 1961) where ammonia reacts with alkaline phenol, and sodium hypochlorite to form indophenol blue. The absorbance of the reaction product is measured at 630 nm, and is directly proportional to the original ammonia concentration in the sample. A standard curve was prepared by analyzing different concentrations of ammonia sulfate (5 mg/L, 10 mg/L, 15 mg/L, 20 mg/L, and 30 mg/L), and the samples were first diluted whenever necessary.

2.3.4 Mcl-PHA quantification

Gas chromatography was used to characterize and quantify mcl-PHA production as described in Braunegg et al (1978) with modifications: 10 mL cultures were collected in 50 mL falcon tubes during time-point sampling, centrifuged at 4,000 x g for 10 min at room temperature, and washed with deionized water. The resulting wet cell pellets were dried in the oven at 60 °C overnight to be used in estimate calculations of cell dry

mass. To quantify the target mcl-PHA, 10 mg of cell mass from the dry cell pellet was mixed with 2 mL of chloroform containing 2 mg of benzoic acid as the internal standard and 2 mL of methanol with 15% (v/v) sulphuric acid in 15 mL conical tubes. Reagents and dried cell biomass were mixed thoroughly in the tubes and placed in a boiling water bath for 4 h. After boiling, the tubes were cooled to room temperature, and 2 mL of deionized water was added, resulting in the formation of an organic layer in the bottom of the tube, which was later extracted for GC analysis. The same GC method was used here as for fatty acid analysis. A mcl-PHA standard, containing a known amount of different mcl-PHA monomers (C6, C8, C10, C12, C14), purchased from Sigma-Aldrich, was methylated as described above and used for peak identification and for calculating response factors for each mcl-PHA monomer mcl-PHA monomer peaks were then quantified by comparing the peak area of internal standard (1 mg/mL benzoic acid), and corrected with its corresponding response factor. Total mcl-PHA content was achieved by adding the individual mcl-PHA monomer concentrations.

2.4 Results

2.4.1 Characterization of waste glycerol and waste free fatty acids

The glycerol content in the WG sample was analyzed by HPLC and indicated a glycerol concentration of 93.7 g/L for WG compared to 126 g/L for PG. The residual free fatty acid content in the WG sample was determined to be approximately 874 mg/L (0.087%), which is close to the data provided by Renewable Energy Group Inc. (0.08%). Therefore, we have calculated the free fatty acid content in the WG medium to be 27 mg/L. For WFA sample, fatty acids containing sixteen (C16) and eighteen (C18) carbons were the dominant fatty acid monomers. A summary of the monomer distribution in the

waste free fatty acid substrate is provided in **Table 2-1**.

2.4.2 Growth of *P. putida* LS46 on waste glycerol

Growth of *P. putida* LS46 on waste glycerol was determined by both optical density (OD_{600}) and plate counts (CFUs/mL). No lag-phase was observed in the growth curve, and the transition from log-phase growth to stationary phase occurred at approximately 16 hours post-inoculation (h pi). In microorganisms like *P. putida*, that synthesize mcl-PHA contained within intracellular occlusion bodies, the use of optical density to monitor cell growth is problematic because the accumulation of the PHA in cell granules contributes to light scattering. This can lead to higher than expected OD_{600} readings and thus over estimate cell growth (Eugenio et al., 2010). In this experiment, CFUs/mL were plotted against OD_{600} readings from the same time point samples in $\log_{10}$ scale, as illustrated in **Figure 2-1**. The relationship between OD_{600} measurements and CFUs was consistent, with both measurements indicating a transition from log-phase growth into the stationary phase at approximately 16 hours, and eventually reaching a plateau by 24 hours. Time points at 8, 12, 16, 24, and 30 hours were sampled to demonstrate the strength of the correlation between the two measurements, and the linear regression of OD_{600} versus CFU/mL was calculated, with an R^2 value of 0.70. However, the correlation between OD_{600} and CFU/mL was poor for time points after 30 hours (data not show). These results suggest that OD_{600} may be used as a relative measure that reflects cell growth and cell numbers over the course of exponential phase and early mcl-PHA accumulation stage.

Table 2-1. Major components of free fatty acids from waste fatty acids.

Free Fatty Acid	Peak Area (%)
C11:0	3.48
C14:0	1.39
C16:0	20.40
C16:1	1.56
C18:0	11.49
C18:1	35.43
C18:2	20.68
C18:3	1.88

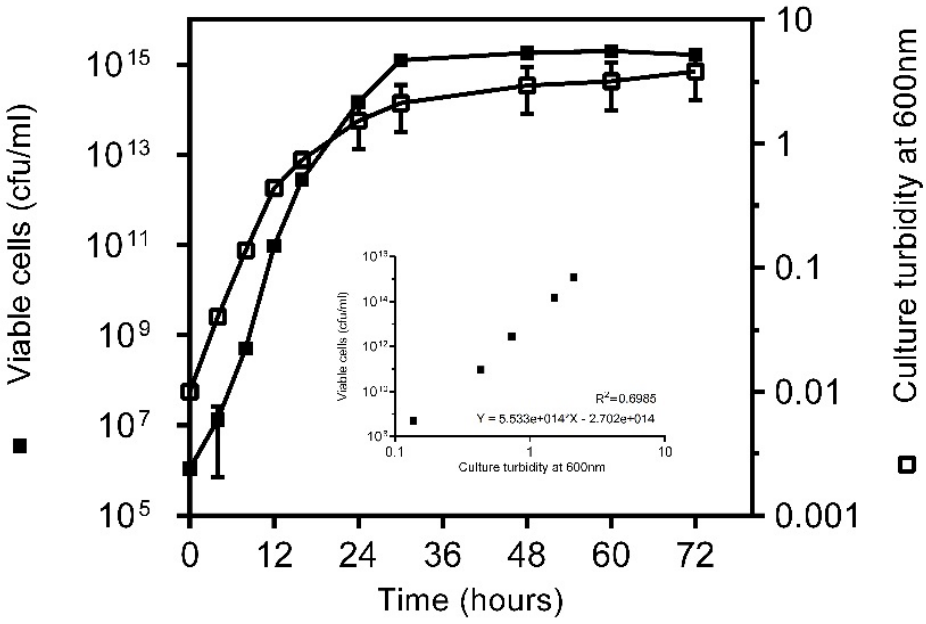

Figure 2-1. Comparison of cell growth measurements. Optical density **(**OD_{600}, open squares) was compared with cell plate counts of the colony forming units per mL (CFU mL^{-1}, solid squares). The correlation between OD_{600} and CFU mL^{-1} measurements was determined by linear regression analysis using 5 selected data points: t = 8, 12, 16, 24, and 30 h pi (insert). Note: data from OD_{600} readings and CFU were plotted in log_{10} scale.

2.4.3 Kinetic study of mcl-PHA synthesis by *P. putida* LS46 from pure and waste glycerol

In order to compare growth and mcl-PHA biosynthesis profiles of *P. putida* LS46 cultured in medium containing pure and waste glycerol (PG-cultures and WG-cultures, respectively), OD_{600}, dry cell biomass, carbon, nitrogen, and mcl-PHA production were tracked over time. An initial glycerol concentration of 30 g/L of was used for both PG- and WG-cultures to compare mcl-PHA production kinetics from the two substrates **(Figures 2-2)**. Cell growth, monitored by OD_{600} was similar for both PG and WG-cultures, reaching a plateau after 24 hours due to depletion of nitrogen. Within the first 12 hours of growth (during exponential phase) *P. putida* LS46 reached slightly higher OD_{600} (0.89 versus 0.76, respectively), and consumed more nitrogen (138.3 mg/L versus 110 mg/L, respectively), in WG-cultures compared with PG-cultures. Glycerol consumption was also greater in WG-cultures than in PG-cultures (1.12 g/L versus 0.98 g/L, respectively) at 12 hours. Finally, although we did not track the fatty acid consumption in WG-cultures over time, no residual free fatty acids could be detected at 12 hours h pi (post inoculation) (initial concentration of the free fatty acids in the WG-cultures was 27 mg/L).

P. putida LS46 did not completely consumed all the available glycerol in the medium of either the PG- or WG-cultures. In fact, only about one third of the glycerol content had been consumed at the end of the experiment (72 h pi). Overall, biomass (measured by dried cell pellet) continued to increase after nitrogen depletion (24 to 48 hours), which was attributed to the production and accumulation of mcl-PHA in the cells. After 48 hours, both the biomass production and corresponding mcl-PHA production rate decreased substantially. The amounts of mcl-PHA synthesized and accumulated in

P. putida LS46 cells in PG- and WG-cultures, were very comparable. The mcl-PHA content reached 17.9 % ± 2 cdw with PG-cultures and 16.3 % ± 1.9 cdw with WG-cultures at 72 h pi. The substrate specific yields of mcl-PHA (g PHA produced per g glycerol consumed) during the accumulation stage (between 18 and 48 h pi) were 0.12 ± 0.013 glycerol in PG-cultures and 0.087 ± 0.03 in WG-cultures. The conversion efficiencies of substrate to mcl-PHA (g mcl-PHA/g substrate) were 0.21 g mcl-PHA/g of glycerol for pure glycerol, and 0.13 g mcl-PHA/g of glycerol for waste glycerol. Nitrogen-limitation triggered mcl-PHA synthesis with either WG or PG as the carbon source. Although some minimal level of mcl-PHA accumulation was observed at late exponential phase, significant production occurred after nitrogen-depletion. Also, a clear reduction in mcl-PHA production rate was observed after 48 h pi despite the availability of glycerol. The monomer distribution of mcl-PHA synthesized by *P. putida* LS46 in PG- and WG-cultures were also similar (**Table 2-2**), with 3-hydroxydecanoate (C10 monomers) and 3-hydroxyoctanoate (C8 monomers) as the dominant subunits.

A

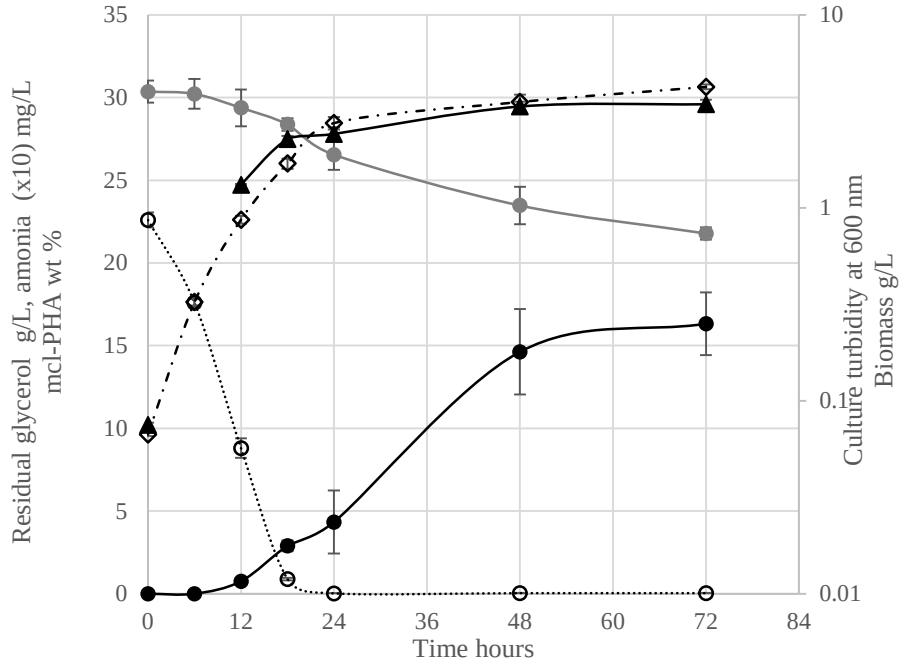

B

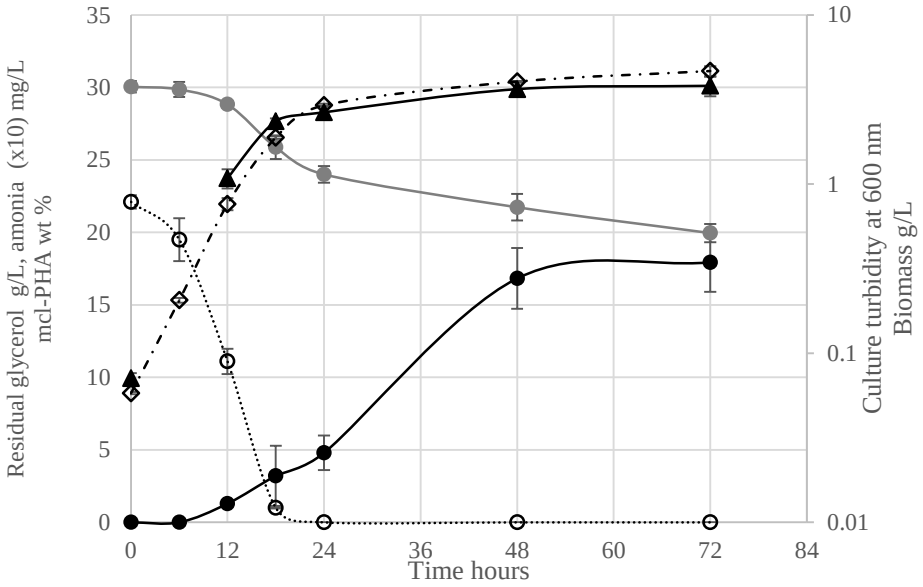

Figures 2-2. Characterization of cell growth and mcl-PHA production by *P. putida* LS46

in cultures containing pure glycerol (**A**) or waste glycerol (**B**). Open diamond (◊) with dashed line, OD measurement; Solid triangle (▲) with solid line, biomass measurement; Solid gray circle ( ) with solid line, residual glycerol concentration. Open circle (○) with dashed line, residual ammonia concentration; Solid circle (●) with solid line, mcl-PHA production overtime.

Table 2-2. Production and monomer composition of mcl-PHA synthesized by *P. putida* LS46 cultured with PG, WG, and WFA.

Samples	Biomass ($g\ L^{-1}$)	mcl-PHAs (% cdw)	3-hydroxy-alkanoaic acid (mole %)							
Pure and waste glycerol			**C6**	**C8**	**C10**	**C12**	**C14**	**C9**	**C12:1**	**C14:1**
PG 24 hours	2.65 ± 0.3	4.79 ± 1.2	2.8 ± 0.85	27.3 ± 0.78	61.3 ±0.43	2.33 ± 0.41	0.70 ± 0.15	nd	5.34 ± 0.46	nd
PG 48 hours	3.64 ± 0.3	16.82 ± 2.1	2.58 ± 0.25	28.9 ± 0.77	61.1 ± 0.84	1.94 ± 0.79	0.62 ± 0.30	nd	4.84 ± 0.11	nd
PG 72 hours	3.8 ± 0.5	17.93 ± 2.0	2.55 ± 0.18	30.8 ± 0.29	59.3 ± 1.2	2.03 ± 0.38	0.41 ± 0.08	nd	4.83 ± 0.07	nd
WG 24 hours	2.42 ± 0.2	4.34 ± 1.9	3.37 ± 0.31	28.3 ± 2.1	59.4 ± 0.5	2.64 ± 0.26	0.94 ± 0.12	nd	5.36 ± 0.92	nd
WG 48 hours	3.35 ± 0.2	14.62 ± 2.6	4.78 ± 0.44	29.1 ± 1.50	58.9 ± 1.3	2.15 ± 0.52	0.52 ± 0.23	nd	4.55 ± 1.65	nd
WG 72 hours	3.44 ± 0.2	16.32 ± 1.9	3.82 ± 0.56	31.7 ± 1.55	56.9 ± 2.05	2.16 ± 0.12	0.7 ± 0.07	nd	4.67 ± 1.29	nd
Waste free fatty acids			**C6**	**C8**	**C10**	**C12**	**C14**	**C9**	**C12:1**	**C14:1**
WFA 12 hours	3.22 ± 0.06	11.75 ± 1.77	4.68 ± 0.17	58 ± 0.96	27.3 ± 0.88	4.76 ± 0.18	1.13 ± 0.03	2.47 ± 0.01	1.65 ± 0.03	2.18 ± 0.14
WFA 24 hours	4.57 ± 0.2	16.79 ± 2.42	4.57 ± 0.07	57.2 ± 0.17	26.4 ± 1.02	6.34 ± 0.44	0.88 ± 0.07	1.90 ± 0.51	2.67 ± 0 .42	1.73 ± 0.2
WFA 36 hours	4.72 ± 0.27	25.08 ± 2.85	4.71 ± 0.14	56.44 ± 0.94	28.2 ± 0.7	6.28 ± 0.17	0.78 ± 0.12	1.13 ± 0.20	2.39 ± 0.49	1.73 ± 0.39
WFA 48 hours	5.25 ± 0.35	28.82 ± 1.01	4.77 ± 0.19	56.9 ± 0.12	27.7 ± 0.35	6.12 ± 0.04	0.75 ± 0.12	0.96 ± 0.31	2.72 ± 0..05	1.86 ± 0.35
WFA 72 hours	5.32 ± 0.26	29.93 ± 2.57	4.59 ± 0.31	56.39 ± 0.32	27.85 ± 0.33	6.27 ± 0.17	0.69 ± 0.03	0.77 ± 0.03	2.11 ± 0.12	1.34 ± 0.22

Note: PG, pure, reagent grade glycerol; WG, waste crude biodiesel-derived glycerol; WFA, free fatty acids extracted from crude biodiesel-derived glycerol; C6, 3-hydroxyhexnoic acid; C8, 3-hydroxyoctanoic acid; C9: 3-hydroxynonanoic acid C10, 3-hydroxydecanoic acid; C12, 3-hydroxydodecanoic acid; C14, 3-hydroxytetradecanoic acid. C12:1 and C14;1: unsaturated 3-hydroxydodecanoic acid and 3-hydroxytetradecanoic acid. nd: not detected.

2.4.4 Kinetic study of mcl-PHA synthesis by *P. putida* LS46 from waste free fatty acids

Cell growth and mcl-PHA synthesis by *P. putida* LS46 in cultures containing waste free fatty acids was different from growth and mcl-PHA synthesis in glycerol-based cultures. Due to the turbidity of the cultures containing WFA, OD_{600} was not an effective method of monitoring cell growth. Therefore, cell growth was monitored via biomass production (dry cell mass) instead. We have observed mcl-PHA production (7.54 wt %) at 0 hour in WFA culture, which was carry-over from the inoculant derived from the WFA subculture. When 9 g/L of waste free fatty acid was used as the sole carbon source, significant production of mcl-PHA was observed as early as 12 h pi. **Figure 2-3** shows both cell growth and mcl-PHA plateaued by 48 hours. Final mcl-PHA accumulation was 29.9 % cdw at 72 h pi. The monomer composition of mcl-PHA synthesized in WFA-cultures was also different from the monomer composition of mcl-PHA synthesized in glycerol- based cultures: 3-hydroxynonanoate (C9 monomer) was detected as a sub-unit in mcl- PHA polymers synthesized by *P. putida* LS46 in WFA-based cultures. Mcl-PHA synthesized in glycerol-based cultures had a greater mole % of 3-hydroxydecanoate (C10 monomers) than the 3-hydroxyoctanoate (C8 monomers), whereas mcl-PHA synthesized in free fatty acid-based cultures contained a greater mole % of C8 monomers than C10 monomers (**Table 2-2**).

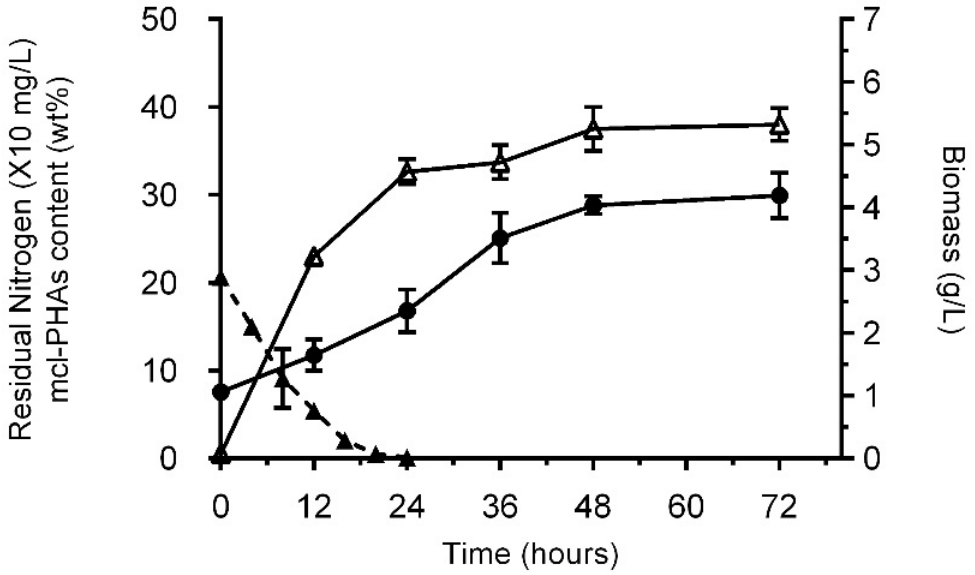

Figure 2-3. Characterization of cell growth and mcl-PHA production by *P. putida* LS46 in cultures containing waste free fatty acids (WFA). Δ (open triangles with solid line), biomass concentration; ● (solid dots with solid line) mcl-PHAs production; ▲ (solid triangles with dashed line), residual nitrogen concentrations.

2.5 Discussion

In this study, the components that make up the ash in WG (7% of the mass, based on the REG Glycerin-80 "Certificate of Analysis" provided by Renewable Energy Group Inc.) were not measured in detail. However, several studies have suggested that sodium salt is a major component of ash in crude glycerol, along with metals such as iron, copper, molybdenum, zinc, and trace amounts of other metals (Cavalheiro et al., 2009; Verhoef et al., 2013). The presence of impurities of crude glycerol had a negligible effect on cell growth of *P. putida* S12, compared to *Escherichia coli* and *Cupriavidus necator*, which were shown to be less tolerant to crude glycerol (Cavalheiro et al., 2009; Verhoef et al., 2013). *P. putida* is well known for its ability to tolerate diverse and toxic compounds, including heavy metals, aromatic compounds, and solvents by using cell surface efflux pumps and corresponding degradation pathways (Weber et al., 1993; Nelson et al., 2002; Jiménez et al., 2002; Cánovas et al., 2003; Chen et al., 2005). Such abilities may thus reduce the negative impact that salts impose to the cell, which would otherwise lead to reduced cell growth activity and potentially lower PHA production.

Higher OD_{600} readings at early growth of the *P. putida* LS46 in WG compare to PG were observed. This may be a result of the residual free fatty acids in the WG sample, although the free fatty acids were present in low concentrations in the (27 mg/L). *P. putida* KT2440 was observed to grow faster on co-substrates (fatty acid and glycerol) than on glycerol alone (Escapa et al., 2013). Studies have also suggested that fatty acids or other growth precursors (glucose, fructose) may act as an inducer of the glycerol uptake system, as GlpK (glycerol kinase) activity increased about 15 times in the presence of the inducers (Saharan et al., 2010; Escapa et al., 2013). Nitrogen-

limitation was requirement for active mcl-PHA accumulation in glycerol-based cultures (both PG and WG), but not in fatty acid-based cultures (WFA). PHA are storage compounds for carbon, energy, and reducing equivalents, and it is well known that synthesis of mcl-PHA in *P. putida* is triggered by nutrition-limitation from carbon sources that are structurally unrelated to PHA polymer subunits, such as glucose and glycerol. However, mcl-PHA could be synthesized acrtively under the exponential phase in fatty acid-based cultures (Sun et al., 2007). This may also explain the observed mcl-PHA carry-over from the WFA subculture only, not in glycerol-based subculture. Both fatty acid oxidation and *de novo* synthesis pathways are used by *P. putida* to synthesize the mcl-PHA precursors used by mcl-PHA cluster genes, and expression levels of these genes may change, depending on the carbon substrate consumed. Analyses of *pha*C1, *pha*C2, and *pha*J4 showed that transcription of these genes is up-regulation in fatty acid cultures compared to glucose cultures (Wang and Nomura, 2010). Furthermore, transcription of the *pha*D gene, which encodes a transcriptional activator of *pha* biosynthesis cluster genes, was shown to be activated in *P. putida* KT4220 cells in fatty acid cultures (De Eugenio et al., 2010a). On the other hand, transcription of *pha*G, the gene, known to code the enzyme (Acyl-transferase) responsible for mcl-PHA biosynthesis from fatty acid *de novo* synthesis, was up-regulated in response to nitrogen-limitation (Hoffmann and Rehm, 2004, Poblete-Castro et al., 2013). More recent work has identified a medium-chain-fatty- acid CoA-ligase from *P. putida* KT2440, and shown that it plays a role in converting 3-hydroxyalkanoic acid into 3-hydroxyacyl-CoA for mcl-PHA biosynthesis under nitrogen-limitation (Wang et al., 2011). However, the mechanisms by which cells regulate gene and gene product expression in response to imbalances in carbon

and nitrogen availability are not yet fully understood. Some of these have been tested by monitoring mRNA and protein expression levels under various mcl-PHA permissive conditions, and will be discussed in detail in Chapter 4.

The monomer composition was also different in mcl-PHA polymers synthesized by *P. putida* LS46 grown in glycerol-based cultures versus fatty acid-based cultures. Synthesis of mcl-PHA by *Pseudomonas* species is carried out by class II PHA synthases, which are genetically different from class I PHA synthases, which synthesize scl-PHA (Rehm, 2003). The monomer composition of PHA polymers is, therefore, highly dependent on the substrate specificity of the PHA synthase enzyme encoded. *Pseudomonas* bacteria, which synthesize mcl-PHA, have two PHA synthase enzymes: PhaC1 and PhaC2. PhaC1 has a strong preference for medium chain length (mcl-) 3-hydroxyacly-CoAs, with highest affinity towards 3-hydroxydecanoyl-CoA (C10) and 3-hydroxyoctanoyl-CoA (C8).

Substrate type is an additional driving force for altering mcl-PHA monomer composition in *P. putida*. 3-hydroxydecanoate (C10) is the dominate monomer in most mcl-PHA synthesized by *P. putida* grown on carbon sources that are structurally un-related to PHA monomers (glucose and glycerol, for example). In contrast, 3-hydroxyoctanoate (C8) is the most abundant monomer (> 80 mole %) in mcl-PHA synthesized by *P. putida* when octanoic acid is used as the sole carbon source. Moreover, C8 monomers are also the dominate monomer in mcl-PHA synthesized when long-chain C16 and C18 fatty acids are used as the carbon source (De Eugenio et al., 2010a; Liu et al., 2011; Gumel et al., 2012; Poblete-Castro et al., 2012). Results reported in this study were consistent with these observation. Production of mcl-PHA polymers containing C9 monomers by *P. putida* LS46 grown in WFA-cultures may due to the fact that WFA has

fatty acids with odd carbon numbers (Sun et al., 2007a). Indeed the WFA contains 3% C11:0 (**Table 2-1**). Therefore, in addition to substrate specificity of PhaC1, observed differences in mcl-PHA monomer composition derived from two fatty acid metabolism pathways (synthesizing and degradation) may be also depended on substrate specificity of PHA monomer supplying enzymes. Comparatively, PhaC2 has broader substrate specificity towards both short chain length and medium chain length PHA (Chen et al., 2004). However, compared to PhaC1, PhaC2 appears to make a minor contribution to mcl-PHA production in *P. putida* (Hein et al., 2002; Kim et al., 2006; Ren et al., 2009b).

In the current study, despite the availability of excess carbon (glycerol) in the medium, the rate of mcl-PHA synthesis was significantly reduced between 48 and 72 h pi compared with the rate between 18 and 48 h pi, suggesting that the mcl-PHA synthesis machinery was not operating at maximal capacity. In late stationary phase, nitrogen-limitation and sometimes phosphate-limitation, has been shown to trigger mcl- PHA synthesis by *P. putida* growing on glucose (Chanprateep, 2010; Sharma et al., 2012), but the rate of mcl-PHA synthesis decreases over time, despite excess carbon availability. This was also reported in studies of scl-PHA production (Wang and Lee, 1997; Cavalheiro et al., 2009; Follonier et al., 2011). This behaviour may be attributed to reduced metabolic activity due to the large amount of storage polymer present within the cell (Kim et al., 1994). High PHA yields have been shown to decrease intercellular ATP, which may in turn affect many cellular metabolic processes leading to lower metabolic activity (Poblete-Castro et al., 2012). In such cases, repression of the TCA cycle and reorganization of the terminal oxidase in electron transport chain were observed during mcl-PHA biosynthesis (Poblete-Castro et al., 2013). Furthermore, given the fact that

glycerol has to be converted into glycerol-3-phosphate with the aid of ATP for mcl-PHA biosynthesis, reduced ATP would hinder mcl-PHA accumulation when glycerol is the sole carbon source (Chee et al., 2010; Escapa et al., 2013).

Chapter 3

Effects of impurities in biodiesel-derived glycerol on growth and expression of heavy metal ion homeostasis genes and gene products in *P. putida* LS46.

This chapter is based on the published manuscript titled, "Effects of impurities in biodiesel-derived glycerol on growth and expression of heavy metal ion homeostasis genes and gene products in *P. putida* LS46", by Jilagamazhi Fu, Parveen Sharma, Vic Spicer, Oleg V. Krokhin, Xiangli Zhang, Brian Fristensky, John A. Wilkins, Nazim Cicek, Richard Sparling, and David. B. Levin in the Journal of Applied Microbiology and Biotechnology, 2015, 99(13): 5583-5592.

3.1 Abstract

Biodiesel-production derived waste glycerol (WG) was previously investigated as potential carbon source for medium chain length polyhydroxyalkanoate (mcl-PHA) synthesis by *Pseudomonas putida* LS46. In this study, we evaluated the effect of impurities in the biodiesel-derived waste glycerol on *P. putida* LS46 physiology during exponential growth, and corresponding changes in transcription and protein expression profiles compared with cells grown on pure, reagent grade glycerol. High concentration of metal ions, such as Na+, and numbers of heavy metals ion, such as copper, ion, zinc, was detected in biodiesel-derived waste glycerol. 'Omics analysis from the corresponding cultures suggested altered expression of genes involved in transport and metabolism of ammonia and heavy metal ions. Expression of three groups of heavy metal homeostasis genes was significantly changed (mostly up-regulated) in waste glycerol cultures, and included: copper-responded cluster 1 and 2

genes primarily containing *cus*ABC, two copies of *cop*AB and heavy metal translocating P-type ATPase; Fur-regulated, TonB- dependent siderophorereceptor; and several cobalt/zinc/cadmium transporters. Expression of these genes suggests regulation of intra-cellular concentrations of heavy metals during growth on biodiesel-derived glycerol. Finally, a number of genes involved in adapting to, or metabolizing free fatty acids and other non-heavy metal contaminants, such as Na^+, were also up-regulated in *P. putida* LS46 grown on biodiesel-derived glycerol.

3.2 Introduction

Substrate cost for microbial production of mcl-PHA (biopolymer) may be reduced by using low cost or negative-value feed stocks derived from industrial by-product streams, and crude biodiesel-derived glycerol has been investigated as a low-cost substrate for mcl-PHA production (Kenny et al., 2012). However, while the use of inexpensive carbon sources derived from industrial waste streams is attractive, it may be problematic because of impurities that may affect cell growth and/or polymer yield.

In general, while the components of crude biodiesel derived glycerol may vary from plant to plant, the two major impurities are residual methanol and sodium or potassium soaps derived from the catalysts used in transesterification. In addition, biodiesel derived glycerol may contain residual free fatty acids, non-reacted mono-, di-, and triacylglycerides, and residual fatty acid methyl esters (Chatzifragkou and Papanikolaou 2012).Various elements such as, calcium, potassium, phosphorus, magnesium, sulphur may also be present in the waste glycerol, and although the biodiesel production process does not include any heavy metals, the oil feedstock used may contain heavy metals in various amounts (Pyle et al., 2008; Thompson and He 2006; Verhoef et al., 2014). Impurities in biodiesel-derived glycerol, such as heavy metals, may be toxic to

cells or toxic at concentrations above a certain concentration. The problem may be exacerbated by the greater substrate loading and high cell density required for large-scale industrial production of mcl-PHA. On the other hand, they could potentially serve as additional nutrients (carbon and minerals) that benefit cell growth (Escapa et al., 2013; Verhoef et al., 2014). In either case, the optimal intracellular heavy metal concentration is important.

P. putida (mcl-PHA producer) is well known for its genome potential of resistance to heavy metals, solvents, and antibiotics (Cánovas et al., 2003; Wu et al., 2011; Sharma et al., 2014) making it good candidate for biopolymer production using industrial by-products, such as waste glycerol. However, the analysis of the potential toxic compounds in an industry derived waste glycerol and their potential effect on *P. putida* in term of gene and gene products expression profile are generally limited. In this study, we have evaluated the major "impurities" in the biodiesel derived waste glycerol, and the gene expression responses of *P. putida* LS46 at transcriptional and/or translational level when exposing to these "contaminants". Waste glycerol induced significant expression changes on genes putatively involved in cell defense/adaptation mechanisms, even though previous study (**Chapter 2**) showed a similar growth pattern of *P. putida* LS46 during the exponential growth on pure versus waste glycerol cultures. These findings may help to identify potential molecular targets that are essential for detoxification when the strain is cultured with the industrial waste glycerol.

3.3 Material and Method

3.3.1 Culture medium and growing condition

P. putida LS46 was isolated from a local wastewater treatment plant in Winnipeg,

Manitoba, Canada. The strain was deposited with the International Depository Authority of Canada (IDAC) at the National Microbiology Laboratory, Health Canada Culture Collection (NML-HCCC), WDCM number 840 (Sharma et al., 2012). Pure, reagent grade glycerol (PG) was purchased from Sigma-Aldrich (Sigma-Aldrich, MO, USA). Biodiesel production-derived waste glycerol (WG) was obtained from the Renewable Energy Group LLC (Danville, Illinois, USA). Ramsay's medium (See medium components in Chapter 2 at section: 2.3.1) was used as culturing medium. Pure glycerol (PG) (Sigma-Aldrich, Missouri, USA) or waste glycerol (WG) was added to the growth medium to give equivalent final glycerol concentration of 30 g/L, respectively. Therefore, both cultures had the same initial concentration of glycerol (30 g/L) at the time of inoculation with *P. putida* LS46. All experiments were conducted in 500-mL shaking flasks, with culture volumes of 150 mL, and were incubated at 30 °C, with mixing at 150 rpm. All flasks containing culture medium with either PG or WG were sterilized by autoclaving for 45 min at 121 °C before inoculation. Before each set of experiments, a single colony of *P. putida* LS46 was picked from a streak plate and used to inoculate 25 mL of Luria-Bertini (LB) medium in a 250-mL flask and incubated overnight at 30 °C. Subsequently, 1 % (v/v) of the culture was transferred into different subcultures containing 30 g/L glycerol from PG or WG as sole carbon sources. Mid-log grown pre- culture was then used to feed the test culture containing 30 g/L PG or WG with the volume of inoculum given an initial OD600 at 0.05. Cell growth was monitored via a Thermo Fisher Biomate 3 spectrophotometer (CAT335905) at 600 nm (OD600). For RNA-seq and proteomics analyses, both RNA and protein samples were taken at mid-log phase, about 8-h post inoculation (h pi), at an OD600nm of 0.58 and 0.50 of WG and PG cultures, respectively.

3.3.2 Compositional characterization of industrial waste glycerol

Glycerol and residual free fatty acid content in WG was previously described (Fu et al., 2014). The metal ion content in WG was performed by CCD simultaneous inductively coupled plasma-optical emission spectroscopy (ICP-OES; Model: VISTA MPX; Varian Inc.) in samples containing WG in sterile distilled water at three concentrations: 1 % (10 g/L), 3 % (30 g/L), and 5 % (50 g/L). These concentrations of WG were prepared separately, rather than from a serial dilution. Pure reagent grade glycerol at 3 % (30 g/L) in distilled water was used as a control (blank) sample.

3.3.3 Transcriptomics and Proteomics

3.3.3.1 RNA isolation and RNA sequencing

Two biological replicates were used for each RNA sample. Five (5) mL of cell culture were collected and centrifuged at 4,000 x g, to pellet the cells. Total RNA was extracted from the cell pellets using a PureLink® RNA Mini Kit (Ambion, Life Technologies, USA). Isolated RNA samples were treated with DNase to remove DNA contamination. The concentration of RNA was determined using a Nanodrop 1000 spectrophotometer (Thermofisher, USA), and RNA integrity was analyzed by electrophoresis using an Experion system (BioRad, USA). RNA samples were shipped to and sequenced by the Genome Quebec Innovation Centre at McGill University (Montreal, Quebec) for creation of cDNA libraries and RNA-seq using the Illumina HiSeq 2000 platform.

3.3.3.2 Protein isolation, digestion, and peptide purification

Culture medium (40 mL) were collected, centrifuged at 4,000 x g, resuspended with phosphate buffer solution (PBS) (0.144 g/L KH_2PO_4; 9 g/L NaCl; 0.795 g/L

Na_2HPO_4- $7H_2O$, pH 7.4) and centrifuged again at 4,000 x g. The PBS wash was repeated once more and the cell pellets were then stored at -80 ^oC for later use. When all samples were collected, frozen pellets were re-dissolved in 4 mL distilled-deionized (DI) water, of which 1 mL was used for total protein isolation. One mL of lysis buffer (8 % of sodium dodecyl sulphate, 200 mM dithiothreatol, 200 mM Tris-HCl, pH 7.6) was added to each 1 mL sample of resuspended cell pellet and solution were mixed thoroughly by pipetting. The solutions were transferred to 10 mL falcon tubes, which were then place in a boiling water bath for 5 minutes (min). After boiling, the samples were sonicated for 30 seconds, and then centrifuged at 16,000 x g at room temperature. 10ul of supernatant was subjected to SDS-PAGE gel (**S1 Figures A**). One mL of each supernatant was then transferred into an Eppendorf tube.

One (1) mL of total protein was transferred to an Amicon Ultra-15 10K filter device (Millipore, Billerica, MA), which followed the purification, digestion, and subsequent peptide purification steps as mentioned in Gungormusler-Yilmaz *et al* 2014 (Gungormusler-Yilmaz et al., 2014) with little modification: the typsin to protein ration at 1:100 instead of 1:50. The purified peptides were lyophilized and re-dissolved in 0.1 % formic acid in water for subsequent 1D-LC-MS/MS analysis.

3.3.3.3 RNA identification and quantification

Identification: Transcriptomic analysis used an in-house alignment and quantitation engine using the R2 element of the Illumina paired-end read sets. Our algorithm detects exact 100-mer read alignments only, relying on the high quality of the HiSeq data to give sufficient counting statistics. Additional filtering steps applied was: RNAseq values were accepted only if there were at least two alignment counts per gene.

P. putida LS46 genome was used as reference for alignment.

Quantification: Transcripts were quantified by expressing the sum of all 100-mer RNA alignments per gene. Values were transformed to a log2 scale for comparison and differential analysis.

3.3.3.4 Protein identification and quantification

Identification: ABSciex TripleTOF 5600 TOF-MS system (Applied Biosystems, Foster City, CA) equipped with a Nano-sprayIII ionization source was used for data acquisition. Each acquisition cycle included 250 ms survey MS acqusition (m/z 400–1500) and up to twenty 100 ms MS/MS measurements on the most intense parent ions (300 counts/s threshold, +2 to +4 charge state, m/z 100–1500 mass range for MS/MS). Two hours runs for each of biological replicates of every experimental samples. Raw spectra files were converted into 200 Mascot Generic File (MGF) format for peptide/protein identification. Peptides were identified from the observed MS/MS spectra using an in-house GPU peptide search engine (McQueen et al., 2012) from a single missed cleavage tryptic database derived from the *P. putida* LS46 genome annotation with only the fixed post-translational modification of the carbamidomethlyation of cysteine residues (+57.021 Da) applied. The GPU search engine settings were 20 ppm on parent mass ions and a 0.2 Da window on fragment ions respectively and peptides with expectation log(e) $\leq$ -1.5 were reported. Proteins with only a single member peptide were excluded from the report, and subsequent analyses.

Quantification: Total ion counts (TIC), which are the sum of all CID (collision induced dissociation) fragment intensities of member peptides, were used for protein quantitation. Values were transformed to a log2 scale for comparison and differential analysis, and differential analysis was constructed by subtracting sets of log2 protein

intensity values derived from the comparing conditions. Note that by plotting these differential expression value in histogram, each set of detected proteins forms a three-lobed histogram, with the central population of data points containing proteins observed in both states (e.g the two comparing condition), while the outer histograms contain proteins observed only in one state, but not the other. While these are manifestations of the instrument's information-directed acquisition (IDA) detection limits, and do not represent the absolute presence or absence of a protein in a sample. Thus, in order to conduct comparative analysis, a simple algorithm has been developed to normalize three population into single population. At last, proteins that only observed in one biological replicate of each physiological condition have been excluded from the subsequent analysis. Note these two additional steps prior to the data analysis were only applied to proteomics analysis, due to relative deeper coverage observed for RNAseq data.

3.3.4 'Omics data analysis and validation

Analysis: Detailed comparative analyses of the expression data gathered from the specific experiments was conducted using an in-house Omics data analysis system called "UNITY" (Gungormusler-Yilmaz et al., 2014). The analysis operations in order were as follows: 1) The overall number of identified protein and RNA molecules were calculated: 2) The overall correlation between transcriptomic and proteomic log2 expression values were observed; 3) Differential expression values were calculated: a) cross-state: Z = (state A – state B); and b): among biological replicates, where R = intra biological replicate differences; 4) A quality control of biological variation signals between any two comparison groups (cross-state) vs system noise among biological replications (intra-replicative viability) were conducted; 5) Transformation of different populations into

final Znet scores as descripted in (Verbeke et al., 2014) (The Znet score for Protein was defined as Pnet, and Rnet for RNA as easily presentation) for relative expression analysis cross-state was conducted. The cutoff scores of ± 1.65 were used to represent outermost 10% of the population defined as an asymmetry (up-regulated or down-regulated) of expression of RNA and protein relative to the expression profiles of the overall population; Thus, gene having a final normalized Znet score (e.g. Pnet for protein and Rnet for RNA) over 1.65 or below -1.65 will be considered as significant up or down regulated under two specific comparing conditions (e.g Pure glycerol vs Waste glycerol at exponential phase). 6) Each gene's set of 'Omics measurements were mapped into Clusters of Orthologous Groups of proteins (COG) for global condition-specific expression analysis (Tatusov et al., 2000).

Validation: Correlation of the RNA and Protein expression data under the tested experimental condition was done by plotting the log2 expression values of transcriptomic and proteomic data. The dynamic range of Log2 expression values was > 4 and > 11 for RNAseq and proteomic analyses, respectively. Furthermore, a simple function was developed to evaluate the statistical significance of a two-state two-replicate dataset on a protein-by-protein basis, which computes an overall measurement of the system quality as the ratio of the mean of the standard deviations of the cross state and intra-replicate populations. This is known as the 'system to noise' (S/N) ratio. On an individual protein level, the S/N is the ratio of the vector magnitudes (protein expression levels) across the experimental states and intra-replicate normalized values, scaled by the overall system S/N values. A simple Monte-Carlo Model was used to derived functions relating 'false discovery rates' (FDR) to a defined S/N cutoff: all proteins with a S/N > 2.8 were found to have a FDR of 10% or less. Thus, for a protein with a Pnet (differential

expression) value, if it (the protein) has a S/N ratio over 2.8, then the analysis of this protein with the Pnet value is statistically significant. In other words, this function allowed us to reliably access smaller differential expression values across experimental states, provided the variation of their corresponding intra-replicate measurements were sufficiently small.

3.3.5 Bioinformatics

Alignments and phylogenetic analyses of sequences for gene cluster analyses was carried out by concatenating each protein sequence of the cluster prior to alignment, using MEGA 6 (Tamura et al., 2011). The evolutionary history was inferred using the Neighbour-joining method with evolutionary distances calculated via the Poisson correction (Zuckerkandl and Pauling 1965). Alignment gaps were deleted via pair-wise sequence comparisons and clusters grouped using the bootstrapping method (Felsenstein 1985), where 500 replicates were taken to represent the evolutionary history of the taxa analyzed. The view of conserved neighborhood orthology of selected genes was done under gene neighborhood comparisons function integrated within the IMG-ER (Integrated Microbial Genomes: Expert Review) platform (Victor et al., 2012). Subcellular location of proteins was predicted by Transportation Classification Database (Saier et al., 2014) integrated with IMG-ER platform.

3.3.6 Data deposit

Raw sequencing data and gene expression abundance value of the RNAseq analysis were deposited in NCBI Sequence Read Archive (SRA) through Gene Expression Omnibus (GEO) with accession number: GSE65029. In addition, the gene expression abundance and differential gene expression values derived from the

'Omics studies were provided in supplemental materials (**S1 Table** and **S2 Table, A).**

3.4 Results

3.4.1 Characterization of biodiesel-derived glycerol (glycerol, free fatty acids, biologically important ions, and metal ions)

Waste glycerol contains approximately 76 % glycerol and 800 mg/L of free fatty acids (Fu et al., 2014), which are residual fatty acids from the upgrading of glycerol bottoms generated during biodiesel production. In addition, we determined the concentrations of both biologically important ions and metal ions present in WG, and found high concentrations of Na, Ca, and P as well as a variety of heavy metal ions (Cu, Fe, Mn, Ni, and Zn) (**Table 3-1**).

3.4.2 Growth of *P. putida* LS46 in pure glycerol and waste glycerol

P. putida LS46 grew equally well in Ramsey's medium contain pure reagent grade glycerol (PG) and biodiesel-derived WG, although slightly greater cell densities were attained by *P. putida* LS46 cultures with PG compared to WG (**S2 Figure**). No lag phase was observed, and cells appeared to immediately enter exponential phase (~4 to 20 h pi). Nitrogen concentrations were depleted between 16 and 20 h pi (**S3 Figure**), and the cell entered stationary phase thereafter. Cell densities (as measured by OD_{600}) of *P. putida* LS46 cultured with PG were 1.87 to 2.45 between 16 and 20 h pi, whereas cell densities of *P. putida* LS46 cultured with WG were 1.77 to 2.29 between 16 and 20 hpi. Samples for transcriptomic and proteomic analyses were collected at 8 h pi, when cell densities of the PG and WG cultures were 0.50 and 0.58 OD_{600} unit, respectively. No detectable mcl-PHA production was observed under both cultures (WG and PG) during the exponential growth.

Table 3-1. Metal ion concentrations in biodiesel-derived waste glycerol (WG).

Metals[a] (ppm)	Na	Ca	P	Cu	Fe	Mn	Ni	Zn
Blank	n.d	n.d	0.12 ± 0.01	n.d	n.d	n.d	n.d	n.d
WG 1%	253 ± 11.5	0.09 ± 0.02	0.57 ± 0.01	0.016 ± 0.001	0.23 ± 0.01	n.d	n.d	n.d
WG 3%	1012 ± 52.1	0.45 ± 0.04	1.98 ± 0.07	0.055 ± 0.002	0.68 ± 0.01	0.013 ± 0.003	n.d	0.024 ± 0.001
WG 5%	1334 ± 41.1	0.53 ± 0.02	3.02 ± 0.12	0.089 ± 0.005	0.98 ± 0.03	0.019 ± 0.001	n.d	0.041 ± 0.002
RM (theoretical)	1150	2.73	1117	0.003	9.9~11.1	0.008	0.005	0.023
RM (measured)	1111 ± 60.1	2.49 ± 0.3	1095 ± 25.6	0.005 ± 0.002	11.03 ± 0.23	0.010 ± 0.003	0.003 ± 0.0002	0.020 ± 0.001
RM + 3% WG	2180 ± 44.7	2.92 ± 0.3	1100 ± 73.5	0.051 ± 0.006	11.90 ± 0.17	0.021± 0.005	0.003 ± 0.0005	0.037 ± 0.006

[a] Waste glycerol at various concentration (1% = 10g/L; 3% = 30g/L and 5% = 50g/L) and chemical reagent pure glycerol at 30g/L (used as blank) were dissolved in sterile deionized water for each test. RM: Ramsay's Medium.
[b/c:] Metal concentrations in the supernatant of WG or PG cultures of *P. putida* LS46 at 8 hour post-inoculation;
n.d: Not detected, below the detection limit. n.a, not analyzed.

3.4.3 Global transcriptomics and proteomics analysis

Transcriptomic analysis identified an average of 5194 genes under two conditions. This constitutes almost 95 % coverage of the *P. putida* LS46 genome, while 1D-LC-MS/MS proteomic analyses detected, on average of approximately 1300 proteins under the two conditions tested (**S3 Table**). Thus, the depth of the transcriptome was much greater than the depth of the proteome. Furthermore, the log2 expression values of transcriptomic and proteomic data under the two conditions largely correlated with each other (with R^2 ratio from about 0.33 to 0.44) indicating that while the full depth of the differential analysis was best done with the transcriptomic data, the proteomic data could be used to support and confirm the transcriptomic data, when the proteins detected were sufficiently abundant. The scatterplots of the log2 expression values of transcriptomic and proteomic data under the two conditions were provided at **S4 Figures**. As a means of quality control, the standard deviation of populations (RNA or Protein) from both cross-states and intra-replicates were compared yielding a "signal to noise ratio" of 2.5 for RNAseq data, suggesting the response of *P. putida* LS46 to waste glycerol is profound on transcriptional level, while the signal to noise ratio for the proteomic data was 1.0, indicating that our proteomic measurement system was not sufficiently sensitive to access these changes (**S4 Tables A**).

The cross-state (WG vs PG) specific gene expression profiles were assigned to different COG classifications (summarized in **Table 3-2**). More than 5 times more RNA transcripts than proteins were identified as having undergone significant changes in expression levels. Fewer gene transcripts, and no proteins putatively involved in central metabolism pathways, such as G for carbohydrate transport and metabolism, changed compared to other COG categories. However, a number of genes/proteins associated with

lipid transportation and metabolism were up regulated in WG culture, likely due to presence of residual fatty acids in this waste source. Interestingly, a greater number of gene transcripts were detected in other COG categories not associated with central metabolic functions, such as inorganic ion transport and metabolism (P). This suggests a response to elevated metal concentrations in the WG culture, which serves as a basis for a more focused analyses of the expression of genes responding (putatively) to metals and other impurities in the waste glycerol derived culture. These aspects were analysed more deeply below.

Table 3-2. Numbers of significant up- and down-regulated[a] genes in specific COG groups under specific growth conditions.

COG Group	Description	Mid-log phase Waste glycerol vs Pure Glycerol			
		RNA		Protein	
		Up [a]	Down	Up	Down
K	Transcription	12	9	1	1
C	Energy production and conversion	9	19	3	1
L	Replication, recombination and repair	3	7	1	1
O	Posttranslational modification, protein turnover, chaperones	4	5	2	3
H	Coenzyme transport and metabolism	8	4	1	1
J	Translation, ribosomal structure and biogenesis	0 [b]	0	1	2
F	Nucleotide transport and metabolism	0	0	0	1
R	General function prediction only	21	17	4	2
G	Carbohydrate transport and metabolism	9	8	1	0
M	Cell wall, membrane, and envelope biogenesis	13	5	1	2
T	Signal transduction mechanisms	9	14	2	1
P	Inorganic ion transport and metabolism	19	8	1	3
S	Function unknown	24	12	1	2
E	Amino acid transport and metabolism	18	31	4	3
I	Lipid transport and metabolism	8	12	3	2
D	Cell cycle control, cell division, chromosome partitioning	1	2	2	0
V	Defense mechanisms	4	5	0	1
Q	Secondary metabolite biosynthesis, transport, and catabolism	5	10	0	0
U	Intracellular trafficking, secretion, and vesicular transport	2	3	2	1
N	Cell motility	0	2	1	0
Total		169	173	31	27

[a] Up- or down-regulation limited to RNA or proteins (with FDR less than 10%) having a Z- score (Rnet for RNA; Pnet for Protein) outside (±) 1.65 standard deviations from the population mean.

[b] Zero means that none of the genes products within the specific COG catagory had a Z-score that corresponded to a significnat change in expression.

3.4.4 Genes and regulatory elements putatively involved in heavy metal resistance

Elevated levels of expression of several *P. putida* LS46 genes and regulatory elements that have been suggested to play a role in cellular response and adaptation to heavy metals were observed (**Table 3-3**). Many of these genes appear to be organized into transcriptional units (see locus tags), and two gene clusters, labelled "cluster 1" and "cluster 2" were identified. Note that, unlike cluster 1, two putative transcriptional units in cluster 2 are not adjacent, but they are close to each other. Greater changes in transcript were observed in cluster 2 genes (higher Rnet value), but gene products (proteins) of cluster 1 genes were expressed at much higher levels than the cluster 2 gene products, according the expression abundant values.

RNASeq analysis revealed two putative transcriptional units in cluster 1, belonging to *cus*ABC and *cop*AB genes, and the putative *cop*AB unit genes were up-regulated either at the transcriptional and/or translational level, which may suggest that different regulatory mechanisms may exist for these two groups cluster 1 genes. The *cus*ABC belongs to well characterized members of the heavy metal efflux (HME)-RND (resistance-modulation-cell division) family proteins, which are involved in detoxifying heavy metal ions, such as silver and copper, in *Cupriavidus metallidurans* (Mergeay et al., 2003). The gene products encoded by *cop*AB are highly conserved in various *Pseudomonas* species and have been shown to be involved in cellular response and adaptation to copper (Teitzel et al., 2006; Miller et al., 2009; Bender and Cooksey, 1987). Furthermore, a two component regulatory system within cluster 1 likely plays an essential role in heavy metal sensing and resistance. Genes in cluster 2 were highly up-regulated (in transcriptome) in WG cultures, including numbers of heavy metal related transporters, a second copy of *cop*AB genes, and one MerR family transcriptional

regulator which is the major regulator that respondes to environmental stress, such as oxidative stress, or contaminants like heavy metals or antibiotics (Brown et al., 2003). Furthermore, 10 additional putative *mer*R genes could be identified in the genome of *P. putida* LS46, but with mostly unchanged expression profiles.

Finally, 'Omics indicated the expression changes on a number of genes scattered across the *P. putida* LS46 genome, which are putatively involved in sensing, transporting, and efflux of (heavy) metal ions, such as iron, cobalt/zinc/cadmium, and nickel. Beyond the annotated genes, a significant number (7) of hypothetical proteins encoded within the *P. putida* LS46 genome displayed statistically significant changes in their expression profiles in response to the WG culture (**S2 Tables A**). This suggests a complexity of the *P. putida* LS46 response to WG that is beyond our current knowledge from annotated genes.

Table 3-3. Identification of *P. putida* LS46 gene clusters putatively involved in heavy metal resistance and up-regulated in WG culture. Differential expression between two culture conditions (WG versus PG) was expressed by Rnet for RNA, and Pnet for Protein. Threshold for up or down regulation (in bold) of RNA and/*or* protein was set at Rnet/Pnet = ± 1.65.

	Locus-tag (PPUTLS46_)[a]	**Annotation**	**Subcellular location [b]**	**Expression abundance (WG) [c]**		**Differential expression (WG vs PG) [d]**	
				RNA	**Protein**	**Rnet**	**Pnet**
Cluster 1	008549	Hypothetical protein	-	11.2	-	0.39	-
	008554	Outer membrane efflux protein (*cus*C)	OM	11.5	17.5	0.47	0.61*
	008559	RND family efflux transporter MFP subunit (*cus*B)	CT	11.3	19	0.09	1.72*
	008564	CzcA family heavy metal efflux protein(*cus*A)	CM	11.2	19.1	0.03	1.3*
	008569	Protein of unknown function	-	8.5	-	0.47	-
	008574	Outer membrane porin	OM	8.9	-	0.78	-
	008579	Predicted metal-binding protein	-	10.3	17.5	**1.73**	0.55*
	008584	Cytochrome C oxidase, cbb3-type, subunit III	-	12.3	18.7	1.59	0.44*
	008589	Copper resistance B	OM	13.2	20.2	1.53	**1.77**
	008594	Hypothetical protein	-	11.4	-	1.41	-
	008599	CopA family copper resistance protein	PP	14.3	21.2	1.54	0.04*
	008604	Hypothetical protein	-	11.4	-	**1.86**	-
	008644	Copper-translocating P-type ATPase	CM	12.9	20.4	0.35	0.03*
	008669	Two component heavy metal response transcriptional regulator	CT	10.6	-	1.14	-
	008674	Heavy metal sensor signal transduction histidine	CM	10.4	-	**2.39**	-
Cluster 2	023578	CopA family copper resistance protein	PP	13.6	-	**3.45**	-
	023583	Hypothetical protein	-	11.1	-	**4.49**	-
	023588	Copper resistance B precursor	OM	12	-	**3.65**	-

	023313	Bcr/CflA family multidrug resistance transporter	CM	12.4	-	**6.44**	-
	023318	heavy metal transport/detoxification protein	-	12.1	-	**6.04**	-
	023323	Hypothetical protein	-	-	-	-	-
	023328	Heavy metal translocating P-type ATPase	CM	13.4	17.8	**2.73**	0.46*
	023333	MerR family transcriptional regulator (MerR-1)	-	10.3	-	**2.16**	-
	023583	Hypothetical protein	-	11.1	-	**4.49**	-
Through out genome	017239	CzcC family cobalt/zinc/cadmium efflux	OM	3.4	-	**2.03**	-
	017244	CzcB family cobalt/zinc/cadmium efflux	-	4.9	-	0.84	-
	017249	Cation efflux system protein czcA	CM	6.6	-	0.04	-
	012843	Cation diffusion facilitator family transporter	-	7.7	15.1	**2.97**	0.73*
	007086	Ferric uptake regulation protein	-	12.1	20.5	0.03	**2.68***
	009189	TonB-dependent siderophore receptor	OM	9.5	17.9	**-4.3**	**-5.61**
	009194	nickel transport system substrate-binding	PP	9.6	18.1	**3.83**	**-1.65***
	011725	Cation transporter	-	9.97	-	**2.23**	-

[a] Locus tag increments by units of 5, such as, PputLS46_008549 and PputLS46_008554, are adjacent genes;

[b] CT, cytoplasmic; CM, cytoplasmic membrane; OM, outer membrane; PP, periplasm;

[c] Log2 expression abundance of gene products (mRNA and Protein) of *P. putida* LS46 grown under mid-log phase of waste glycerol culture. Values were averaged from two biological replicates;

[d] Gene differential expression value, mRNA and/or Protein that were significantly up/down-regulated were bold. Proteins that did not pass the threshold for protein detection have no abundance value, and therefore no Pnet value.-; proteins expression was not detected in both waste glycerol and pure glycerol cultures, and therefore no Pnet values associated.

A * symbol besides the individual Pnet value of the protein indicates the protein (if detected) with S/N (signal to noise) ratio less than 2.8, and thus having FDR greater than 10 %.

3.4.5 *P. putida* LS46 responses to non-heavy metal impurities in waste glycerol

In addition to heavy metal ions, waste biodiesel-derived glycerol may contain other impurities that co-extracted during glycerol refinery process. Our current 'Omics study revealed that *P. putida* LS46 responded to three other classes of non-metal contaminants during growing on waste glycerol (**Table 3-4**), including: 1) putative anti-osmotic stress response genes (due to high sodium content in waste glycerol); 2) a putative fusaric acid resistance system; 3) genes responsible for fatty acid oxidation;

Expression of a number of genes may be changed in response to elevated sodium concentrations, which may induce osmotic stress to the cells. These genes include an efflux system for hydrophobic molecules and Na^+/H^+ exchanger. A gene cluster that is putatively involved in resistance to fusaric acid was highly up-regulated at the transcriptional level in WG-glycerol cultures, but corresponding proteins were not detected in the proteome. Transcription of this gene cluster may be regulated under a MarR (Multiple antibiotic resistance regulator) family transcriptional regulator (PputLS46_025448) which locates downstream of the putative gene cluster for fusaric acid resistance. Finally, up-regulation of numbers of fatty acid β-oxidation pathway genes in *P. putida* LS46 is likely due to the presence of residual free fatty acids in the waste biodiesel derived glycerol (Fu et al., 2014).

Table 3-4. Expression profiles of *P. putida* LS46 genes responding to non-heavy metal impurities in waste biodiesel-derived glycerol. The threshold for up or down (bold) regulation of RNA and protein was set at Rnet/Pnet = ± 1.65.

Locus-tag (PPUTLS46_)	Annotation	Expression abundance (WG)[a]		Differential expression (WG vs PG)	
		RNA	Protein	Rnet	Pnet
025428	RND efflux transporter	9.3	-	**3.05**	-
025433	Secretion protein HlyD family protein	9.3	-	**3.68**	-
025438	Protein of unknown function	5.8	-	**5.59**	-
025443	Fusaric acid resistance protein region	9.9	-	**5.39**	-
025448	MarR family transcriptional regulator	9.14	-	**5.36**	-
018286	Efflux system OM protein	10.5	17.1	**-2.50**	**-4.1**
018281	Transporter hydrophobe/amphiphile efflux1	10.5	17.7	**-3.47**	**-3.17**
018276	Efflux transporter RND family, MFP subunit	9.13	17.7	**-3.53**	**-3.8**
005321	Choline dehydrogenase	10.5	17.5	-0.41	1.4*
016544	Glucose-methanol-choline oxidoreductase	13.3	21.2	**3.68**	**6.05**
005771	Sodium/hydrogen exchanger	9.2	-	**2.07**	-
024448	Acyl-CoA dehydrogenase	14	20.3	0.9	**5.16***
000715	Acetyl-CoA acetyltransferase	9.4	18.5	**4.14**	**2.64**
004404	3-ketoacyl-CoA thiolase	12.5	19.7	0.81	**2.28**
004399	Multifunctional fatty acid oxidation complex	12.4	20.6	1.05	1.53*
021046	Long-chain-fatty-acid--CoA ligase	10.8	18.5	0.14	1.4

[a] Log2 expression abundance of gene products (mRNA and Protein) of *P. putida* LS46 grown under mid-log phase of waste glycerol culture. Values were averaged from two biological replicates;

A * symbol besides the individual Pnet value of the protein indicates the protein (if detected) with S/N (signal to noise) ratio less than 2.8, and thus having FDR greater than 10%.

3.5 Discussion

Impurities in biodiesel-derived glycerol include residual methanol and free fatty acids, sodium or potassium salts used as catalysts during transesterification, and heavy metal ions (Verhoef et al., 2013; Brown et al., 2003). Under the experimental conditions described in this work, the concentrations of heavy metal ions in the WG culture were most likely not toxic to *P. putida* LS46. Instead, these impurities (residual fatty acids, divalent cations) may serve as additional nutrients to the cell. Verhoef et al grew *P. putida* S12 in crude glycerol cultures (40 mM) without adding a trace element solution, and showed that the replacement of minerals from crude glycerol promoted cell growth to certain point, while no growth was observed in cultures with pure glycerol in the absence of trace minerals (Verhoef et al., 2013). Our result revealed a similar pattern in that the residual free fatty acids and divalent cations in biodiesel- derived glycerol potentially served as additional carbon and micronutrients for *P. putida* LS46. This is associated with higher ammonia consumption during the early exponential phase growth of *P. putida* LS46 in WG cultures (**S3 Figure**).

Biodiesel-derived waste glycerol induced differential expression of genes putatively involved in heavy metal ion transport and metabolism (**Table 3-2**). *P. putida* is well known for heavy metals resistance, and intra-cellular concentration of these toxic compounds are putatively regulated via various mechanisms including metal transportation, reduction, or segregation (Wu et al., 2011; Cánovas et al., 2003; Nies, 1999). Three groups of up-regulated genes were observed in *P. putida* LS46 WG cultures (**Table 3-3**), which putatively served as the primary regulatory response to elevated heavy metal uptake.

It may be worth mentioning that *cus*ABC has been wrongly annotated as *czc*ABC in various *P. putida* genomes and should be re-annotated based on phylogenetic analyses of the *cus*ABC cluster presented in this work (**S5 Figure**) and previous phylogenetic studies (Gutiérrez-Barranquero et al., 2013). Orthologs of *cus*ABC efflux genes (cluster 1) in *Cupriavidus metallidurans* (Mergeay et al., 2003), *Pseudomonas syringae* (Gutiérrez- Barranquero et al., 2013), and *Pseudomonas aeruginosa* PAO1 (Teitzel et al., 2006) were shown to involved in copper resistance, however our 'Omics analysis suggested that their expression did not changed under the current experimental conditions of *P. putida* LS46 cultured with WG compare to PG. This suggests over-expression of *cus*ABC cluster may not be the primary response of *P. putida* LS46 to the elevated level of heavy metals ions (such as, copper) in the WG culture.

Initial studies of copper resistance in *P. syringae* pv. Tomato identified the *cop*ABCD gene cluster as crucial for copper tolerance (Cha and Cooksey, 1991). *P. putida* species lack of *cop*CD genes, but also encode a second copy of the copper binding protein CopAB in the genome, which may compensate the lack of *cop*CD gene products for copper resistance (Cánovas et al., 2003). CopB is an outer membrane protein that binds copper in the medium (Cha and Cooksey, 1991), while CopA is a periplasmic protein which has a multi-copper oxidase domain, and may be involved in oxidation Cu^{1+} to its less toxic form Cu^{2+} in *P. aeruginosa* (Teitzel et al., 2006). Expression of two copies of CopAB has been observed in a 2D-proteomic/Microarray analysis in copper- stressed *P. putida* KT2440 (Miller et al., 2009). In the Miller *et al* (2009) study, CopB1 and CopA2 were the most up-regulated proteins of the two copies of CopAB responding to copper stress, whereas there was little changed in the expression level of the CopA1 protein, and no detected expression of CopB2. CopB1

has been suggested to be the major protein for cellular surface protection from excess copper-binding (Pabst et al., 2010). The result of our transcriptomic and proteomic expression studies in *P. putida* LS46 were similar to those of Miller et al (2009), in that CopB1 (in cluster 1) was the most up- regulated protein of the two *cop*AB gene copies, while expression of the CopA1 protein did not change much, even though increased transcription of the *cop*A1 gene was observed.

Two heavy metal translocating P-type ATPases were identified in the two clusters. The gene PputLS46_023328 in cluster 2 displayed increased levels of transcription and is presumably induced by the presence of Cu^{+}. The ortholog of PputLS46_023328 in *P. putida* KT2440 appears works as a copper exporter, and in *P. aeruginosa* PAO, it is crucial for Cu^{+} resistance by exporting Cu^{+} from the cytosol to the periplasmic space through an ATP-dependant reaction (Miller et al., 2009; González-Guerrero et al., 2010). Furthermore, cluster 2 heavy metal translocating P-type ATPases (PputLS46_023328) and four up-regulated adjacent genes form a putative transcription unit (**Table 3-3**), which is likely regulated by the highly up-regulated MerR family transcriptional regulator (coded by Pputls46_02333) of the unit. The archetype of MerR family transcriptional regulator is involved in mercury resistance, and is found on several transposable elements. Many MerR family proteins have been identified and are known to respond to various environmental stimuli, including heavy metals (Brown et al., 1983). In addition to previous mentioned *mer*R gene, we have identified additional 10 putative MerR regulatory genes and their corresponding gene products in *P. putida* LS46 which suggests that this strain has the genetic capacity to respond to various environmental stimuli (Wu et al., 2011).

A cation transport-related gene (PputLS46_012843) was up-regulated in *P. putida*

LS46 cells grown in WG-cultures. The gene product of PputLS46_012843 is a cation diffusion facilitator (CDF) family protein, which is putatively involved in translocating heavy metals such as Zn^{++}, Cd^{++}, and Co^{++} (Haney et al., 2005). These metals can also be exported by a RND multi-drug efflux transporter system, but expression of the system (*czc*ABC cluster in **Table 3-3**) was very low, suggesting CDF seems the first line of defense against heavy metals by *P. putida* LS46. This is similar to some other gram-negative bacteria (Hantke, 2001).

High expression abundance of ferric uptake regulator (Fur) coded by PputLS46_007086 (protein abundance: 20.1) may be important in regulating iron acquisition by *P. putida* LS46 with increased iron concentration (i.e. waste glycerol derived culture, **Table 3-1**). The Fur regulator is well conserved in many gram-negative bacteria, and it governs (represses) the iron acquisition-related genes, such as siderophore-mediated iron transport systems, when iron is plentiful (Hassett et al., 1996). Interestingly, a TonB-dependent siderophore receptor (PputLS46_009189) has been greatly repressed in *P. putida* LS46 in WG-cultures, which may be a response to the level of the Fur regulator protein.

We have also observed changes in expression levels of a group of *P. putida* LS46 genes putatively involved in adaptation to osmotic-stress (Kosono et al., 2005), which may be caused by elevated concentrations of sodium present in WG-cultures (**Table 3-1**). PputLS46_005321 was identified as a putative ortholog of the characterized choline dehydrogenase enzyme of *P. aeruginosa* PAO1, due to high amino acid sequence identity (85%). Moreover, the organization and arrangements of genes up-stream and down-stream of PputLS46_005321 in *P. putida* LS46 was identical to the choline dehydrogenase gene neighbourhood in *P. aeruginosa* PAO1 (Wargo et al., 2008). The

choline dehydrogenase enzyme oxidizes choline to glycine betaine, a compatible solute that prevents dehydration in high osmotic environments (Fan et al., 2004; Wargo et al., 2008).

In addition to the above-mentioned RND family of efflux systems for heavy metals, there are also numbers of RND-type efflux pumps that are putatively sensitive to non-metal contaminants in WG-cultures. A fusaric acid resistance related efflux system was significantly up-regulated in the WG culture. Fusaric acid is generally produced by numbers of filamentous fungi widely distributed in soil, and is known to decrease plant cell variability, therefore trace amount of the compound may present in the plant-derived biodiesel production process. Fusaric acid is also known to be toxic to many gram-negative bacterial, such as *P. fluorescens, Burkholderia cepacia,* and more recently *Stenotrophomonas maltophilia,* which expresses an inducible efflux pump for fusaric acid resistance (Utsumi et al., 1991; Hu et al., 2012; Pan et al., 2011). An up-stream MarR family transcriptional regulator may control the expression of this gene cluster in *P. putida* LS46. Furthermore, a tripartite efflux pump was found to be significantly down-regulated in WG culture of *P. putida* LS46 (PputLS46_018286/018281/018276). The analog of this system in *P. aeruginosa* PAO1 (mexE-mexF-oprN) is involved in the resistance to a variety of antibiotics (Michéa et al., 1997). Interestingly, the expression of this system is inversely correlated with expression another major multi-drug efflux system, namely mexA-mexB-oprM, in *P. aseuginosa* PAO1, suggesting the two systems are coordinately regulated (Li et al., 2000). An analog of mexA-mexB-oprM was identified in the *P. putida* LS46 genome (PputLS46_013778/013773/013768), however with no significant expression changes in WG culture. Finally, a number of fatty acid metabolism genes were significantly up-regulated in *P. putida* LS46 WG culture, which

is consistent with the presence of free fatty acids in the biodiesel-derived waste glycerol used as substrate (Fu et al., 2014). In conclusion, the physiology of *P. putida* LS46 grown in waste glycerol derived culture and current 'Omics study revealed that *P. putida* LS46 is capable to adapt effectively to impurities in the industry waste glycerol streams making it an effective candidate for bioplastics production.

Chapter 4

Quantitative 'Omics analyses of medium chain length polyhydroxyalkanaote metabolism in *Pseudomonas putida* LS46 cultured with waste glycerol and waste fatty acids

This chapter is based on published manuscript submitted to PLOS ONE titled, "Quantitative 'Omics analyses of medium chain length polyhydroxyalkanaote metabolism in *Pseudomonas putida* LS46 cultured with waste glycerol and waste fatty acids", by Jilagamazhi Fu, Parveen Sharma, Vic Spicer, Oleg V. Krokhin, Xiang Li Zhang, Brian Fristensky, John A. Wilkins, Nazim Cicek, Richard Sparling, and David B. Levin. PLoS ONE, 2015, 10(11): e0142322.

4.1 Abstract

The transcriptomes and proteomes of *Pseudomonas putida* LS46 cultured with biodiesel-derived waste glycerol (WG) or waste free fatty acids (WFA), as sole carbon source, were compared under conditions that were either permissive or non-permissive for synthesis of medium chain length polyhydroxyalkanoates (mcl-PHA). The objectives of this study were to help to elucidate mechanisms that influence activation of biopolymer synthesis, intra-cellular accumulation, and monomer composition, and determine if these were physiologically specific to the carbon sources used for the growth of *P. putida* LS46. Active mcl-PHA synthesis by *P. putida* LS46 was associated with high expression levels of key mcl-PHA biosynthesis genes and/or gene products including monomer supplying proteins, PHA synthases, and granule-associated proteins. 'Omics data suggested that expression of these genes were regulated by different genetic mechanisms in *P. putida* LS46 cells in different physiological states,

when cultured on the two waste carbon sources. Genetic targets whose expression may potentially effect carbon flux to mcl-PHA biosynthesis were studied under the active mcl-PHA synthesis stage of WG and WFA cultures. In the WG culture, the significant variations in gene expression were identified primarily involved in: 1) glycerol transportation; 2) enzymatic reactions that recycle reducing equivalents and produce key mcl-PHA biosynthesis pathway intermediates (e.g. NADH/NADPH, acetyl-CoA, 3-hydroxyacyl-ACP). A putative thioesterase in the fatty acid beta-oxidation pathway has been identified, and it may regulate the level of fatty acid beta-oxidation intermediates during the cell grown on WFA, and thus carbon flux to mcl-PHA biosynthesis. Finally, the data suggested that differences in expression of selected fatty acid metabolism and mcl-PHA monomer supplying enzymes may play a role in determining the monomer composition of mcl-PHA polymers. Understanding the relationships between genome content, gene and gene product expression, and how these factors influence polymer synthesis, will aid in the optimization of mcl-PHA production by *P. putida* LS46 using biodiesel waste streams.

4.2 Introduction

Medium chain length polyhydroxyalkanoates (mcl-PHA) are mostly produced by bacteria in the genus *Pseudomonas* as reserve sources of carbon and energy under conditions of nutritional stress (Akaraonye et al., 2010). Mcl-PHA polymers may be used to manufacture biodegradable plastics and resins, but large-scale production of these polymers is currently hindered by high product costs, of which substrate cost is a major component (Akaraonye et al., 2010). A number of studies have explored the use of microorganisms to convert agro-industrial waste streams into value-added PHA polymers (Koller et al., 2005; Cavalheiro et al., 2009). The by-products from industrial

biodiesel production, such as biodiesel-derived glycerol and biodiesel-derived free fatty acids, contain certain amount of impurities making them less useful for other downstream industrial applications. For example, waste glycerol contains methanol, residual free fatty acids, sodium or potassium soaps derived from the catalysts used to synthesize biodiesel, and numbers of identified heavy metals (Li et al., 2013; Verhoef et al., 2014; Fu et al., 2015). Waste glycerol is normally refined in order to use in food, cosmetics, and pharmaceutical industrial. Non-refined waste glycerol was used as animal feedstuff, but concerns still remain regarding the acceptable level of the impurities (Cerrate et al., 2006; Yang et al., 2012). Biological conversion of biodiesel derived waste carbon sources into high-value added product, such as synthesis of mcl-PHA by *Pseudomonas putida* (Fu et al., 2014; Kenny et al., 2012), is of great interests currently. Understanding the effects of these low cost "waste" carbon sources on the metabolism of *P. putida* in general, and mcl-PHA synthesis pathways in particular, will provide a rational basis for optimization of fermentation strategies for large-scale mcl-PHA production.

Phenotypically, it is the cellular content and monomer composition of mcl-PHA mostly determines its final applications, while these "parameters" are genetically regulated by the "factors" that involved to activate mcl-PHA biosynthesis machinery, regulate carbon flux and monomer pattern during the polymer biosynthesis under different physiological conditions. Previous study in Chapter 2 has provided a significant different mcl-PHA production profiles between waste glycerol and waste fatty acids cultures, which potentially allows us to explore the genetic variations behind the phenotypical differences using 'Omics' technologies (transcriptomics and proteomics). The technology could provide an informative and rather complete

"snapshot" of gene expression profiles under specific growth conditions. The advantages of this approach include, but are not limited to: i) identification of pathway genes that are actively involved in metabolic processes; ii) differentiation of active genes from redundantly encoded genes in the genome; iii) prediction of carbon and electron flow, which influence metabolic flux, and therefore determine end-product synthesis patterns; and iv) insight into mechanisms of gene regulation and regulatory variation at transcriptional or translational level (Joyce et al., 2006).

Previously, mapping the gene expression data to mcl-PHA biosynthesis pathway at the polymer synthesis stage has been evaluated in *P. putida* KT2440 grown on pure fatty acids, such as octanoic and decanoic acid (Poblete-Castro et al., 2012; Escapa et al., 2012). However, a systematic analysis of gene expression pertinent to mcl-PHA biosynthesis by *P. putida* cultured with biodiesel derived waste glycerol and waste fatty acids at both the transcriptome and proteome level has not been reported, although few studies has studied the transcriptome of exponentially grown *P. putida* KT2440 on pure reagent grade glycerol cultures (Nikel et al., 2014; Kim et al., 2013).

In this work, we have studied two specific mcl-PHA producing conditions of *P. putida* LS46 using waste glycerol and waste fatty acids as sole carbons source: Stationary phase of WG culture and Exponential phase of WFA culture. A non-mcl-PHA producing condition (derived from exponential phase of WG culture) was used as reference for comparison purpose. Quantitative transcriptomics by RNA sequencing (RNAseq) and proteomics (1D-LC-MS/MS) was applied help to understand: a) the activation of mcl-PHA biosynthesis in cultures containing biodiesel-derived glycerol versus biodiesel- derived free fatty acids; and b) the potential genetic targets that effect

intra-cellular polymer accumulation and monomer composition.

4.3 Materials and Methods

4.3.1 Bacterial strain and culture conditions

Pseudomonas putida LS46 was isolated from a local wastewater treatment plant in Winnipeg, Manitoba, Canada. The strain was deposited with International Depository Authority of Canada (IDAC) at the National Microbiology Laboratory, Health Canada Culture Collection (NML-HCCC), WDCM number 840 (Sharma et al., 2012). Crude biodiesel-derived (waste) glycerol (WG) and (waste) free fatty acids (WFA) were obtained from the Renewable Energy Group LLC (Danville, Illinois, USA). *P. putida* LS46 was cultured in Ramsay's medium supplemented with either 30 g/L waste glycerol, or 1 v/v % (about 9 g/L) of waste fatty acids as studied in our previous work (Fu et al., 2014). The components of Ramsay's medium are (per liter): 6.7 g of Na_2HPO_4-$7H_2O$, 1.5 g of KH_2PO_4, 1.0 g of $(NH_4)_2SO_4$, 0.2 g of $MgSO_4$-$7H_20$, 60 mg of ferrous ammonium citrate, 10 mg of $CaCl_2 \cdot 2H_2O$, 1 ml of trace element solution. Each liter of trace element solution contains the following: 0.3 g of H_3BO_3, 0.2 g of $CoCl_2$-$6H_2O$, 0.1 g of $ZnSO_4$-$7H_2O$, 30 mg of $MnCl_2$-$4H_2O$, 30 mg of $NaMoO_4$-$2H_2O$, 20 mg of $NiCl_2$-$6H_2O$, 10 mg of $CuSO_4$-$5H_2O$. The major fatty acids of triacylglycerides in the biodiesel-derived waste fatty acids used as substrate in these experiments was previously reported (Fu et al., 2014), and were C16 (20.4%), C18:0 (11.5), C18:1 (35.4) and C18:2 (20.7), based on the peak area percentage.

4.3.2 Cell growth measurements

Dry cell weight was used as an indicator of the cell growth. Ten (10) mL cultures medium were collected in 50 mL falcon tubes during time-point sampling, centrifuged at

4,000 x g for 10 min at room temperature, and washed with deionized water. The resulting wet cell pellets were dried in the oven at 60 °C overnight before determining the dry cell weight.

4.3.3 Nutrition consumption and mcl-PHA quantification

Residual glycerol in medium was measured using a WATERS Breeze^{TM} 2 HPLC system (model number: MO915P795A) (Milford, MA, US). Pure glycerol was used as an external standard for quantification purposes. Residual ammonia concentrations in the medium were measured using the Quikchem method 10-107-06-1-I, by flow injection analysis (Lachat Instrument, Colorado, USA) same as mentioned in Chapter 2 at the section of **2.3.3.**

To quantify free fatty acid content in waste free fatty acids culture overtime, a step of recovering residual free fatty acids from the culture medium was required. This method was based on the method described by Budde et al., 2011, and modified as follows: 10 mL of the culture medium was centrifuged (4,400 x g) for 10 min, supernatant was collected. The cell pellet was washed with 5 mL DI (deionized) water, and centrifuged (4,400 x g for 5 min), the resulting supernatant was combined with the supernatant from the first centrifugation (above). Chloroform (10 mL) and 5 mL methanol were then added to the mixture, vortexed vigorously for 1 min, and centrifuged for 5 min at 4,400 x g. After centrifugation, the organic layer was collected and transferred to a pre-weighted glass tube and dried in the oven (60 ^{o}C overnight). The lipid content in the 10 mL culture medium was therefore calculated gravimetrically. To calculate the lipid (total fatty acid content) concentration in the medium, the following equation was used:

$$Lipid\ concentration = Mass\ recovered \times \frac{Vorganic}{Vtransferred} \times \frac{1}{Vsample}$$

where, "Mass recovered" is the mass of lipid recovered from the 10 mL culture; "V*organic*is" is the volume of the organic phase (chloroform layer) after the extraction; "V*transferred*" is the volume of organic layer transferred (or used) to calculate the mass recovery; and "V*sample*" is the volume of medium taken from the culture (10 mL in this case).

Mcl-PHA production over time was measured using the same method as described previously (Fu et al., 2014). Note that, cells from overnight cultures of *P. putida* LS46 grown in WFA, and used to inoculate fresh cultures for the experiments described below contained 10.74 wt % of mcl-PHA.

4.3.4 Transcriptomics and Proteomics

4.3.4.1 Sampling conditions for RNA and protein isolation

Samples of *P. putida* LS46 cells were collected during the exponential and stationary phases for WG cultures, and from the exponential phase only in WFA cultures. Triplicate shake flask experiments have been carried out for physiological analysis (e.g. growth characterization, and polymer production). Subsequently, two replicates derived from the same triplicates shake-flasks experiments were taken for each of the above sampling conditions for RNAseq and proteomic analyses.

4.3.4.2 RNA isolation and RNA sequencing

Five (5) mL of cell culture were collected and centrifuged at 4,000 x g, to pellet the cells. Total RNA was extracted from the cell pellets using a PureLink® RNA Mini Kit (Ambion, Life Technologies, USA). Isolated RNA samples were treated with DNase to

remove DNA contamination. The concentration of RNA was determined using a Nanodrop 1000 spectrophotometer (Thermofisher, USA), and RNA integrity was analyzed by electrophoresis using an Experion system (BioRad, USA). RNA samples were shipped to and sequenced by the Genome Quebec Innovation Centre at McGill University (Montreal, Quebec) for creation of cDNA libraries and RNA-seq using the Illumina HiSeq 2000 platform.

4.3.4.3 Protein isolation, digestion, and peptide purification

Culture medium (40 mL) were collected, centrifuged at 4,000 x g, resuspended with phosphate buffer solution (PBS) (0.144 g/L KH_2PO_4; 9 g/L NaCl; 0.795 g/L Na_2HPO_4-$7H_2O$, pH 7.4) and centrifuged again at 4,000 x g. The PBS wash was repeated once more and the cell pellets were then stored at -80^oC for later use. When all samples were collected, frozen pellets were re-dissolved in 4 mL distilled-deionized (DI) water, of which 1 mL was used for total protein isolation. One mL of lysis buffer (8 % of sodium dodecyl sulphate, 200 mM dithiothreatol, 200 mM Tris-HCl, pH 7.6) was added to each 1 mL sample of resuspended cell pellet and solution were mixed thoroughly by pipetting. The solutions were transferred to 10 mL falcon tubes, which were then place in a boiling water bath for 5 minutes (min). After boiling, the samples were sonicated for 30 seconds, and then centrifuged at 16,000 x g at room temperature. 10ul of supernatant was subjected to SDS-PAGE gel (**S1 Figures**). One (1) mL of each supernatant was then transferred into an Eppendorf tube.

One (1) mL of total protein was transferred to an Amicon Ultra-15 10K filter device (Millipore, Billerica, MA), which followed the purification, digestion, and subsequent peptide purification steps as mentioned in Gungormusler-Yilmaz *et al* 2014

(Gungormusler-Yilmaz et al., 2014) with little modification: the typsin to protein ration at 1:100 instead of 1:50. The purified peptides were lyophilized and re-dissolved in 0.1 % formic acid in water for subsequent 1D-LC-MS/MS analysis.

4.3.4.4 RNA identification and quantification

Identification: Transcriptomic analysis used an in-house alignment and quantitation engine using the R2 element of the Illumina paired-end read sets. Our algorithm detects exact 100-mer read alignments only, relying on the high quality of the HiSeq data to give sufficient counting statistics. Additional filtering steps applied was: RNAseq values were accepted only if there were at least two alignment counts per gene. *P. putida* LS46 genome was used as reference for alignment.

Quantification: Transcripts were quantified by expressing the sum of all 100-mer RNA alignments per gene. Values were transformed to a log2 scale for comparison and differential analysis.

4.3.4.5 Protein identification and quantification

Identification: ABSciex TripleTOF 5600 TOF-MS system (Applied Biosystems, Foster City, CA) equipped with a Nano-sprayIII ionization source was used for data acquisition. Each acquisition cycle included 250 ms survey MS acqusition (m/z 400–1500) and up to twenty 100 ms MS/MS measurements on the most intense parent ions (300 counts/s threshold, +2 to +4 charge state, m/z 100–1500 mass range for MS/MS). Two hours runs for each of biological replicates of every experimental samples. Raw spectra files were converted into 200 Mascot Generic File (MGF) format for peptide/protein identification. Peptides were identified from the observed MS/MS spectra using an in-house GPU peptide search engine (McQueen et al., 2012) from a single

missed cleavage tryptic database derived from the *P. putida* LS46 genome annotation with only the fixed post-translational modification of the carbamidomethlyation of cysteine residues (+57.021 Da) applied. The GPU search engine settings were 20 ppm on parent mass ions and a 0.2 Da window on fragment ions respectively and peptides with expectation log (e) ≤ -1.5 were reported. Proteins with only a single member peptide were excluded from the report, and subsequent analyses.

Quantification: Total ion counts (TIC), which are the sum of all CID (collision induced dissociation) fragment intensities of member peptides, were used for protein quantitation. Values were transformed to a log2 scale for comparison and differential analysis, and differential analysis was constructed by subtracting sets of log2 protein intensity values derived from the comparing conditions. Note that by plotting these differential expression value in histogram, each set of detected proteins forms a three-lobed histogram, with the central population of data points containing proteins observed in both states (e.g. any two comparing conditions), while the outer histograms contain proteins observed only in one state, but not the other. While these are manifestations of the instrument's information-directed acquisition (IDA) detection limits, and do not represent the absolute presence or absence of a protein in a given sample. Thus, in order to conduct comparative analysis, a simple algorithm has been developed to normalize three population into single population. At last, proteins that only observed in one biological replicate of each physiological condition have been excluded from the subsequent analysis. Note these two additional steps prior to the data analysis were only applied to proteomics analysis, due to relative deep coverage observed for RNAseq data.

4.3.5 'Omics data analysis and validation

Analysis: Detailed comparative analyses of the expression data gathered from the specific experiments was conducted using an in-house 'Omics' data analysis system called "UNITY" (Gungormusler-Yilmaz et al., 2014). The analysis operations in order were as follows: 1) The overall number of identified protein and RNA molecules were calculated: 2) The overall correlation between transcriptomic and proteomic log2 expression values were observed; 3) Differential expression values were calculated: a) cross-state: Z = (state A - state B); and b): among biological replicates, where R = intra biological replicate differences; 4) A quality control of biological variation signals between any two comparison groups (cross-state) vs system noise among biological replications (intra-replicative viability) were conducted; 5) Transformation of different populations into final Znet scores as descripted in (Verbeke et al., 2014) (The Znet score for Protein was defined as Pnet, and Rnet for RNA as easily presentation) for relative expression analysis cross-state was conducted. The cutoff scores of ± 1.65 were used to represent outermost 10 % of the population defined as an asymmetry (up-regulated or down-regulated) of expression of RNA and protein relative to the expression profiles of the overall population; Thus, gene having a final normalized Znet score (e.g. Pnet for protein and Rnet for RNA) over 1.65 or below -1.65 will be considered as significant up or down regulated under two specific comparing conditions. 6) Each gene's set of 'Omics measurements were mapped into clusters of orthologous group (COG) classes for global condition-specific expression analysis (Tatusov et al., 2000) (**S5 Table**).

Validation: Correlation of the RNA and Protein expression data under the tested experimental condition was done by plotting the Log2 expression values of

transcriptomic and proteomic data. The dynamic range of Log2 expression values was > 4 and > 11 for RNAseq and proteomic analyses, respectively. Furthermore, a simple function was developed to evaluate the statistical significance of a two-state two-replicate dataset, on a protein-by-protein basis, which computes an overall measurement of the system quality as the ratio of the mean of the standard deviations of the cross state and intra-replicate populations. This is known as the 'system to noise' (S/N) ratio. On an individual protein level, the S/N is the ratio of the vector magnitudes (protein expression levels) across the experimental states and intra-replicate normalized values, scaled by the overall system S/N values. A simple Monte-Carlo Model was used to derived functions relating 'false discovery rates' (FDR) to a defined S/N cutoff: all proteins with a S/N > 2.8 were found to have a FDR of 10 % or less. Thus, for a protein with a Pnet (differential expression) value, if it (the protein) has a S/N ratio over 2.8, then the analysis of this protein with the Pnet value is statistically significant. In other words, this function allowed us to reliably access smaller differential expression values across experimental states, provided the variation of their corresponding intra-replicate measurements were sufficiently small.

4.3.6 Bioinformatics

To map the expression data within the metabolic pathways of interested (e.g biosynthesis of mcl-PHA from glycerol and fatty acids), identification of putative metabolic pathway genes was done within the IMG-ER platform: genes were compared across the annotated and closely-related *P. putida* strains (such as, type strain *P. putida* KT2440) through build-in functional identifiers including Enzyme Commission number (Dixon and Wedd 1964), Clusters of Orthologous Groups (COG) (Tatusov et al., 2000),

KEGG Orthology (Kanehisa et al., 2014), Pfam (Finn et al., 2014) and TIGRFAMs (Daniel et al., 2003). Gene homologs were screened with an E-value < 10^{-5} and at 60 % identity via a pBLAST using the amino acid sequence. Literature research was also used wherever available for functional annotation. Gene expression data was then mapped to the metabolic pathways by matching the locus-tag of gene products (mRNA and Proteins) identified with the corresponding pathway gene.

4.3.7 Reverse transcription Quantitative PCR analysis

The transcriptional level of genes *pha*C1 and *pha*C2 were analyzed via RT-qPCR from the same culture as for 'Omics analysis (above). Total RNA from three biological replicates of each sampling condition were isolated the same way as for RNA-seq analysis. Standard curves using primer sets for *pha*C1 and *pha*C2 at final concentration of 0.2 µm and 0.3 µm, respectively, were amplified against various concentration of *P. putida* LS46 genomic DNA (200 ng, 20 ng, 2 ng, 0.2 ng. 0.02 ng) using SsoAdvanced™ universal SYBR® Green supermix (Bio-Rad, CA, USA). The amplification of the standard curves was initiated by denaturing at 98 ^{o}C for 2 min, followed by 39 cycles of 98 ^{o}C 15 s, 58 ^{o}C 15 s for annealing/extention/plate read using CFX Connect Real-Time System (Bio-Rad, CA, USA). Next, 100 ng total RNA were reverse transcripted into cDNA using the iScript reverse transcription supermix (Bio-Rad, CA, USA) under the condition: 25^{o}C, 5 min; 42 ^{o}C 30 min; 85 ^{o}C 5 min. Subsequently, 10 ng of synthesized cDNA was directly amplified via qPCR as mentioned above along with the standard curves. For every gene under each condition, the average transcriptional level from biological triplicates samples were reported. Sequence of two primer sets: *pha*C1 forward primer: 5'-CCGACCAATACCCTGTCCACCC-3'; *pha*C1 reverse primer: 5'-

GCCGCC GTTATTGACCATGTCC-3'; *pha*C2 forward primer: 5'-CCTGGCGCAGTGGTATTT- 3'; phaC2 reverse: 5'-GCTGAGGTCGAAGATGTAGAAC-3'.

4.3.8 Data deposit

Raw sequencing data and gene expression abundance value of the RNAseq analysis were deposited in NCBI Sequence Read Archive (SRA) through Gene Expression Omnibus (GEO) with accession number: GSE65029. In addition, the gene expression abundance and differential gene expression values generated from the current 'Omics studies were provided in supplemental materials (**S1 Table and S2 Tables, B**).

4.4 Results

4.4.1 Physiology of *P. putida* LS46 growing in waste glycerol and waste fatty acids

Growth of *P. putida* LS46 in cultures containing biodiesel-derived glycerol (WG) and biodiesel-derived free fatty acids (WFA), and the points at which samples were taken (arrows) for the 'Omics analyses are indicated in **Figures 4-1**. The exponential growth phase of *P. putida* LS46 on WG was completed by 16 hours post inoculation (h pi), when nitrogen was mostly depleted, and active mcl-PHA synthesis began (**Figure 4-1A**). Consumption of glycerol slowed down during active polymer synthesis (after 16 h pi), and no further increase in mcl-PHA production was observed after 48 h pi, although glycerol was still in excess (**Figure 4-1A**). Thus, samples taken for 'Omics analyses were at 8 h pi, representing the "non-permissive" condition for mcl-PHA synthesis, and at 32 h pi, representing the "permissive" condition for active mcl-PHA synthesis.

For mcl-PHA accumulation in WFA culture, it is worth to mention that, the waste fatty acids inoculum contained about 13 wt % mcl-PHA. Thus, we observed a

decrease in intra-cellular mcl-PHA to about 8.6 wt % by 4 h pi. The mcl-PHA content of the cells started to increase gradually up to 24 h pi, and then increased at a much greater rate after nitrogen concentrations in the medium were exhausted (**Figure 4-1B**). This suggested that mcl-PHA biosynthesis was not restricted to nitrogen-limitation under WFA culture, although the maximum productivity was triggered by nitrogen depletion. Therefore, samples were taken from WFA cultures only during the exponential growth at 8 h pi, representing a different "permissive" condition for mcl- PHA synthesis.

The monomer composition of mcl-PHA polymers synthesized by *P. putida* LS46 cultured with WG and WFA varied primarily in the content of C8 and C10 monomers. C10 was the dominant monomer in polymers synthesized from WG culture, while C8 was observed as the most abundant monomer in polymers synthesized from WFA culture. According to our previous study, such monomer distribution profile of the mcl-PHA derived from two waste carbon sources was generally stable overtime (Fu et al., 2014). Production of unsaturated mcl-PHA monomers was observed in both cultures. The polymer derived from WG cultures contained more C12:1 monomer, while polymers from WFA cultures contained greater mol % of monomers with longer chain length 3-hydroxyalkanoate monomers, such as C14 and C14:1. Unsaturated monomers were determined via GC/MS with 2 mass unit smaller than their saturated 3-hydroxyalkanoic acid standards (**S6 Table**).

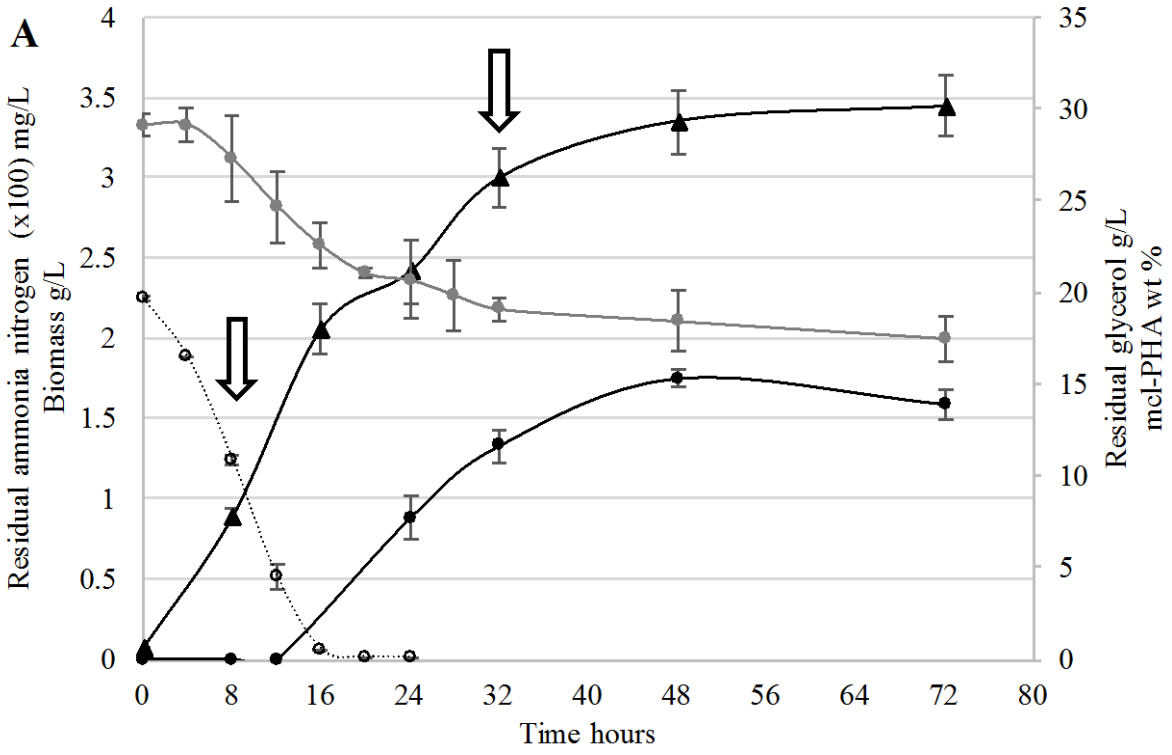
A
Residual ammonia nitrogen (x100) mg/L
Biomass g/L
Residual glycerol g/L
mcl-PHA wt %
Time hours
0
0.5
1
1.5
2
2.5
3
3.5
4
0
5
10
15
20
25
30
35
0
8
16
24
32
40
48
56
64
72
80

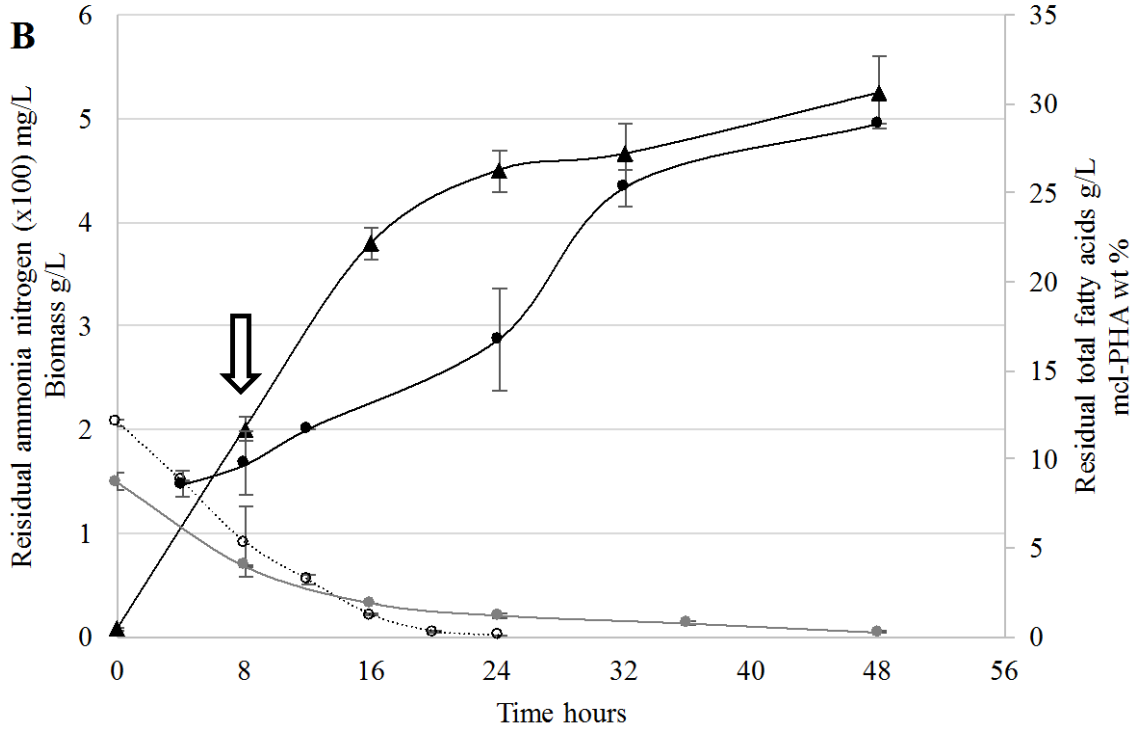
B
Reisidual ammonia nitrogen (x100) mg/L
Biomass g/L
Residual total fatty acids g/L
mcl-PHA wt %
Time hours
0
1
2
3
4
5
6
0
5
10
15
20
25
30
35
0
8
16
24
32
40
48
56

Figures 4-1. Growth of *P. putida* LS46 cultured with waste glycerol (WG) and waste fatty acids (WFA). *P. putida* LS46 was cultured in Ramsay's Minimal Medium containing A) WG and B) WFA. Solid triangle ▲, Biomass production; Solid black circle ●, mcl-PHA synthesis; Solid gray circle ●, glycerol concentrations (A) and fatty acid concentration (B); Open circle ○, nitrogen concentrations. Error bars represent standard deviations about the means calculated from three independent, biological replicate experiments. Arrows indicate samples taken for subsequent RNA and Protein isolation.

4.4.2 Whole cell transcriptomics and proteomics analyses

RNAseq analysis identified approximately 5200 genes under each of three conditions, representing about 95 % coverage of all protein coding genes in the *P. putida* LS46 genome. The 1D LC MS/MS label free proteomic analysis yielded an average number of 1362 final proteins from three tested conditions **(S3 Table)**. Thus, the depth of the transcriptome was much greater than the depth of the proteome.

The log2 expression values of transcriptomic and proteomic data largely correlated with each other (with R^2 ratio from about 0.24 to 0.42), suggesting that while the full depth of the differential analysis was best achieved with the transcriptomic data, the proteomic data could be used to support and confirm the transcriptomic data, when the proteins detected were sufficiently abundant (**S6 Figures**). Note that the correlation was relatively low in WG cultures during stationary culture (average R^2 ratio of 0.25), suggesting overall translation of gene transcripts (mRNA) into protein was more unstable under this condition, which could be expected under the assumption of higher protein degradation during the stationary stage of the culture compared to exponentially growth resulting in higher degree of differences in transcriptome and proteome correlation (Christian et al., 2013).

An average "signal to noise ratio" ratio of 3.48 was obtained for RNAseq data, suggesting the responses of *P. putida* LS46 to two mcl-PHA permissive conditions are biologically significant at the transcriptional level, while the signal to noise ratio for the proteomic data was, on average, 1.55, indicating that the proteomic measurement system was not sufficiently sensitive to access changes in protein expression levels under the experimental conditions (**S4 Table B**).

4.4.2 Levels of expression of genes involved in mcl-PHA biosynthesis

Expression of mcl-PHA biosynthesis cluster genes and several previously identified monomer supplying genes are essential for the active mcl-PHA synthesis by *P. putida* LS46. Many of these genes were up-regulated, as shown in **Table 4-1**. However, expression levels of the genes appear to be linked to the specific growth conditions that are permissive for mcl-PHA synthesis. The data in support of this observation are: 1) The two tested mcl-PHA permissive conditions induced the over-expression of key mcl-PHA synthases (PhaC1 and PhaC2) at the protein level. However, while the transcriptional level of these genes (*phaC1* and *phaC2)* was stable under the two comparing conditions in the WG culture (i.e. during the stationary phase relative to exponential phase), transcription of the *pha*C1 gene during the exponential phase of the WFA culture (mcl-PHA permissive condition) was elevated relative to exponential phase during growth on glycerol (mcl-PHA non-permissive condition). This key observation was confirmed using RT-qPCR. The qPCR results (**Table 4-2**) supported the RNASeq data, and showed that the transcription level of *pha*C1 was clearly higher in the WFA culture. Analysis of the qPCR data by T-test revealed that abundance of *pha*C1 transcripts in the WFA culture were significantly different from the abundance of *pha*C1 transcripts in the WG cultures ($P = 0.04$), whereas all the others were not significant from each other. The lack of correlation between mRNA and protein expression profiles of two mcl-PHA synthases suggests the potential for post-transcriptional regulation that is specific to the WG culture. 2) Specific expression patterns of several mcl-PHA monomer supplying proteins (PhaG, PhaJ1, and PhaJ4) across the growth phase and substrates were observed. Expression of the *pha*G gene was specific to WG cultures but not WFA cultures. However, surprisingly, we noticed that the *pha*J4 gene (which usually

proposed to be the key protein for mcl-PHA biosynthesis from fatty acids (Sato et al., 2011) was significantly up-regulated in the WG culture during the mcl-PHA synthesis condition; 4) Two putative mcl-PHA granule associated protein coding genes, *pha*I and *pha*F, had the highest Pnet and Rnet values, which indicats that these gene products were most up-regulated in the mcl-PHA biosynthesis gene cluster under the conditions tested that favoured PHA production (WG-stationary phase and WFA-exponential phase). The enzymes encoded by these genes were also the most abundant proteins among all mcl-PHA biosynthesizing enzymes detected (**Table 4-1**) suggesting their essential role for active mcl-PHA synthesis. Interestingly, unlike PhaF, the expression of PhaI was not detectable at mid-log WG culture (e.g. non-mcl-PHA producing condition).

Table 4-1. Expression values of key mcl-PHA biosynthesis genes under three experimental conditions [a].

				WG (Sta vs Exp)		WFA vs WG (Exp)	
Locus-tag (PPUTLS46_)	**Gene symbol**	**Expression abundance [b]**		**Differential expression [c]**		**Differential expression [c]**	
		RNA	**Protein**	**Rnet**	**Pnet**	**Rnet**	**Pnet**
005596	*pha*I	10.1	**- [d]**	**5.90**	**+ [e]**	**6.61**	+
005601	*pha*F	12.7	21.5	**2.49**	**2.47**	**3.91**	**2.42**
005606	*pha*D	9.7	-	-0.53	-	0.07	-
005611	*pha*C2	11.3	17.0	-0.17	**2.53**	0.72	**2.05**
005616	*pha*Z	10.6	-	0.1	-	-	-
005621	*pha*C1	12.1	19.0	0.83	**2.04**	**1.94**	**1.74**
013888	*pha*G*	13.1	-	**2.09**	+	**-2.27**	-
021056	*pha*J1*	10.5	17.4	-	-	0.46	0.03
006576	*pha*J4	11.4	-	0.79	+	0.94	+

[a] Exponential versus stationary growth phase in waste glycerol versus exponential growth phase in waste free fatty acids;

[b] Log2 expression abundance of gene products (mRNA and Protein) of *P. putida* LS46 grown under mid-log phase of waste glycerol culture (non-mcl-PHA synthesis condition). Values were averaged from two biological replicates;

[c] Differential expression values (see details in the Materials and Method section) of gene products under the specific comparing conditions: Sta, Stationary phase; Exp, Exponential phase; Significantly up and/or down-regulated proteins are indicated in bold;

[d] a "-" symbol means not detected mRNA and/or protein expression under mid-log phase of WG culture and/or two tested mcl-PHA synthesis condition(s);

[e] a "+" symbol means protein expression of the gene was detectable under the specific mcl-PHA synthesis conditions: stationary culture of WG and/or exponential culture of WFA, respectively (e.g. protein expression abundance of PhaI: 22.9 and 23.5; PhaG: 17.1 under stationary culture of WG; PhaJ4: 19.1 and 18.9);

a * symbol indicates proteins (if detected) with S/N (signal to noise) ratio less than 2.8, and thus having FDR greater than 10 %.

Table 4-2. Transcription levels of the two *P. putida* LS46 mcl-PHA Synthases under three experimental conditions, as determined by RT-qPCR.

Locus-tag (PPUTLS46_)	**Gene symbol**	**RT-qPCR[a] (cDNA ng x 10)**		
		WG (Exp)	**WG (Sta)**	**WFA (Exp) [b]**
005611	*pha*C2	0.19 ± 0.02	0.13 ± 0.06	0.20 ± 0.09
005621	*pha*C1	0.36 ± 0.09	0.49 ± 0.18	0.89 ± 0.15

[a] cDNA values of each gene from10 ng total cDNA input for RT-qPCR under three studied experimental conditions;

[b] Analysis of the qPCR data by a Two-tail T-test revealed that abundance of *pha*C1 transcripts in the WFA culture were significantly different from the abundance of *pha*C1 transcripts in theWG cultures (P = 0.04, where the threshold was P=0.05), whereas all the others were not significant from each other.

4.4.3 State-specific gene expression profile pertinent to mcl-PHA biosynthesis

The potential driving force behind the observed specific mcl-PHA production profiles, induced either by growth phase or substrate was further studied by evaluating the gene expression profiles of the pathways in addition to mcl-PHA biosynthesizing genes, which may further control the polymer content and monomer composition.

4.4.3.1 Waste glycerol derived gene expression variations during mcl-PHA biosynthesis

The substrate (glycerol) consumption rate of *P. putida* LS46 in WG culture was decreased once the cells reached stationary phase under the active mcl-PHA biosynthesis conditions (**Figure 4-1A**). This was associated with significant reduction in protein expression of *glp*F gene, a transmembrane glycerol transportation facilitator, in the proteome of *P. putida* LS46 (**Figure 4-2**) suggesting the efficient transportation of extra-cellular glycerol into cytoplasm was restrained during stationary phase. The expression of other essential genes and homologs (i.e. *opr*B porin homologs) for glycerol transportation and catabolic initiation did not change significantly.

	Locus PPUTLS46_	RNA	Protein	waste glycerol (Sta vs Exp) Rnet	Pnet
OprB	022486	9.8	18.3	-1.16	-1.08
	014019	-	-	-	-
	002137	10.5	-	-1.36	-
	017699	6.7	-	1.46	-
GlpF	022196	11.8	20.5	-0.91	**-2.38**
GlpK ★	022201	13.8	23.0	-1.22	0.17
GlpD ★	022211	15.5	21.4	-0.03	-0.07
AccA	023463	11.5	21.7	-0.3	-0.92
AccB ★	023468	13.9	22.3	-0.64	0.09
AccC	000435	-	-	-	-
AccD ★	014614	12.3	20.7	0.75	0
FabD ★	000250	12	18.6	-0.02	0.45
FabH	020461	-	-	-	-
FabG ★	000255	12.6	20.1	0.23	0.01
	015924	10.1	19.5	-0.59	-0.43
	023353	11.3	17.7	-1.39	**1.82**
FabA	012710	11.7	17.4	1.13	1.42
FabZ	014589	11.1	19.6	-0.39	-0.8
FabV ★	012998	12.1	21.2	0.44	-0.19
FabB ★	012715	13.5	20.3	0.46	-0.49
FabF ★	000265	12.1	18.3	1.05	-0.14
IDH2	011960	20.4	22.8	-1.27	1.63
6PGD	012100	10.0	19.6	0.77	1.3
IDH1	011965	12.4	17.1	-0.6	**-4.29**
PDC	023483	7.0	19.7	-0.02	**-2.5**
	023488	7.8	20.2	0.03	**-2.32**
	023493	7.7	19.0	0.14	**-2.11**

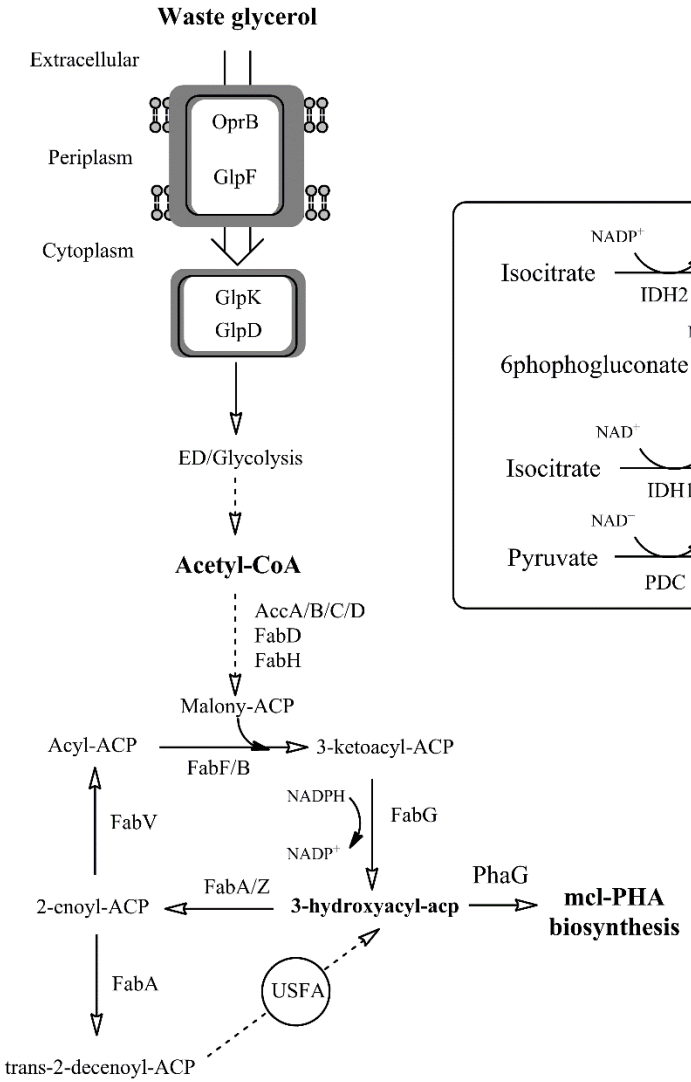

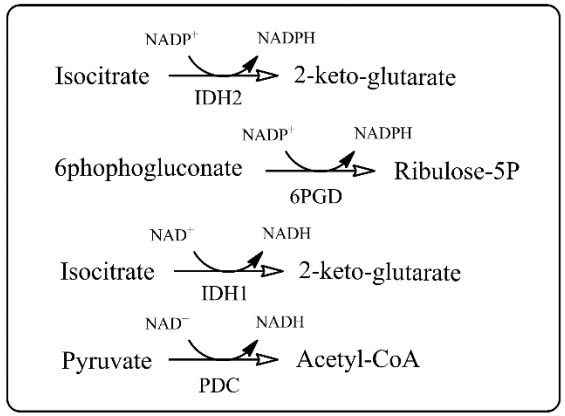

Figure 4-2. Expression values of genes and gene products involved in proposed mcl-PHA metabolism derived from waste glycerol (WG) culture of *P. putida* LS46. Numbers in each column (from left to right) represent: the gene locus tag; RNA abundance during Exponential phase of WG cultures; Protein abundance during Exponential phase of WG cultures; Values were averaged from two biological replicates; Rnet and Pnet values from WG cultures in Stationary phase versus Exponential phase; Significantly up-regulated mRNAs or proteins are indicated in green font; Significantly down-regulated mRNA or proteins are indicated in red font; -, not detected, and therefore no Rnet or Pnet value associated. A star symbol in front of gene locus tag indicates proteins (if detected) with S/N (signal to noise) ratio less than 2.8, and thus having FDR greater than 10 %. USFA: unsaturated fatty acid. Gene symbols for each putative pathway protein were also given. IDH1: putative NAD^+ dependent isocitrate dehydrogenase; IDH2: putative $NADP^+$-dependent isocitrate dehydrogenase; PDC: Pyruvate dehydrogenase complex; 6PGD: 6-phosphogluconate dehydrogenase.

During *de novo* fatty acid synthesis in *P. putida* LS46, acetyl-CoA was used by the pathway enzymes to generate 3-hydroxyacyl-ACP, a key precursor molecule for mcl-PHA biosynthesis (**Figure 4-2**). The 'Omics data suggested a few gene products were up-regulated during active mcl-PHA synthesis, putatively at the steps that provide key pathway intermediates for polymer synthesis (**Figure 4-2**). Protein levels of a putative ketoacyl-ACP reductase (FabG, encoded by PPUTLS46_023353) which is one of 8 homologs identified in the *P. putida* LS46 genome (**S7 Table**) that provide various 3-hydroxyacyl-ACP intermediates was highly up-regulated in stationary phase of WG cultures when there was active mcl-PHA synthesis. RNAseq analysis, however, indicated down-regulation of this gene at the transcriptional level. In addition, increased expression level of the *fab*A gene was observed though not considered as statistically significant up-regulated during stationary phase in WG cultures (i.e. during active mcl-PHA synthesis). Two isoforms of beta-hydroxyacyl-ACP dehydratases (FabA and FabZ) identified in the genome of *P. putida* LS46 carry-out dehydration reactions to produce *trans*-2-acyl-ACP, and FabA also carries out an isomerization reaction leading to the unsaturated fatty acids biosynthesis (Kimber et al., 2004), which could also be a critical point for unsaturated mcl- PHA production from fatty acid *de novo* synthesis (**Figure 4-2**).

Over-expression of the genes for trehalose biosynthesis was observed during mcl- PHA synthesis in WG culture, and these genes are located in a gene cluster with putative glycogen metabolism genes (**Table 4-3**). Trehalose can be synthesized from maltose by trehalose synthase (coded by *tre*S), or synthesized from maltodextrine by enzymes encoded by *tre*Z and *tre*Y (Roca et al., 2013; Su et al., 2014). Under the current study, putative trehalose synthase (*tre*S, PPUTLS46_012155) has been up-

regulated. Simutaneously, putative glycogen degrading enzymes coded by *mal*Q (PPUTLS46_012120) and *glg*P (PPUTLS46_005431) which putatively offered the precursor for trehalose biosynthesis (Simon et al., 2014). An additional trehalose synthase coding gene (PPUTLS46_002907) was identified in *P. putida* LS46, however detected only at mRNA level (i.e. no protein was detected). Finally, 'Omics analysis has revealed differential expression level (mostly at protein level) of genes putatively involved in recycling of cellular reducing equivalents, such as NADH and NADPH, under the mcl-PHA synthesizing stage (**Figure 4-2**).

Table 4-3. Expression values of gene clusters putatively involved in trehalose biosynthesis and polyphosphate degradation in *P. putida* LS46 under mcl-PHA permissive vs non-permissive conditions in WG cultures.

					WG (Sta vs Exp)	
Locus-tag PPUTLS46_	**Gene symbol**	**Gene product**	**Expression abundance [a]**		**Differential expression [b]**	
			RNA	**Protein**	**Rnet**	**Pnet**
012110	*glg*A	glycogen synthase	- [c]	-	-	-
012115	*tre*Y	Malto-oligosyltrehalose trehalohydrolase	-	-	-	-
012120	*mal*Q	4-alpha-glucanotransferase	9.94	19.10	-0.07	**2.06**
012125	*tre*Z	maltooligosyl trehalose synthase	-	-	-	-
012130	*	protein of unknown function	8.98	20.04	-0.07	0.06
012135	*glg*X	glycogen debranching protein	-	-	-	-
012140		hypothetical protein	9.07	-	-0.44	-
012145		outer membrane autotransporter	7.34	-	0.99	-
012150	*glg*B*	glycogen branching enzyme	11.34	19.80	-0.42	1.21
012155	*tre*S	trehalose synthase	9.95	21.02	-0.59	**2.76**
012160		alpha amylase family protein	10.19	20.09	-0.9	1.28
002907	*tre*S	trehalose synthase (*Pseudomonas stutzeri* type)	7.66	-	0.11	-
005431	*glg*P	glycogen phosphorylase	11.14	22.36	-0.47	**2.45**

[a] Log2 expression abundance of gene products (mRNA and Protein) of *P. putida* LS46 grown under mid-log phase of waste glycerol culture (non-mcl-PHA synthesis condition). Values were averaged from two biological replicates;

[b] Differential expression value of gene products under the specific comparing conditions: Sta, Stationary phase; Exp, Exponential phase; Significantly up-regulated mRNA and/or proteins are indicated in bold;

[c] a "-" symbol means not detected mRNA and/or protein expression under mid-log phase of WG culture and stationary culture of WG culture.

a * symbol indicates proteins (if detected) with S/N (signal to noise) ratio less than 2.8, and thus having FDR greater than 10 %.

4.4.3.2 Waste fatty acids derived gene expression variations during mcl-PHA biosynthesis

'Omics analysis identified putative enzymes essential for waste fatty acids transport, activation and catabolism via fatty acid β-oxidation. The expression level of most of these genes were significantly up-regulated in WFA cultures compared with the WG cultures as expected (**Figure 4-3**).

	Locus PPUTLS46_	RNA	Protein	WFA vs WG (Exp) Rnet	Pnet
FadL	015009	12.0	21.1	**3.57**	**3.31**
FadD ★	021046	10.8	18.5	0	0.18
	021041	11.0	18.6	**2.7**	**2.89**
	016739	8.8	-	-0.21	-
FadE	024448	16.6	24.3	**3.25**	**3.54**
★	006756	10.8	18.7	-0.33	0.59
★	000145	11.1	18	-0.7	0.15
★	002522	9.6	17.6	0.46	0.52
FadA	004399	16.1	25.5	**4.4**	**4.65**
FadB	004404	15.6	24.7	**3.79**	**4.8**
Cluster 4	026256	9.6	-	1.56	-
	026251	11.1	11.7	**1.73**	**2.19**
	026246	11.7	20.8	**1.66**	**1.76**
ACTO	009584	10.1	19.1	0.16	**3.17**
AceA	012430	16.2	26.3	**4.08**	**5.85**
GlcB	024508	13.2	23.2	**1.98**	**2.82**

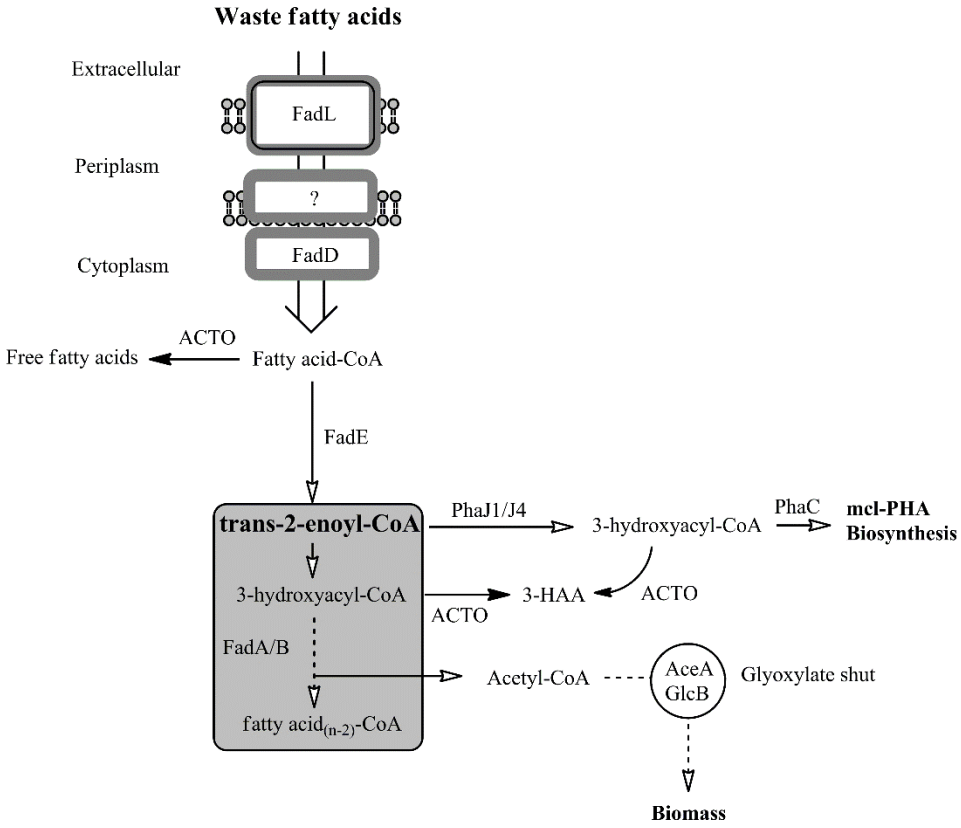

Figure 4-3. Expression values of genes and gene products involved in proposed mcl-PHA metabolism derived from waste fatty acids (WFA) culture of *P. putida* LS46. Numbers in each column (from left to right) represent: the gene locus tag; RNA abundance during Exponential phase of WFA cultures; Protein abundance during Exponential phase of WFA cultures; Values were averaged from two biological replicates; Rnet and Pnet values from the Exponential phase of WFA versus WG cultures; Significantly up-regulated mRNAs or proteins are indicated in green font; -, protein expression was not detected, and therefore no Pnet value associated. A star symbol in front of gene locus tag indicates proteins (if detected) with S/N (signal to noise) ratio less than 2.8, and thus having FDR greater than 10 %. ACTO: putative acyl-CoA thioesterase. Gene symbols for each putative pathway protein were also given. 3-HAA: 3-hydroxyalkanoic acid; AceA: isocitrate lyase; GlcB: malate synthase.

P. putida encodes large numbers of fatty acid β-oxidation enzymes that putatively carry out parallel biochemical reactions, and differential expression of these pathway genes was shown to potentially effect mcl-PHA synthesis as well as the monomer composition of the polymer (Poblete-Castro et al., 2012; Guzik et al., 2013). Of the 18 identified *fad*E homologs identified in the *P. putida* LS46 genome, expression values of four FadE proteins were most abundant (**Figure 4-3 and S8 Table)**. The gene encoded by locus tag PUTLS46_024448 was the most significantly up-regulated *fad*E gene in the WFA culture. The multifunctional fatty acid β-oxidation complex, coded by the *fad*AB gene cluster (cluster 1), was highly up-regulated in the WFA culture. Furthermore, we found three more gene clusters in the genome of *P. putida* LS46 that are putatively involved in fatty acid oxidation (**S9 Table**), and cluster 4 genes were expressed at higher levels, and putatively under the regulation of the in-cluster TetR family regulator (PPUTILS46_026256) (**Figure 4-3**). The annotation of this gene cluster suggests its putative role in short chain fatty acid (≤ 4) degradation **(S9 Table**).

Finally, during the fatty acid oxidation, various CoA intermediates of the pathway are converted into their corresponding free acids by acyl-CoA thioesterase, which helps to control an optimal concentration of different pathway intermediates (Hunt et al., 2002). Expression of an acyl-CoA thioesterase-like protein (PPUTILS46_009584) was expressed at much higher levels in WFA cultures than in WG cultures (**Figure 4-3**). In addition, significant amount of acetyl-CoA from the fatty acid oxidation may flux to the "glyoxylate shunt", as suggested by highly up-regulated isocitrate lyase and malate synthase, which may serve as an important route for C2 assimilation to prevent carbon spillage in the form of CO_2 (Maloy et al., 1980).

4.5 Discussion

Using biodiesel derived waste streams, such as waste glycerol and waste fatty acids, for mcl-PHA synthesis would potentially decrease the product cost, and therefore benefits the industrial biopolymer production. To study and predict the potential genetic targets that regulate mcl-PHA biosynthesis profile of *P. putida* LS46 grown under biodiesel derived waste carbon sources, multi-level 'Omics analyses were used to correlate the observed variations in mcl-PHA synthesis with differences in gene expression profiles with respect to: 1) mcl-PHA biosynthesis activation; 2) itracellular accumulation of mcl-PHA polymers; and 3) differences in monomer composition of the polymers.

4.5.1 mcl-PHA biosynthesis activation machineries

Converting fatty acid metabolism pathway intermediates for mcl-PHA synthesis was dependent on two processes: monomer supplying genes (*pha*G, *pha*J1, and *pha*J4) and the PHA synthesis cluster genes (*pha*C1/Z/C2/D, and *pha*I/F). Induction of mcl-PHA synthesis by nitrogen limitation has been well reported in *P. putida* strains using structurally non-related carbon sources, such as glucose (Poblete-Castro et al., 2013) and glycerol (Fu et al., 2014). This was due to induction of transcription of the key mcl-PHA monomer supplying gene, *pha*G, by nitrogen depletion (Poblete-Castro et al., 2012; Hoffmann et al., 2004). This was also observed under the current study (**Table 4-1**). Under the exponential phase in WG culture, transcription levels of the *pha*G gene was much lower compare to the stationary WG culture, and expression of PhaG protein did not detected (**Table 4-1**). Whereas the expression of PhaG protein was detectable in the stationary phase in WG culture with an expression abundance value at 17.1.

In addition to PhaG mediated induction of mcl-PHA biosynthesis, stationary phase WG cultures may also activate PhaJ4-driven polymer synthesis route (**Table 4-1**). A possible mechanism for this would be conversion of acyl-ACP from fatty acid biosynthesis into free fatty acids by thioesterase, which is used in PhaJ4 mediated polymer synthesis (Qiu et al., 2005). Homologs of *E. coli* type I and II thioesterase that hydrolyze both acyl-ACP and acyl-CoA (Spencer et al., 1978) were identified in the *P. putida* LS46 genome (PPUTLS46_009584/006916/009634), however, with no significant changes in the levels of either transcription or protein expression in stationary versus exponential phases of WG cultures of *P. putida* LS46.

When grown on waste fatty acids, mcl-PHA biosynthesis was observed even in the presence of adequate nitrogen concentrations (**Figure 4-1B**) suggesting activation of mcl-PHA synthesis in culture containing free fatty acids did not require strict nitrogen limitation (Sun et al., 2007). Rather, the mcl-PHA precursor was putatively synthesized by two proposed monomer supplying proteins: PhaJ4 and PhaJ1 (Sato et al., 2011; Fukui et al., 1998), which were both expressed in the WFA culture while nitrogen was still in excess (**Table 4-1 and Figure 4-1 B)**. Within the two proteins, expression of PhaJ4 was observed during mcl-PHA biosynthesis under both WFA and WG cultures suggesting the primary role in mcl-PHA biosynthesis derived from fatty acid beta-oxidation pathway (Sato et al., 2011).

In terms of the mcl-PHA biosynthesis gene cluster, up-regulation of the PHA synthase enzymes, PhaC1 and PhaC2, was observed for mcl-PHA biosynthesis under the two mcl-PHA synthesizing conditions: i.e. stationary phase of WG cultures and exponential phase of WFA culture (**Table 4-1**). However, expression of these two

enzymes may be regulated by different mechanisms under the different growth specific conditions: 1) Although there were differences in the levels of PhaC1 and PhaC2 protein expression levels, no differences in the levels of *pha*C1 and *pha*C2 transcripts were observed between the stationary and exponential phases of WG cultures. These data suggest post-transcriptional regulation of PHA synthase enzyme expression in WG cultures (**Table 4-1 and 4-2**). It has been demonstrated that PhaC1 expression is repressed in *P. putida* KT2442 when cultured in media containing balanced carbon and nitrogen concentrations by regulatory mechanisms mediated by RsmA and Crc (Ryan et al., 2013; La et al., 2014). The Crc (Catabolite repression control) protein was showen to repress PhaC1 translation under balanced carbon and nitrogen conditions, during exponential growth in LB culture (La et al., 2014). However, the Crc regulator was not detected the under conditions tested in the current work at either the mRNA or Protein level. RsmA (Regulator of secondary metabolites), another regulator of metabolism, belongs to CsrA (Carbon storage regulator) superfamily, and its role typically involves management of carbon storage, expression of virulence or biocontrol factors (Karine et al., 2008). Recently, it has been suggested that the RsmA protein is involved in post-transcriptional regulation of the PhaC1 protein putatively through a Gac/Rsm regulatory cascade (Ryan et al., 2013). Two CsrA homologs (PPUTLS46_02063 and PPUTLS46_015344) were detected in the current transcriptome, but not in the proteome, of *P. putida* LS46, suggesting these regulators were likely expressed at low levels, and with no significant changes in expression levels across the tested experimental conditions. RNA abundance of the two *csr*A homologs during the exponential growth phase in waste glycerol (WG) cultures were 7.69 and 6.04, respectively. The exact mechanism of this regulator on mcl-PHA biosynthesis is still

unclear in *P. putida*. 2) In contrast, higher levels of *pha*C1 transcripts and PhaC1 protein were observed in WFA cultures compared to WG cultures during exponential phase (**Table 4-1 and 4-2)**. The in-cluster transcriptional activator, PhaD, likely activated *pha*C1 transcription when *P. putida* LS46 was cultured with waste free fatty acids (Yang et al., 2012).

A previous study of the PhaF protein has suggested that it has an essential role in mcl-PHA segregation during active cell division of *P. putida* KT2442 (grown on fatty acids), through binding polymer granules to the bacterial chromosome (Perito et al., 2011). In our study, significant up-regulation of *pha*F transcripts and gene product (PhaF) was observed during mcl-PHA synthesis in WFA cultures during exponential phase and WG cultures during stationary phase. This suggested that detectable amount of mcl-PHA synthesized during stationary WG culture requires more phasin protein (e.g PhaF) for proper distribution of polymer into daughter cells, even though the cells may have a relatively low rate of cell division compared to cells in exponential growth phase in WFA cultures. The biological function of PhaI protein is still unknown. However, expression of the PhaI protein could only be detected during mcl-PHA synthesis (**Table 4-1**), suggesting expression of this protein may be tightly regulated during the time when mcl-PHA were not being actively synthesized.

4.5.2 Molecular targets potentially affect the cellular mcl-PHA content

Attempts have been made to identify genetic targets that potentially affect mcl-PHA synthesis under the current experimental conditions (i.e. in the WG and WFA cultures). Reduced glycerol uptake rate was observed during the active mcl-PHA synthesis in WG culture **(Figure 4-1A**), which potentially counteracted with the

efficient mcl-PHA production. Physiologically, limiting glycerol transport in the stationary phase of *P. putida* LS46 WG culture would reduce the energy requirement for converting intra-cellular glycerol into glycerol-3-phosphate, and further metabolism (Schweizer et al., 1997), and repressed expression of the transmembrane glycerol uptake facilitator (GlpF) (Escapa et al., 2013) may be the most efficient strategy for cells to suppress further glycerol transport (**Figure 4-2**). Reduced glycerol uptake, may have an effect on cell osmolality, as the high glycerol content of the culture medium could putatively create a hypertonic environment for *P. putida* LS46 cells. To counter this osmotic stress in WG cultures during active mcl-PHA synthesis, *P. putida* LS46 may specifically responded by up-regulating trehalose synthase (TreS)(**Table 4-3**), putatively increasing the intracellular concentration of trehalose (Borrero-de Acuña et al., 2014; Ma et al., 2006). Trehalose has been identified as protective agent under varies stress conditions, such as osmotic stress (Su et al., 2014; Freeman et al., 2010), thermoltolerance (Regine et al., 1991), desiccation (Roca et al., 2012) although the biosynthesis pathway, along with clustered putative glycogen synthesis pathway (Follonier et al., 2014), potentially compete with mcl-PHA biosynthesis by diverting acetyl-CoA into gluconeogenesis. During mcl-PHA synthesis via the fatty acid *de novo* synthesis pathway in WG cultures, over-expression of putative FabG (PPUTLS46_023353) potentially increased the cellular 3-hydroxyacyl-ACP pool, a key precursor for mcl-PHA biosynthesis (**Figure 4-2**). In addition, the reaction also couples with NADPH consumption, although some FabG homologs are also NADH-dependent (Javidpour et al., 2014). Up-regulation of FabG protein may facilitate a higher proportion of reducing equivalents directed to fatty acids biosynthesis during the active mcl-PHA synthesis stage of *P. putida* LS46 grown on waste glycerol.

Simultaneously, *P. putida* LS46 up-regulated enzymatic reactions putatively to replenish the cellular NADPH pool via NADP-dependent isocitrate dehydrogenase (PPUTLS46_011960) (Wang et al., 2015) and 6-phosphogluconate dehydrogenase (PPUTLS46_012100), whereas expression of numerous tricarboxylic acid (TCA) cycle enzymes that supply bulk of NADH, such as putative NAD^+-dependent isocitrate dehydrogenase and pyruvate dehydrogenase, were significantly down-regulated during the mcl-PHA synthesis stage in WG cultures (**Figure 4-2**). A similar pattern of expression for these enzymes was observed in *P. fluorescence* under oxidative stress (Singh et al., 2007), suggesting their essential roles in balancing cellular reducing equivalents (i.e. level of NADH/NADPH). Elevated intracellular ratios of $NADH/NAD^+$ and $NADPH/NADP^+$ are known to be important for PHA biosynthesis in many gram-negative bacteria (Lee et al., 1995; Lee et al., 1996; Ren et al., 2010; Ren et al., 2009). Over-expression of pyruvate dehydrogenase subunit (*aco*A) was shown to have positive effect on maximizing mcl-PHA production of *P. putida* KT2440 grown on glucose (Borrero-de Acuña et al., 2014), which putatively increased the acetyl-CoA and NADH pool used in fatty acid biosynthesis during mcl-PHA biosynthesis stage.

P. putida LS46 growth on waste fatty acids was maintained simultaneously with synthesis of mcl-PHA (**Figure 4-1 B**), which corresponds with the high levels of expression observed for mcl-PHA biosynthesis and glyoxylate shunt enzymes (**Figure 4-3**). Elevated levels of the glyoxalate shunt have also been observed in *Escherichia coli* during growth on fatty acids (Maloy et al., 1980). The two pathways may thus prevent large amounts of carbon being oxidized to through the TCA cycle by directing the carbon to biomass production and polymer synthesis in waste fatty acid cultures. As for mcl-PHA biosynthesis, production of the key precursor pathway trans-2-enoyl-CoA is

putatively provided by acyl-CoA dehydrogenase (FadE, PPUTLS46_024448) (**Figure 4-3**). Expression level of this enzyme were found to be a limiting factor for PHA synthesis by recombinant *E. coli* (Lu et al., 2003).

Highly expressed putative acyl-CoA thioesterase (PPUTLS46_009584) has 23 % amino acid sequence identity to the well-studied *E. coli* type II acyl-CoA thioesterase (encoded by *tes*B) and 40 % amino acid identity to a *tes*B-like 3-hydroxyacyl-CoA specific thioesterase in a PHA producing, hydrocarbon degrading gram-negative bacterium, *Alcanivorax borkumensis* SK2 (Sabirova et al., 2006). Till now, effect of *P. putida* thioesterase expression on mcl-PHA production has not been studied in *P. putida* strains. The expression of acyl-CoA thioesterase may be strongly associated with the fatty acid metabolism in term of mediating the amount of the pathway intermediates for optimized fatty acid oxidation (Hunt et al., 2002), and in some case, resulted in phenotypic benefit for cell grown on hydrocarbon (Déziel et al., 2003; Tuleva et al., 2002). Such that this enzyme represents a "branch-point" allowing either the storage of the metabolic precursors in the form of PHA or the ability to hydrolyze fatty acids CoA esters.

4.5.3 Factors that potentially determine the mcl-PHA monomer composition

Although PhaC1 and PhaC2 are the enzymes that carry-out PHA polymerization, the composition of the polymer may be also determined by several monomer supplying enzymes that convert fatty acids to various 3-hydroxyacyl-CoA precursors which are then utilized by the PHA synthases. The monomer supplying enzymes were differentially expressed under the two mcl-PHA permissive conditions used in this study. The PhaG enzyme has been associated with a preference for 3-hydroxydecanoyl-ACP in *P. putida*

KT2440 (Rehm et al., 2001; Wang et al., 2011). High levels of PhaG expression were also observed in *P. putida* LS46 cultured with WG, which synthesized mcl-PHA that contained a high mol % of 3-hydroxydecanoic acid (C10) subunits. Mcl-PHA polymers synthesized by *P. putida* LS46 cultured with WFA contained a high mol % of 3- hydroxyoctanoic acid (C8) subunits. PhaJ1 has been shown to synthesize R-3-hydroxyoctanoyl-CoA (Sato et al., 2011). Considering the fact that PhaJ4 was expressed under both mcl-PHA permissive conditions, specific expression of PhaJ1 in *P. putida* LS46 cultured with WFA may contribute to the increased mol% of C8 monomers in the polymers synthesized. In addition to the monomer supplying proteins synthesized by *P. putida* LS46 in the presence of free fatty acids, this strain also encodes and expresses a large number of putative "redundant" fatty acid oxidation genes that carry out parallel reactions, and whose expression may vary under different growth condition (Guzik et al., 2014; Poblete- Castro et al., 2012). FadE carries out the dehydration of acyl-CoA into trans-enoyl-CoA, an important intermediate for mcl-PHA synthesis **(Figure 4-3**). Except for its potential role in mcl-PHA production as mentioned above, effect of expression of FadE (as well as other fatty acid oxidation enzymes) on mcl-PHA monomer composition is largely unknown, due to large number of isozymes with limited data on enzymatic activity analysis or knockout experiments (Nelson et al., 2002). In the current study, PPUTLS46_024448 (one of a number of FadE homologs in *P. putida* LS46) and Cluster 1 fatty acid oxidation enzymes (**Figure 4-3**) were up-regulated in WFA cultures, and thus may play a primary role in synthesis of acyl-CoA intermediates. Ortholog of these enzymes were shown to induced by long chain fatty acids ($\geq$ C14) in *P. putida* KT2440 and *P. aeruginosa* PAO1 (McMahon and Mayhew, 2007; Kang et al., 2008), which agrees with the fact that long chain fatty acids are the

primary substrate in WFA cultures in the current study. Non-detected Cluster 2 and 3 proteins (some of these clusters genes were identified in RNAseq, however at much lower transcription level compare to Cluster 1 genes, **S9 Table**) in *P. putida* LS46 cultured with WFA likely serve as alternative fatty acid oxidation enzymes induced when expression of major fatty acid oxidation enzymes (Cluster 1) were not favoured or been knockout out (Kang et al., 2008). Over-expression of Cluster 3 proteins led to a higher proportion of C10 monomers in mcl-PHA polymers synthesized by *P. putida* KT2440 grown on decanoic acid (Poblete-Castro et al., 2012), suggesting expression of different fatty acid oxidation enzymes effect the polymer composition.

Finally, in the current study, we have suggested a correlation between expression of the FabA protein (**Figure 4-3**) and synthesis of mcl-PHA with unsaturated subunits by in *P. putida* LS46 cultured with WG during active PHA synthesis (i.e. stationary phase). The FabA enzyme has been shown to carry-out an essential step in unsaturated fatty acid biosynthesis from the fatty acid *de novo* synthesis in *P. aeruginosa* PAO1 (Kimber et al., 2004), and forms cis-3-decenoyl-ACP (Hoang and Schweizer, 1997) which is then converted to 3-hydroxy-cis-5-dodecanoyl-ACP (C12:1), which may be used in the synthesis of unsaturated mcl-PHA monomers. The monomer profile observed in mcl-PHA synthesized by *P. putida* LS46 cultured with WG (**S6 Table**) is consistent with this process. This mechanism may be more generally applied to other mcl-PHA structurally non-related carbon sources, such as glucose (Poblete-Castro et al., 2013).

Chapter 5

Summary, Conclusions, and Future Work

5.1 Summary of the major findings

Soil bacteria have very versatile metabolisms, which is one of the reasons that they are of great interest for a wide variety of biotechnology applications, including synthesis of biofuels, biopolymers, fine chemicals, and bioremediation, as well as plant growth promoting and pathogen protection properties (Schmid et al., 2001; Espinosa-Urgel et al., 2002).

Pseudomonas putida, a non-pathogenic heterotrophic soil bacteria, is able to catabolize various carbon sources into precursor metabolites, which are used as building blocks for cell growth (biomass) and storage compounds (biopolymers) with industry applications, although polymer biosynthesis is often neither the primary goal, nor the only survival strategy for bacteria that colonize various ecological niches (Espinosa-Urgel et al., 2002; Nelson et al., 2002). Thus, polymer synthesis does not usually reach its maximum potential in nature, but can be optimized under laboratory and industrial conditions (Akaraonye et al., 2010; Sun et al., 2007).

Fortunately, the ability of *Pseudomonas* species to catabolize a variety of carbon sources has broadened the range of feedstocks that can be used for polymer synthesis for industrial purposes. The initial uptake and metabolism of carbon sources by *P. putida* is accomplished by various nutrient transport systems, that may then be metabolized via a variety of pathways: the Entner-Doudoroff (ED) (as the strain lack of the complete glycolysis pathway) for sugars and polyols; Fatty acid β-oxidation for various free fatty acids, and the β-ketoadipate (ortho-cleavage) pathway for degradation of aromatic

hydrocarbon compounds, like as benzoate (Sudarsan et al., 2014). Dicarboxylic acids, such as succinate, enter the TriCarboxylic Acid (TCA) cycle directly. However, *P. putida* is not able to grow on pentose sugars, such as xylose (Meijnen et al., 2009).

These pathways produce essential precursor metabolites for anabolism. Acetyl-CoA is key precursor for both fatty acid biosynthesis and PHA production by *P. putida* from non-fatty acid carbon sources, while the fatty acid β-oxidation directly channels free fatty acids into polymer biosynthesis (Rehm, 2010). Mcl-PHA biosynthesis in *P. putida* is, therefore, potentially regulated by the metabolic demands of the cell (i.e. growing on different carbon sources). In Chapter 2, we have shown that mcl-PHA synthesis profiles (with regard to cellular content and monomer composition) were different in *P. putida* LS46 cultured with biodiesel-derived waste glycerol versus waste fatty acids culture. These results support Hypothesis 1, that the percent dry cell weight accumulation and monomer composition of mcl-PHA in *P. putida* LS46 are substrate-specific.

Although as potential candidate carbon source, culturing *P. putida* LS46 with industrial waste carbon sources such as biodiesel-derived glycerol or free fatty acids, comes with the potential problem that "impurities" in these substrates may have a negative impact on growth and/or polymer synthesis. In Chapter 3, we detected the presence of metal ions, including a number of heavy metal ions, in biodiesel-derived waste glycerol. However, we observed that growth and polymer synthesis by *P. putida* LS46 cultured with pure glycerol versus waste glycerol were similar, suggesting the impurities of waste glycerol have no (or very little) effect on *P. putida* LS46 growth under the studied conditions. This may suggest potential adaptation of *P. putida* LS46 to waste glycerol culture. The genome of *P. putida* is known to encode genes that play a role in resisting various toxic materials, including heavy metals (Wu et al., 2011). In

the Chapter 3, comparative transcriptomics and proteomics analyses revealed the up-regulation of genes putatively involved in heavy metal resistance when cultured with waste glycerol versus pure glycerol. The finding supports Hypothesis 2, that *P. putida* LS46 would express heavy metal resistance genes and gene products, and/or regulatory elements associated with heavy metal resistance genes, when growing on biodiesel-derived waste glycerol.

In Chapter 4, transcriptomic and proteomic analyses of *P. putida* LS46 cultured with biodiesel-derived glycerol or free fatty acids, and under three different physiological conditions, were explored. Two active mcl-PHA biosynthesis conditions were compared with a condition in which mcl-PHA biosynthesis was not active during exponential growth of *P. putida* LS46 on waste glycerol culture. The corresponding transcriptomic and proteomic analyses revealed the specific expression profile of genes and/or gene products in mcl-PHA biosynthesizing cluster and monomer supplying pathways in waste glycerol versus waste free fatty acid cultures. Enzymatic reactions that putatively competes or favors mcl-PHA biosynthesis under the current study conditions were also predicted. Hence, Hypothesis 3, that differences in mcl-PHA synthesis patterns observed when *P. putida* LS46 was grown on different carbon sources are a consequence of differences in gene and/or gene product expression levels, was verified in Chapter 4.

5.2 Conclusions and future works

Bacterial medium chain length poly-3-hydroxyalkanoate (mcl-PHA) biopolymers have great potential for a variety of industrial applications (Chen, 2009). Development of an economically feasible biopolymer production platform, however, depends heavily on substrate cost and the bacterial strain used. Biodiesel-derived waste streams (waste

glycerol and waste fatty acids) are of great interest as carbon sources due to their abundance and low cost. A robust and high mcl-PHA yielding bacterial strain is critical for optimized industrial fermentation processes.

The capacity and adaptability of *P. putida* LS46 to grow and produce mcl-PHA polymers using industrial waste carbon sources were explored in Chapters 3 and 4. However, the relatively low waste glycerol utilization and mcl-PHA production in these experiments suggests the need for optimization of the polymer production process. This could be achieved by using bioreactors with better control of the process parameters and overcome some of the potential metabolic constraints that limit the intracellular mcl-PHA production. For mcl-PHA production using waste glycerol, high biomass concentrations are needed prior to the initiation of polymer synthesis in order to maximize polymer production during the stationary phase. To achieve high biomass concentration, ideally, cell growth could be maintained exponentially at a certain growth rate in a fed-batch with major nutrients (such as carbon/nitrogen) fed continuously. Alternatively, these nutrients can also be fed dis-continuously (i.e. pulsed). In addition, increasing polymer production by *P. putida* LS46 genetically will require a better understanding of the cell metabolism. The complexity of the *P. putida* genome endows this bacterium with great metabolic and regulatory versatility. The use of 'Omics analyses, including genomics, transcriptomics, and proteomics can provide the insight required to develop strategies to maximize cell specific polymer yield. Data from this thesis revealed that the potential capacity of *P. putida* LS46 to maximize mcl-PHA under the experimental conditions used was likely effected by the abundance of the gene products carrying out the enzymatic reactions of glycerol transportation, synthesis of mcl-PHA precursor molecules, and synthesis of cellular reducing equivalents. Thus, in the future, metabolic engineering

(knockout or over- expression of key genes) may be carried out for manipulation of following suggested enzymatic reactions and/or pathways involved with: i) substrate transportation; ii) synthesis of key polymer biosynthetic precursors (acetyl-CoA, 3-hydroxyacyl-ACP, and 3-hydroxyacyl-CoA); and iii) synthesis of cellular reducing equivalents (level of NADH/NADPH). Finally, the monomer composition of the polymers is an important character affecting the thermal and physical properties of mcl-PHA. Substrate-specific monomer composition appeared to be associated with different gene expression profiles of fatty acid metabolism and mcl-PHA monomer supplying proteins that (putatively) carry out the enzymatic steps that provide precursor molecules for mcl-PHA biosynthesis (Chapter 4); (Rehm et al., 2001; Sato et al., 2011). For example, FabA (3- hydroxydecanoyl-ACP dehydrase) was identified putatively as part of unsaturated mcl- PHA monomer synthesis pathway, chemically important functional groups (Sun et al., 2009), using the non-fatty acids carbon source, a topic that merits further study.

To sum up, by overcoming the metabolic constraints on mcl-PHA biosynthesis, together with optimized industrial-scale fermentation and down-stream extraction processes, medium chain length polyhydroxyalkanoate (mcl-PHA) production by *P. putida* has significant commercial potential with versatile applications.

References

Abraham, G. A., Gallardo, A., San Roman, J., Olivera, E. R., Jodra, R., García, B., Minambres, B., García, J. L., Luengo, J. M. 2001. Microbial synthesis of poly (β-hydroxyalkanoates) bearing phenyl groups from *Pseudomonas putida*: chemical structure and characterization. Biomacromolecules 2: 562-567.

Abedi, D. 2006. Biodegradable Biopolymers: An Overview on Polyhydroxyalkanoates. Iranian Journal of Pharmaceutical Research 2: 77-78.

Akaraonye, E., Keshavarz, T., Roy, I. 2010. Production of polyhydroxyalkanoates: the future green materials of choice. Journal of Chemical Technology and Biotechnology 85: 732-743.

Albuquerque, M., Eiroa, M., Torres, C., Nunes, B., Reis, M. 2007. Strategies for the development of a side stream process for polyhydroxyalkanoate (PHA) production from sugar cane molasses. Journal of Biotechnology 130: 411-421.

Amara, A., Rehm, B. 2003. Replacement of the catalytic nucleophile cysteine-296 by serine in class II polyhydroxyalkanoate synthase from *Pseudomonas aeruginosa* mediated synthesis of a new polyester: identification of catalytic residues. Journal of Biochemistry 374: 413-421.

Arias, S., Sandoval, A., Arcos, M., Cañedo, L. M., Maestro, B., Sanz, J. M., Naharro, G., Luengo, J. M. 2008. Poly-3-hydroxyalkanoate synthases from *Pseudomonas putida* U: substrate specificity and ultrastructural studies. Journal of Microbial Biotechnology 1: 170-176.

Ashby, R., Solaiman, D., Foglia, T. 2002. The synthesis of short-and medium-chain-length poly (hydroxyalkanoate) mixtures from glucose or alkanoic acid grown *Pseudomonas oleovorans*. Journal of Industrial Microbiology and Biotechnology

28: 147-153.

Ashby, R. D., Solaiman, D. K., Foglia, T. A. 2005. Synthesis of short/medium-chain-length poly (hydroxyalkanoate) blends by mixed culture fermentation of glycerol. Biomacromolecules 6: 2106-2112.

Babu, R. P., O'connor, K., Seeram, R. 2013. Current progress on bio-based polymers and their future trends. Progress in Biomaterials 2: 1-16.

Baker, M. 2011. Metabolomics: from small molecules to big ideas. Nature Methods 8: 117-121.

Bender, C., Cooksey, D. 1987. Molecular cloning of copper resistance genes from *Pseudomonas syringae* pv. tomato. Journal of Bacteriology 169: 470-474.

Bengtsson, S., Pisco, A. R., Johansson, P., Lemos, P. C., Reis, M. A. 2010a. Molecular weight and thermal properties of polyhydroxyalkanoates produced from fermented sugar molasses by open mixed cultures. Journal of Biotechnology 147: 172-179.

Bengtsson, S., Pisco, A. R., Reis, M. A., Lemos, P. C. 2010b. Production of polyhydroxyalkanoates from fermented sugar cane molasses by a mixed culture enriched in glycogen accumulating organisms. Journal of Biotechnology 145: 253-263.

Bolleter, W. T., Bushman, C. J., Tidwell, P. W. 1961. Spectrophotometric determination of ammonia as indophenol. Analytical. Chemistry 33: 592-594.

Borrero-De Acuña, J. M., Bielecka, A., Häussler, S., Schobert, M., Jahn, M., Wittmann, C., Jahn, D., Poblete-Castro, I. 2014. Production of medium chain length polyhydroxyalkanoate in metabolic flux optimized *Pseudomonas putida*. Microbial Cell Factories 13: 88-103.

Braunegg, G., Sonnleitner, B., Lafferty, R. M. 1978. A rapid gas chromatographic method for the determination of poly-beta-hydroxybutyric acid in microbial biomass. European Journal of Applied Microbiology 6: 29-37.

Braunegg, G., Lefebvre, G., Genser, K. F. 1998. Polyhydroxyalkanoates, biopolyesters from renewable resources: physiological and engineering aspects. Journal of Biotechnology 65: 127-161.

Brown, N. L., Ford, S. J., Pridmore, R. D., Fritzinger, D. C. 1983. Deoxyribonucleic acid sequence of a gene from the *Pseudomonas* transposon TN501 encoding mercuric reductase. Biochemistry 22: 4089-4095.

Brown, N. L., Stoyanov, J. V., Kidd, S. P., Hobman, J. L. 2003. The MerR family of transcriptional regulators. FEMS Microbiology Reviews 27: 145-163.

Budde, C. F., Riedel, S. L., Hübner, F., Risch, S., Popović, M. K., Rha, C., Sinskey, A. J. 2011. Growth and polyhydroxybutyrate production by *Ralstonia eutropha* in emulsified plant oil medium. Applied Microbiology and Biotechnology 89: 1611-1619.

Cai, L., Yuan, M. Q., Liu, F., Jian, J., Chen, G. Q. 2009. Enhanced production of medium-chain-length polyhydroxyalkanoates (PHA) by PHA depolymerase knockout mutant of *Pseudomonas putida* KT2442. Bioresource Technology 100: 2265-2270.

Cánovas, D., Cases, I., De Lorenzo, V. 2003. Heavy metal tolerance and metal homeostasis in *Pseudomonas putida* as revealed by complete genome analysis. Environmental Microbiology 5: 1242-1256.

Castillo, T. D., Ramos, J. L., Rodrıguez-Herva, J .J., Fuhrer, T., Sauer, U., Duque, E. 2007. Convergent peripheral pathways catalyze initial glucose catabolismin

Pseudomonas putida: genomic and flux analysis. Journal of Bacteriology 189: 5142-5152.

Cavalheiro, J. M., De Almeida, M., Grandfils, C., Da Fonseca, M. 2009. Poly-3-hydroxybutyrate production by *Cupriavidus necator* using waste glycerol. Process Biochemistry 44: 509-515.

Cerrate, S., Yan, F., Wang, Z., Coto, C., Sacakli, P., Waldroup, P. W. 2006. Evaluation of glycerine from biodiesel production as a feed ingredient for broilers. International Journal of Poultry Science 5: 1001-1007.

Cha, J. S., Cooksey, D. A. 1991. Copper resistance in *Pseudomonas syringae* mediated by periplasmic and outer membrane proteins. Proceedings of the National Academy of Sciences 88: 8915-8919.

Chan, S., Kanchanatawee, S., Jantama, K. 2012. Production of succinic acid from sucrose and sugarcane molasses by metabolically engineered *Escherichia coli*. Bioresource Technology 103: 329-336.

Chanprateep, S. 2010. Current trends in biodegradable polyhydroxyalkanoates. Journal of Bioscience and Bioengineering 110: 621-632.

Chatzifragkou, A and Papanikolaou, S. 2012. Effect of impurities in biodiesel-derived waste glycerol on the performance and feasibility of biotechnological processes. Applied microbiology and Biotechnology 95: 13-27.

Chee, J. Y., Tan, Y., Samian, M. R., Sudesh, K. 2010. Isolation and characterization of a *Burkholderia* sp. USM (JCM15050) capable of producing polyhydroxyalkanoate (PHA) from triglycerides, fatty acids and glycerols. Journal of Polymers and the Environment 18: 584-592.

Chen, G. Q. 2009. A microbial polyhydroxyalkanoates (PHA) based bio and materials

industry. Chemical Society Reviews 38: 2434-2446.

Chen, J. Y., Liu, T., Zheng, Z., Chen, J. C., Chen, G. Q. 2004. Polyhydroxyalkanoate synthases PhaC1 and PhaC2 from *Pseudomonas stutzeri* 1317 had different substrate specificities. FEMS Microbiology Letters 234: 231-237.

Chen, X. C., Wang, Y. P., Lin, Q., Shi, J. Y., Wu, W. X., Chen, Y. X. 2005. Biosorption of copper (II) and zinc (II) from aqueous solution by *Pseudomonas putida* CZ1. Colloids and Surfaces B: Biointerfaces 46: 101-107.

Choi, M. H., Xu, J., Gutierrez, M., Yoo, T., Cho, Y. H., Yoon, S. C. 2011. Metabolic relationship between polyhydroxyalkanoic acid and rhamnolipid synthesis in *Pseudomonas aeruginosa*: comparative 13C NMR analysis of the products in wild-type and mutants. Journal of Biotechnology 151: 30-42.

Christian, T., Stefan, P. A., Ansgar, P. 2013. Proteome turnover in bacteria: current status for *Corynebacterium glutamicum* and related bacteria. Microbial Biotechnology 6: 708-719.

Chuah, J. A., Tomizawa, S., Yamada, M., Tsuge, T., Doi, Y., Sudesh, K., Numata, K. 2013. Characterization of site-specific mutations in a short-chain-length/medium-chain-length polyhydroxyalkanoate synthase: In vivo and in vitro studies of enzymatic activity and substrate specificity. Applied and Environmental Microbiology 79: 3813-3821.

Chung, A. L., Jin, H. L., Huang, L. J., Ye, H. M., Chen, J. C., Wu, Q., Chen, G. Q. 2011. Biosynthesis and characterization of poly (3-hydroxydodecanoate) by β-oxidation inhibited mutant of *Pseudomonas entomophila* L48. Biomacromolecules 12: 3559-3566.

Costa, S. G., Lépine, F., Milot, S., Déziel, E., Nitschke, M., Contiero, J. 2009.

Cassava wastewater as a substrate for the simultaneous production of rhamnolipids and polyhydroxyalkanoates by *Pseudomonas aeruginosa*. Journal of Industrial Microbiology & Biotechnology 36: 1063-1072.

Da Silva, G. P., Mack, M., Contiero, J. 2009. Glycerol: a promising and abundant carbon source for industrial microbiology. Biotechnology Advances 27: 30-39.

Daniel, H. H., Jeremy D. S., Owen, W. 2003. The TIGRFAMs database of protein families. Nulceic Acid Research. 31: 317-373.

De Eugenio, L. I., Escapa, I. F., Morales, V., Dinjaski, N., Galán, B., García, J. L., Prieto, M. A. 2010a. The turnover of medium chain length polyhydroxyalkanoates in *Pseudomonas putida* KT2442 and the fundamental role of PhaZ depolymerase for the metabolic balance. Environmental Microbiology 12: 207-221.

De Eugenio, L. I., Galán, B., Escapa, I. F., Maestro, B., Sanz, J. M., García, J. L., Prieto, M. A. 2010b. The PhaD regulator controls the simultaneous expression of the *pha* genes involved in polyhydroxyalkanoate metabolism and turnover in *Pseudomonas putida* KT2442. Environmental Microbiology 12: 1591-1603.

de Smet, M. J., Eggink, G., Witholt, B., Kingma, J., Wynberg, H. 1983. Characterization of intracellular inclusions formed by *Pseludomonas oleovorans* during growth on octane. Journal of Bacteriology 154: 870-878.

Deretic, V., Hibler, N., Holt, S. 1992. Immunocytochemical analysis of AlgP (Hp1), a histonelike element participating in control of mucoidy in *Pseudomonas aeruginosa*. Journal of Bacteriology 174: 824-831.

Deretic, V and Konyecsni, W. 1990. A procaryotic regulatory factor with a histone H1-like carboxy-terminal domain: clonal variation of repeats within *alg*P, a gene involved in regulation of mucoidy in *Pseudomonas aeruginosa*. Journal of

Bacteriology 172: 5544-5554.

Desuoky, A., El-Haleem, A., Zaki, S., Abuelhamd, A., Amara, A., Aboelreesh, G. 2007. Biosynthesis of polyhydroxyalkanotes in wildtype yeasts. Journal of Applied Sciences and Environmental Management 11:5-10.

Dixon, M and Webb, E. C. 1964. Enzymes, 2nd edn.Longmans Green, London, and Academic Press, New York.

Diniz, S. C., Taciro, M. K., Gomez, J. G. C., Da Cruz Pradella, J. G. 2004. High-cell-density cultivation of *Pseudomonas putida* IPT 046 and medium-chain-length polyhydroxyalkanoate production from sugarcane carbohydrates. Applied Biochemistry and Biotechnology 119: 51-69.

Escapa, I., Del Cerro, C., García, J., Prieto, M. 2013. The role of GlpR repressor in *Pseudomonas putida* KT2440 growth and PHA production from glycerol. Environmental Microbiology 15: 93-110.

Escapa, I. F., García, J., Bühler, B., Blank, L., Prieto, M. A. 2012. The polyhydroxyalkanoate metabolism controls carbon and energy spillage in *Pseudomonas putida*. Environmental Microbiology 14: 1049-1063.

Espinosa-Urgel, M., Kolter, R., Ramos, J. L. 2002. Root colonization by *Pseudomonas putida*: love at first sight. Microbiology 148: 341-343.

Fan, F., Ghanem, M., Gadda, G. 2004. Cloning, sequence analysis, and purification of choline oxidase from *Arthrobacter globiformis*: a bacterial enzyme involved in osmotic stress tolerance. Archives of Biochemistry and Biophysics 421: 149-158.

Felsenstein, J. 1985. Confidence limits on phylogenies: an approach using the bootstrap. Evolution. 39: 783-791.

Finn, R. D., Bateman, A., Clements, J., Coggill, P., Eberhardt, R. Y., Eddy, S. R.,

Heger, A., Hetherington, K., Holm, L., Mistry, J., Sonnhammer, E. L. L., Tate, J., Punta.

M. 2014. The Pfam protein families database. Nucleic Acid Research 42: D222-D230.

Follonier, S., Panke, S., Zinn, M. 2011. A reduction in growth rate of *Pseudomonas putida* KT2442 counteracts productivity advances in medium-chain-length polyhydroxyalkanoate production from gluconate. Microbial Cell Factories 10: 25-36.

Freeman, B. C., Chen, C., Beattie, G. A. 2010. Identification of the trehalose biosynthetic loci of *Pseudomonas syringae* and their contribution to fitness in the phyllosphere. Environmental Microbiology 12: 1486-1497.

Fu, J., Sharma, U., Sparling, R., Cicek, N., Levin, D. B. 2014. Evaluation of Medium-Chain Length Polyhydroxyalkanoate production by *Pseudomonas putida* LS46 using biodiesel by-product streams. Canadian Journal of Microbiology 60:461- 468.

Fukui, T., Shiomi, N., Doi, Y. 1998. Expression and characterization of (R)-specific enoyl coenzyme A hydratase involved in polyhydroxyalkanoate biosynthesis by *Aeromonas caviae*. Journal of Bacteriology 180: 667-673.

Galán, B., Dinjaski, N., Maestro, B., De Eugenio, L., Escapa, I., Sanz, J., García, J., Prieto, M. 2011. Nucleoid-associated PhaF phasin drives intracellular location and segregation of polyhydroxyalkanoate granules in *Pseudomonas putida* KT2442. Molecular Microbiology 79: 402-418.

González-Guerrero, M., Raimunda, D., Cheng, X., Argüello, J. M. 2010. Distinct

functional roles of homologous Cu^{+} efflux ATPases in *Pseudomonas aeruginosa*. Molecular Microbiology 78: 1246-1258.

Gumel, A. M., Annuar, M. S. M., Heidelberg, T. 2012. Biosynthesis and characterization of polyhydroxyalkanoates copolymers produced by *Pseudomonas putida* Bet001 isolated from palm oil mill effluent. PLoS One 7: e45214.

Gungormusler-Yilmaz, M., Shamshurin, D., Grigoryan, M., Taillefer, M., Spicer, V., Krokhin, O. V., Sparling, R., Levin, D. B. 2014. Reduced catabolic protein expression in *Clostridium butyricum* DSM 10702 correlate with reduced 1, 3-propanediol synthesis at high glycerol loading. AMB Express 4: 63-77.

Guo, W., Song, C., Kong, M., Geng, W., Wang, Y., Wang, S. 2011. Simultaneous production and characterization of medium-chain-length polyhydroxyalkanoates and alginate oligosaccharides by *Pseudomonas mendocina* NK-01. Applied Microbiology and Biotechnology 92: 791-801.

Gutiérrez-Barranquero, J. A., De Vicente, A., Carrión, V. J., Sundin, G. W., Cazorla, F. M. 2013. Recruitment and rearrangement of three different genetic determinants into a conjugative plasmid increase copper resistance in *Pseudomonas syringae*. Applied and Environmental Microbiology 79: 1028-1033.

Guzik, M. W., Narancic, T., Ilic-Tomic, T., Vojnovic, S., Kenny, S. T., Casey, W. T., Duane, G. F., Casey, E., Woods, T., Babu, R. P. 2014. Identification and characterisation of an acyl-CoA dehydrogenase from *Pseudomonas putida* KT2440 that shows preference towards medium to long chain fatty acids. Microbiology 160: 1760-1771.

Haney, C. J., Grass, G., Franke, S., Rensing, C. 2005. New developments in the understanding of the cation diffusion facilitator family. Journal of Industrial

Microbiology and Biotechnology 32: 215-226.

Hantke, K. 2001. Bacterial zinc transporters and regulators. Biometals 14: 239-249.

Hassett, D. J., Sokol, P. A., Howell, M. L., Ma, J.-F., Schweizer, H. T., Ochsner, U., Vasil, M. L. 1996. Ferric uptake regulator (Fur) mutants of *Pseudomonas aeruginosa* demonstrate defective siderophore-mediated iron uptake, altered aerobic growth, and decreased superoxide dismutase and catalase activities. Journal of Bacteriology 178: 3996-4003.

He, W., Tian, W., Zhang, G., Chen, G. Q., Zhang, Z. 1998. Production of novel polyhydroxyalkanoates by *Pseudomonas stutzeri* 1317 from glucose and soybean oil. FEMS Microbiology Letters 169: 45-49.

Hein, S., Paletta, J., Steinbüchel, A. 2002. Cloning, characterization and comparison of the *Pseudomonas mendocina* polyhydroxyalkanoate synthases PhaC1 and PhaC2. Applied Microbiology and Biotechnology 58: 229-236.

Hoang, T. T and Schweizer, H. P. 1997. Fatty acid biosynthesis in *Pseudomonas aeruginosa*: cloning and characterization of the *fab*AB operon encoding beta-hydroxyacyl-acyl carrier protein dehydratase (FabA) and beta-ketoacyl-acyl carrier protein synthase I (FabB). Journal of Bacteriology 179: 5326-5332.

Hoffmann, N., Amara, A. A., Beermann, B. B., Qi, Q., Hinz, H. J., Rehm, B. H. 2002. Biochemical characterization of the *Pseudomonas putida* 3-hydroxyacyl ACP: CoA transacylase, which diverts intermediates of fatty acid *de novo* biosynthesis. Journal of Biological Chemistry 277: 42926-42936.

Hoffmann, N and Rehm, B. H. 2004. Regulation of polyhydroxyalkanoate biosynthesis in *Pseudomonas putida* and *Pseudomonas aeruginosa*. FEMS Microbiology Letters 237: 1-7.

Hrabak, O. 1992. Industrial production of poly-β-hydroxybutyrate. FEMS Microbiology Letters 103: 251-255.

Hu, R. M., Liao, S. T., Huang, C. C., Huang, Y. W., Yang, T. C. 2012. An inducible fusaric acid tripartite efflux pump contributes to the fusaric acid resistance in *Stenotrophomonas maltophilia*. PLoS One 7: e51053.

Hunt, M. C., Alexson, S. E. 2002. The role Acyl-CoA thioesterases play in mediating intracellular lipid metabolism. Progress in Lipid Research 41: 99-130.

Imamura, T., Kenmoku, T., Honma, T., Kobayashi, S., Yano, T. 2001. Direct biosynthesis of poly (3-hydroxyalkanoates) bearing epoxide groups. International Journal of Biological Macromolecules 29: 295-301.

Javidpour, P., Pereira, J. H., Goh, E.-B., Mcandrew, R. P., Ma, S. M., Friedland, G. D., Keasling, J. D., Chhabra, S. R., Adams, P. D., Beller, H. R. 2014. Biochemical and structural studies of NADH-dependent FabG used to increase the bacterial production of fatty acids under anaerobic conditions. Applied and Environmental Microbiology 80: 497-505.

Jendrossek, D., Pfeiffer, D. 2014. New insights in the formation of polyhydroxyalkanoate granules (carbonosomes) and novel functions of poly (3-hydroxybutyrate). Environmental Microbiology 16: 2357-2373.

Jiménez, J. I., Miñambres, B., Garcia, J. L., Díaz, E. 2002. Genomic analysis of the aromatic catabolic pathways from *Pseudomonas putida* KT2440. Environmental Microbiology 4: 824-841.

Johnstone, B. 1990. A throw away answer. Far Eastern Economic. Review 147: 62-63.

Joyce, A. R., Palsson, B. O. 2006. The model organism as a system: integrating 'omics' data sets. Nature Reviews Molecular Cell Biology 7: 198-210.

Ramsay, B. A., Lomaliza, K., Charvarie, C., Dude, B., Bataille, P., Ramsay, J. A., 1990. Production of Poly-(P-Hydroxybutyric-Co-3-Hydroxyvaleric) Acids. Applied and Environmental Microbiology 56: 2093-2098.

Kahar, P., Tsuge, T., Taguchi, K., Doi, Y. 2004. High yield production of polyhydroxyalkanoates from soybean oil by *Ralstonia eutropha* and its recombinant strain. Polymer Degradation and Stability 83: 79-86.

Kanehisa, M., Goto, S., Sato, Y., Kawashima, M., Furumichi, M., Tanabe, M. 2014. Data, information, knowledge and principle: back to metabolism in KEGG. Nucleic Acids Res 42: D199–D205.

Kang, Y., Nguyen, D. T., Son, M. S., Hoang, T. T. 2008. The *Pseudomonas aeruginosa* PsrA responds to long-chain fatty acid signals to regulate the *fadBA5* β-oxidation operon. Microbiology 154: 1584-1598.

Kenny, S. T., Runic, J. N., Kaminsky, W., Woods, T., Babu, R. P., O'connor, K. E. 2012. Development of a bioprocess to convert PET derived terephthalic acid and biodiesel derived glycerol to medium chain length polyhydroxyalkanoate. Applied Microbiology and Biotechnology 95: 623-633.

Kim, B. S., Lee, S. C., Lee, S. Y., Chang, H. N., Chang, Y. K., Woo, S. I. 1994. Production of poly (3-hydroxybutyric acid) by fed-batch culture of *Alcaligenes eutrophus* with glucose concentration control. Biotechnology and Bioengineering 43: 892-898.

Kim, D. Y., Kim, Y. B., Rhee, Y. H. 2000. Evaluation of various carbon substrates for the biosynthesis of polyhydroxyalkanoates bearing functional groups by *Pseudomonas putida*. International Journal of Biological Macromolecules 28: 23-29.

Kim, J., Oliveros, J. C., Nikel, P, I., Lorenzo, V., Silva-Rocha, R. 2013. Transcriptomic fingerprinting of *Pseudomonas putida* under alternative physiological regimes. Environmental Microbiology 5: 883-891.

Kim, S. N., Shim, S. C., Kim, D. Y., Rhee, Y. H., Kim, Y. B. 2001. Photochemical crosslinking and enzymatic degradation of poly (3-hydroxyalkanoate)s for micropatterning in photolithography. Macromolecular Rapid Communications 22: 1066-1071.

Kim, T. K., Jung, Y. M., Vo, M. T., Shioya, S., Lee, Y. H. 2006. Metabolic engineering and characterization of *pha*C1 and *pha*C2 genes from *Pseudomonas putida* KCTC1639 for overproduction of medium-chain-length polyhydroxyalkanoate. Biotechnology Progress 22: 1541-1546.

Kimber, M. S., Martin, F., Lu, Y., Houston, S., Vedadi, M., Dharamsi, A., Fiebig, K. M., Schmid, M., Rock, C. O. 2004. The structure of (3R)-hydroxyacyl-acyl carrier protein dehydratase (FabZ) from *Pseudomonas aeruginosa*. Journal of Biological Chemistry 279: 52593-52602.

Koller, M., Bona, R., Braunegg, G., Hermann, C., Horvat, P., Kroutil, M., Martinz, J., Neto, J., Pereira, L., Varila, P. 2005. Production of polyhydroxyalkanoates from agricultural waste and surplus materials. Biomacromolecules 6: 561-565.

Kosior, E., Braganca, R. M., Fowler, P. 2006. Lightweight compostable packaging: literature review. Oxon: The Waste & Resources Action Programme.

Kosono, S., Haga, K., Tomizawa, R., Kajiyama, Y., Hatano, K., Takeda, S., Wakai, Y., Hino, M., Kudo, T. 2005. Characterization of a multigene-encoded sodium/hydrogen antiporter (Sha) from *Pseudomonas aeruginosa*: its involvement in pathogenesis. Journal of Bacteriology 187: 5242-5248.

Kulkarni, M. G and Dalai, A. K. 2006. Waste cooking oil an economical source for biodiesel: a review. Industrial & Engineering Chemistry Research 45: 2901-2913.

La Rosa, R., Peña, F., Prieto, M. A., Rojo, F. 2014. The Crc protein inhibits the production of polyhydroxyalkanoates in *Pseudomonas putida* under balanced carbon/nitrogen growth conditions. Environmental Microbiology 16: 278-290.

Le Meur, S., Zinn, M., Egli, T., Thöny-Meyer, L., Ren, Q. 2012. Production of medium-chain-length polyhydroxyalkanoates by sequential feeding of xylose and octanoic acid in engineered *Pseudomonas putida* KT2440. BMC Biotechnology 12: 53-65.

Lee, E., Jendrossek, D., Schirmer, A., Choi, C., Steinbüchel, A. 1995a. Biosynthesis of copolyesters consisting of 3-hydroxybutyric acid and medium-chain-length 3-hydroxyalkanoic acids from 1,3-butanediol or from 3-hydroxybutyrate by *Pseudomonas sp*. A33. Applied Microbiology and Biotechnology 42: 901-909.

Lee, H. J., Choi, M. H., Kim, T. U., Yoon, S. C. 2001. Accumulation of polyhydroxyalkanoic acid containing large amounts of unsaturated monomers in *Pseudomonas fluorescens* BM07 utilizing saccharides and its inhibition by 2-bromooctanoic acid. Applied and Environmental Microbiology 67: 4963-4974.

Lee, I. Y., Kim, M. K., Chang, H. N., Park, Y. H. 1995b. Regulation of poly-β-hydroxybutyrate biosynthesis by nicotinamide nucleotide in *Alcaligenes eutrophus*. FEMS Microbiology Letters 131: 35-39.

Lee, I. Y., Kim, M. K., Park, Y. H., Lee, S. Y. 1996. Regulatory effects of cellular nicotinamide nucleotides and enzyme activities on poly (3-hydroxybutyrate) synthesis in recombinant *Escherichia coli*. Biotechnology and Bioengineering 52: 707-712.

Lenz, R. W., Kim, Y. B., Fuller, R. C. 1992. Production of unusual bacterial polyesters

by *Pseudomonas oleovorans* through cometabolism. FEMS Microbiology Letters 103: 207-214.

Li, C., Lesnik, K. L., Liu, H. 2013. Microbial conversion of waste glycerol from biodiesel production into value-added products. Energies 6: 4739-4768.

Li, X. Z., Barré, N., Poole, K. 2000. Influence of the MexA-MexB-OprM multidrug efflux system on expression of the MexC-MexD-OprJ and MexE-MexF-OprN multidrug efflux systems in *Pseudomonas aeruginosa*. Journal of Antimicrobial Chemotherapy 46: 885-893.

Liebergesell, M., Rahalkar, S., Steinbüchel, A. 2000. Analysis of the *Thiocapsa pfennigii* polyhydroxyalkanoate synthase: subcloning, molecular characterization and generation of hybrid synthases with the corresponding Chromatium vinosum enzyme. Applied Microbiology and Biotechnology 54: 186-194.

Liu, Q., Luo, G., Zhou, X. R., Chen, G. Q. 2011. Biosynthesis of poly (3-hydroxydecanoate) and 3-hydroxydodecanoate dominating polyhydroxyalkanoates by β-oxidation pathway inhibited *Pseudomonas putida*. Metabolic Engineering 13: 11-17.

Lu, X., Zhang, J., Wu, Q., Chen, G. Q. 2003. Enhanced production of poly (3-hydroxybutyrate-co-3-hydroxyhexanoate) via manipulating the fatty acid β-oxidation pathway in *E. coli*. FEMS Microbiology Letters 221: 97-101.

Ma, Y., Xue, L., Sun, D. W. 2006. Characteristics of trehalose synthase from permeablized *Pseudomonas putida* cells and its application in converting maltose into trehalose. Journal of Food Engineering 77: 342-347.

Mallick, P and Kuster, B. 2010. Proteomics: a pragmatic perspective. Nature Biotechnology 28: 695-709.

Maloy, S., Bohlander, M., Nunn, W. 1980. Elevated levels of glyoxylate shunt enzymes in *Escherichia coli* strains constitutive for fatty acid degradation. Journal of Bacteriology 143: 720-725.

Marques, A., Reis, R., Hunt, J. 2002. The biocompatibility of novel starch-based polymers and composites: in vitro studies. Biomaterials 23: 1471-1478.

Marsudi, S., Unno, H., Hori, K. 2008. Palm oil utilization for the simultaneous production of polyhydroxyalkanoates and rhamnolipids by *Pseudomonas aeruginosa*. Applied Microbiology and Biotechnology 78: 955-961.

Matsusaki, H., Abe, H., Taguchi, K., Fukui, T., Doi, Y. 2000. Biosynthesis of poly (3- hydroxybutyrate-co-3-hydroxyalkanoates) by recombinant bacteria expressing the PHA synthase gene *pha*C1 from *Pseudomonas sp*. 61-3. Applied Microbiology and Biotechnology 53: 401-409.

Mccool, G. J and Cannon, M. C. 2001. PhaC and PhaR are required for polyhydroxyalkanoic acid synthase activity in *Bacillus megaterium*. Journal of Bacteriology 183: 4235-4243.

Mcmahon, B and Mayhew, S. G. 2007. Identification and properties of an inducible phenylacyl-CoA dehydrogenase in *Pseudomonas putida* KT2440. FEMS Microbiology Letters 273: 50-57.

McQueen, P., Spicer, V., Rydzak, T., Sparling, R., Levin, D., Wilkins, J. A., Krokhin, O. 2012. Information-dependent LC-MS/MS acquisition with exclusion lists potentially generated on-the-fly: case study using a whole cell digest of *Clostridium thermocellum*. Journal of Proteomics 12:1160–1169.

Meijnen, J. P., De Winde, J. H., Ruijssenaars, H. J. 2009. Establishment of oxidative D- xylose metabolism in *Pseudomonas putida* S12. Applied and Environmental

Microbiology 75: 2784-2791.

Mergeay, M., Monchy, S., Vallaeys, T., Auquier, V., Benotmane, A., Bertin, P., Taghavi, S., Dunn, J., Lelie, D., Wattiez, R. 2003. *Ralstonia metallidurans*, a bacterium specifically adapted to toxic metals: towards a catalogue of metal-responsive genes. FEMS Microbiology Reviews 27: 385-410.

Michéa, H., Mehri, Henze, U., Gotoh, N., Kocjancic Curty, L., Pechère, J. C. 1997. Characterization of MexE–MexF–OprN, a positively regulated multidrug efflux system of *Pseudomonas aeruginosa*. Molecular Microbiology 23: 345-354.

Miller, C., Pettee, B., Zhang, C., Pabst, M., Mclean, J., Anderson, A. 2009. Copper and cadmium: responses in *Pseudomonas putida* KT2440. Letters in Applied Microbiology 49: 775-783.

Mukherjee, T and Kao, N. 2011. PLA based biopolymer reinforced with natural fibre: a review. Journal of Polymers and the Environment 19: 714-725.

Nelson, K., Weinel, C., Paulsen, I., Dodson, R., Hilbert, H., Martins Dos Santos, V., Fouts, D., Gill, S., Pop, M., Holmes, M., et al., 2002. Complete genome sequence and comparative analysis of the metabolically versatile *Pseudomonas putida* KT2440. Environmental Microbiology 4: 799-808.

Ni, Y. Y., Kim, D. Y., Chung, M. G., Lee, S. H., Park, H.Y., Rhee, Y. H. 2010. Biosynthesis of medium-chain-length poly (3-hydroxyalkanoates) by volatile aromatic hydrocarbons-degrading *Pseudomonas fulva* TY16. Bioresource Technology 101: 8485-8488.

Nies, D. H. 1999. Microbial heavy-metal resistance. Applied Microbiology and Biotechnology 51: 730-750.

Nikel, P. I., Kim, J., Lorenzo, V. 2014. Metabolic and regulatory rearrangements

underlying glycerol metabolism in *Pseudomonas putida* KT2440. Environmental Microbiology 16: 239-254.

Noda, I., Green, P. R., Satkowski, M. M., Schechtman, L. A. 2005. Preparation and properties of a novel class of polyhydroxyalkanoate copolymers. Biomacromolecules 6: 580-586.

Nomura, C. T., Tanaka, T., Gan, Z., Kuwabara, K., Abe, H., Takase, K., Taguchi, K., Doi, Y. 2004. Effective enhancement of short-chain-length-medium-chain-length polyhydroxyalkanoate copolymer production by coexpression of genetically engineered 3-ketoacyl-acyl-carrier-protein synthase III (*fab*H) and polyhydroxyalkanoate synthesis genes. Biomacromolecules 5: 1457-1464.

Nopharatana, A., Pullammanappallil, P. C., Clarke, W. P. 2007. Kinetics and dynamic modelling of batch anaerobic digestion of municipal solid waste in a stirred reactor. Waste Management 27: 595-603.

Ojumu, T., Yu, J., Solomon, B. 2004. Production of polyhydroxyalkanoates, a bacterial biodegradable polymer. African Journal of Biotechnology 3: 18-24.

Ouyang, S. P., Luo, R. C., Chen, S. S., Liu, Q., Chung, A., Wu, Q., Chen, G. Q. 2007. Production of polyhydroxyalkanoates with high 3-hydroxydodecanoate monomer content by *fad*B and *fad*A knockout mutant of *Pseudomonas putida* KT2442. Biomacromolecules 8: 2504-2511.

Pabst, M. W., Miller, C. D., Dimkpa, C. O., Anderson, A. J., Mclean, J. E. 2010. Defining the surface adsorption and internalization of copper and cadmium in a soil bacterium, *Pseudomonas putida*. Chemosphere 81: 904-910.

Pan, J. H., Chen, Y., Huang, Y. H., Tao, Y. W., Wang, J., Li, Y., Peng, Y., Dong, T., Lai, X. M., Lin, Y. C. 2011. *Antimycobacterial* activity of fusaric acid from a

mangrove endophyte and its metal complexes. Archives of Pharmacal Research 34: 1177-1181.

Patel, V. J., Thalassinos, K., Slade, S. E., Connolly, J. B., Crombie, A., Murrell, J. C., Scrivens, J. H. 2009. A comparison of labeling and label-free mass spectrometry- based proteomics approaches. Journal of Proteome Research 8: 3752-3759.

Patti, G. J., Yanes, O., Siuzdak, G. 2012. Innovation: Metabolomics: the apogee of the omics trilogy. Nature Reviews Molecular Cell Biology 13: 263-269.

Pfeiffer, D., Wahl, A., Jendrossek, D. 2011. Identification of a multifunctional protein, PhaM, that determines number, surface to volume ratio, subcellular localization

and distribution to daughter cells of poly (3-hydroxybutyrate), PHB, granules in *Ralstonia eutropha* H16. Molecular Microbiology 82: 936-951.

Pham, T. H., Webb, J. S., Rehm, B. H. 2004. The role of polyhydroxyalkanoate biosynthesis by *Pseudomonas aeruginosa* in rhamnolipid and alginate production as well as stress tolerance and biofilm formation. Microbiology 150: 3405-3413.

Poblete-Castro, I., Escapa, I. F., Jäger, C., Puchalka, J., Lam, C. M. C., Schomburg, D., Prieto, M. A., Dos Santos, V. A. M. 2012. The metabolic response of *P. putida* KT2442 producing high levels of polyhydroxyalkanoate under single-and multiple-nutrient-limited growth: Highlights from a multi-level omics approach. Microbial Cell Factories 11: 1-21.

Poblete-Castro, I., Binger, D., Rodrigues, A., Becker, J., Dos Santos, V. A. M., Wittmann, C. 2013. In-silico-driven metabolic engineering of *Pseudomonas putida* for enhanced production of poly-hydroxyalkanoates. Metabolic

Engineering 15: 113- 123.

Prieto, M. A., Bühler, B., Jung, K., Witholt, B., Kessler, B. 1999. PhaF, a polyhydroxyalkanoate-granule-associated protein of *Pseudomonas oleovorans* GPo1 involved in the regulatory expression system for *pha* genes. Journal of Bacteriology 181: 858-868.

Pyle, D. J., Garcia, R. A., Wen, Z. 2008. Producing docosahexaenoic acid (DHA)-rich algae from biodiesel-derived crude glycerol: effects of impurities on DHA production and algal biomass composition. Journal of Agricultural Food and Chemistry 56: 3933-3939.

Qi, Q and Rehm, B. H. 2001. Polyhydroxybutyrate biosynthesis in *Caulobacter crescentus*: molecular characterization of the polyhydroxybutyrate synthase. Microbiology 147: 3353-3358.

Qi, Q., Steinbüchel, A., Rehm, B. 2000. In vitro synthesis of poly (3-hydroxydecanoate): purification and enzymatic characterization of type II polyhydroxyalkanoate synthases PhaC1 and PhaC2 from *Pseudomonas aeruginosa*. Applied Microbiology and Biotechnology 54: 37-43.

Qiu, Y. Z., Han, J., Guo, J. J., Chen, G. Q. 2005. Production of poly (3-hydroxybutyrate-co-3-hydroxyhexanoate) from gluconate and glucose by recombinant *Aeromonas hydrophila* and *Pseudomonas putida*. Biotechnology Letters 27: 1381-1386.

Rai, R., Keshavarz, T., Roether, J., Boccaccini, A. R. Roy, I. 2011a. Medium chain length polyhydroxyalkanoates, promising new biomedical materials for the future. Materials Science and Engineering: Reports 72: 29-47.

Rai, R., Yunos, D. M., Boccaccini, A. R., Knowles, J. C., Barker, I. A., Howdle, S. M., Tredwell, G. D., Keshavarz, T., Roy, I. 2011b. Poly-3-hydroxyoctanoate P (3HO),

a medium chain length polyhydroxyalkanoate homopolymer from *Pseudomonas mendocina*. Biomacromolecules 12: 2126-2136.

Reddy, C., Ghai, R., Kalia, V. C. 2003. Polyhydroxyalkanoates: an overview. Bioresource Technology 87: 137-146.

Rehm, B. H. 2003. Polyester synthases: natural catalysts for plastics. Biochem. J 376: 15-33.

Rehm, B. H. 2010. Bacterial polymers: biosynthesis, modifications and applications. Nature Reviews Microbiology 8: 578-592.

Rehm, B. H., Mitsky, T. A., Steinbüchel, A. 2001. Role of fatty acid *de novo* biosynthesis in polyhydroxyalkanoic acid (PHA) and rhamnolipid synthesis by *pseudomonads*: establishment of the transacylase (PhaG)-mediated pathway for PHA biosynthesis in *Escherichia coli*. Applied and Environmental Microbiology 67: 3102-3109.

Rehm, B. H and Steinbüchel, A. 1999. Biochemical and genetic analysis of PHA synthases and other proteins required for PHA synthesis. International Journal of Biological Macromolecules 25: 3-19.

Ren, Q., De Roo, G., Ruth, K., Witholt, B., Zinn, M., Thö Ny-Meyer, L. 2009a. Simultaneous accumulation and degradation of polyhydroxyalkanoates: futile cycle or clever regulation? Biomacromolecules 10: 916-922.

Ren, Q., De Roo, G., Witholt, B., Zinn, M., Thöny-Meyer, L. 2009b. Over-expression and characterization of medium-chain-length polyhydroxyalkanoate granule bound polymerases from *Pseudomonas putida* GPo1. Microbial Cell Factories 8: 60-69.

Ren, Q., De Roo, G., Witholt, B., Zinn, M., Thöny-Meyer, L. 2010. Influence of growth stage on activities of polyhydroxyalkanoate (PHA) polymerase and PHA

depolymerase in *Pseudomonas putida* U. BMC Microbiology 10: 254-263.

Ren, Q., Sierro, N., Witholt, B., Kessler, B. 2000. FabG, an NADPH-dependent 3-ketoacyl reductase of *Pseudomonas aeruginosa*, provides precursors for medium-chain-length poly-3-hydroxyalkanoate biosynthesis in *Escherichia coli*. Journal of Bacteriology 182: 2978-2981.

Roca, A., Pizarro-Tobías, P., Udaondo, Z., Fernández, M., Matilla, M. A., Molina Henares, M. A., Molina, L., Segura, A., Duque, E., Ramos, J. L. 2013. Analysis of the plant growth-promoting properties encoded by the genome of the rhizobacterium *Pseudomonas putida* BIRD-1. Environmental Microbiology 15: 780-794.

Ross, P. L., Huang, Y. N., Marchese, J. N., Williamson, B., Parker, K., Hattan, S., Khainovski, N., Pillai, S., Dey, S., Daniels, S. 2004. Multiplexed protein quantitation in *Saccharomyces cerevisiae* using amine-reactive isobaric tagging reagents. Molecular & Cellular Proteomics 3: 1154-1169.

Roy, D., Semsarilar, M., Guthrie, J. T., Perrier, S. 2009. Cellulose modification by polymer grafting: a review. Chemical Society Reviews 38: 2046-2064.

Ryan, W. J., O'leary, N. D., O'mahony, M., Dobson, A. D. 2013. GacS-dependent regulation of polyhydroxyalkanoate synthesis in *Pseudomonas putida* CA-3. Applied and Environmental Microbiology 79: 1795-1802.

Sabirova, J. S., Ferrer, M., Lünsdorf, H., Wray, V., Kalscheuer, R., Steinbüchel, A., Timmis, K. N., Golyshin, P. N. 2006. Mutation in a "*tes*B-like" hydroxyacyl-coenzyme A-specific thioesterase gene causes hyperproduction of extracellular polyhydroxyalkanoates by *Alcanivorax borkumensis* SK2. Journal of Bacteriology 188: 8452-8459.

Saharan, K., Sarma, M., Roesti, A., Prakash, A., Johri, B., Aragno, M., Bisaria, V., Sahai,

V. 2010. Cell growth and metabolites produced by fluorescent *pseudomonad* R62 in modified chemically defined medium. World Academy Science, Enggineering and Technology 67: 867-871.

Saier, M. H., Reddy, V. S., Tamang, D. G., Västermark, Å. 2014. The transporter classification database. Nucleic Acids Research 42: D251-D258.

Sánchez, R. J., Schripsema, J., Da Silva, L. F., Taciro, M. K., Pradella, J. G., Gomez, J. G.C. 2003. Medium-chain-length polyhydroxyalkanoic acids (PHA_{mcl}) produced by *Pseudomonas putida* IPT 046 from renewable sources. European polymer Journal 39: 1385-1394.

Sato, S., Kanazawa, H., Tsuge, T. 2011. Expression and characterization of (R)-specific enoyl coenzyme A hydratases making a channeling route to polyhydroxyalkanoate biosynthesis in *Pseudomonas putida*. Applied Microbiology and Biotechnology 90: 951-959.

Schmid, A., Dordick, J., Hauer, B., Kiener, A., Wubbolts, M., Witholt, B. 2001. Industrial biocatalysis today and tomorrow. Nature 409: 258-268.

Schneider, M. V. Orchard, S. 2011. 'Omics technologies, data and bioinformatics principles. Methods in Molecular Biology 719: 3-30.

Scholz, C., Fuller, R. C., Lenz, R. W. 1994. Growth and polymer incorporation of *Pseudomonas oleovorans* on alkyl esters of heptanoic acid. Macromolecules 27: 2886-2889.

Schweizer, H. P., Jump, R., Po, C. 1997. Structure and gene-polypeptide relationships of the region encoding glycerol diffusion facilitator (*glpF*) and glycerol kinase (*glp*K) of *Pseudomonas aeruginosa*. Microbiology 143: 1287-1297.

Shang, L., Jiang, M., Yun, Z., Yan, H. Q., Chang, H. N. 2008. Mass production of medium-chain-length poly (3-hydroxyalkanoates) from hydrolyzed corn oil by fed-batch culture of *Pseudomonas putida*. World Journal of Microbiology and Biotechnology 24: 2783-2787.

Sharma, P. K., Fu, J., Cicek, N., Sparling, R., Levin, D. B. 2012. Kinetics of medium-chain-length polyhydroxyalkanoate production by a novel isolate of *Pseudomonas putida* LS46. Canadian Journal of Microbiology 58: 982-989.

Sharma, P. K., Fu, J., Zhang, X., Fristensky, B., Sparling, R., Levin, D. B. 2014. Genome features of *Pseudomonas putida* LS46, a novel polyhydroxyalkanoate producer and its comparison with other *P. putida* strains. AMB Express 4: 1-18.

Shrivastav, A., Mishra, S. K., Shethia, B., Pancha, I., Jain, D., Mishra, S. 2010. Isolation of promising bacterial strains from soil and marine environment for polyhydroxyalkanoates (PHA) production utilizing Jatropha biodiesel byproduct. International Journal of Biological Macromolecules 47: 283-287.

Silva, L., Taciro, M., Ramos, M. M., Carter, J., Pradella, J., Gomez, J. 2004. Poly-3-hydroxybutyrate (P3HB) production by bacteria from xylose, glucose and sugarcane bagasse hydrolysate. Journal of Industrial Microbiology and Biotechnology 31: 245-254.

Simon, O., Klaiber, I., Huber, A., Pfannstiel, J. 2014. Comprehensive proteome analysis of the response of *Pseudomonas putida* KT2440 to the flavor compound vanillin. Journal of Proteomics 109: 212-227.

Singh, R., Mailloux, R. J., Puiseux-Dao, S., Appanna, V. D. 2007. Oxidative stress evokes a metabolic adaptation that favors increased NADPH synthesis and decreased NADH production in *Pseudomonas fluorescens*. Journal of

Bacteriology 189: 6665-6675.

Solaiman, D. K., Ashby, R. D., Crocker, N., Lai, B. H., Zerkowski, J. A. 2013. Rhamnolipid and poly (hydroxyalkanoate) biosynthesis in 3-hydroxyacyl-ACP: CoA transacylase (*pha*G)-knockouts of *Pseudomonas chlororaphis*. Biocatalysis and Agricultural Biotechnology 3: 159-166.

Song, J. H., Jeon, C. O., Choi, M. H., Yoon, S. C., Park, W. 2008. Polyhydroxyalkanoate (PHA) production using waste vegetable oil by *Pseudomonas sp.* strain DR2. Journal of Microbiology and Biotechnology 18: 1408-1415.

Song, S., Hein, S., Steinbüchel, A. 1999. Production of poly (4-hydroxybutyric acid) by fed-batch cultures of recombinant strains of *Escherichia coli*. Biotechnology Letters 21: 193-197.

Spencer, A. K., Greenspan, A. D., Cronan, J. E. 1978. Thioesterases I and II of *Escherichia coli*. Journal of Biology and Chemistry 253: 5922-5926.

Steinbüchel, A and Valentin, H. E. 1995. Diversity of bacterial polyhydroxyalkanoic acids. FEMS Microbiology Letters 128: 219-228.

Su, J., Wang, T., Ma, C., Li, Z., Li, Z., Wang, R. 2014. Homology modeling and function of trehalose synthase from *Pseudomonas putida* P06. Biotechnology Letters 36: 1009-1013.

Sudarsan, S., Dethlefsen, S., Blank, L. M., Siemann-Herzberg, M., Schmid, A. 2014. The functional structure of central carbon metabolism in *Pseudomonas putida* KT2440. Applied and Environmental Microbiology 80: 5292-5303.

Sudesh, K., Abe, H., Doi, Y. 2000. Synthesis, structure and properties of polyhydroxyalkanoates: biological polyesters. Progress in Polymer Science

25: 1503-1555.

Sun, Z., Ramsay, J. A., Guay, M., Ramsay, B. A. 2007. Carbon-limited fed-batch production of medium-chain-length polyhydroxyalkanoates from nonanoic acid by *Pseudomonas putida* KT2440. Applied Microbiology and Biotechnology 74: 69-77.

Sun, Z., Ramsay, J. A., Guay, M., Ramsay, B. A. 2009. Fed-batch production of unsaturated medium-chain-length polyhydroxyalkanoates with controlled composition by *Pseudomonas putida* KT2440. Applied Microbiology and Biotechnology 82: 657-662.

Takase, K., Taguchi, S., Doi, Y. 2003. Enhanced synthesis of poly (3-hydroxybutyrate) in recombinant *Escherichia coli* by means of error-prone PCR mutagenesis, saturation mutagenesis, and in vitro recombination of the type II polyhydroxyalkanoate synthase gene. Journal of Biochemistry 133: 139-145.

Tamura, K., Peterson, D., Peterson, N., Stecher, G., Nei, M., Kumar, S. 2011. MEGA5: molecular evolutionary genetics analysis using maximum likelihood, evolutionary distance, and maximum parsimony methods. Molecular Biology and Evolution 28: 2731-2739.

Tan, I. K. P., Kumar, K. S., Theanmalar, M., Gan, S. N., Gordon III, B. 1997. Saponified palm kernel oil and its major free fatty acids as carbon substrates for the production of polyhydroxyalkanoates in *Pseudomonas putida* PGA1. Applied Microbiology and Biotechnology 47: 207-211.

Tatusov, R. L., Galperin, M. Y., Natale, D. A., Koonin, E. V. 2000. The COG database: a tool for genome-scale analysis of protein functions and evolution. Nucleic Acids Research 28: 33-36.

Teitzel, G. M., Geddie, A., Susan, K., Kirisits, M. J., Whiteley, M., Parsek, M. R. 2006. Survival and growth in the presence of elevated copper: transcriptional profiling of copper-stressed *Pseudomonas aeruginosa*. Journal of Bacteriology 188: 7242- 7256.

Tian, W., Hong, K., Chen, G. Q., Wu, Q., Zhang, R. Q., Huang, W. 2000. Production of polyesters consisting of medium chain length 3-hydroxyalkanoic acids by *Pseudomonas mendocina* 0806 from various carbon sources. Antonie van leeuwenhoek 77: 31-36.

Tobin, K. M., Mcgrath, J. W., Mullan, A., Quinn, J. P., O'connor, K. E. 2007. Polyphosphate accumulation by *Pseudomonas putida* CA-3 and other medium-chain-length polyhydroxyalkanoate-accumulating bacteria under aerobic growth conditions. Applied and Environmental Microbiology 73: 1383-1387.

Thompson, J and He, B. 2006. Characterization of crude glycerol from biodiesel production from multiple feedstocks. Applied Engineering in Agricultural 22: 261-267.

Tsuge, T., Taguchi, K., Doi, Y. 2003. Molecular characterization and properties of (R)-specific enoyl-CoA hydratases from *Pseudomonas aeruginosa*: metabolic tools for synthesis of polyhydroxyalkanoates via fatty acid beta-oxidation. International Journal of Biological Macromolecules 31: 195-205.

Utsumi, R., Yagi, T., Katayama, S., Katsuragi, K., Tachibana, K., Toyoda, H., Ouchi, S., Obata, K., Shibano, Y., Noda, M. 1991. Molecular cloning and characterization of the fusaric acid-resistance gene from *Pseudomonas cepacia*. Agricultural and Biological Chemistry 55: 1913-1918.

Valappil, S. P., Boccaccini, A. R., Bucke, C., Roy, I. 2007a. Polyhydroxyalkanoates in

Gram-positive bacteria: insights from the genera *Bacillus* and *Streptomyces*. Antonie van leeuwenhoek 91: 1-17.

Valappil, S. P., Peiris, D., Langley, G., Herniman, J., Boccaccini, A. R., Bucke, C., Roy, I. 2007b. Polyhydroxyalkanoate (PHA) biosynthesis from structurally unrelated carbon sources by a newly characterized *Bacillus* spp. Journal of Biotechnology 127: 475-487.

Verbeke, T. J., Spicer, V., Krokhin, O. V., Zhang, X., Schellenberg, J. J., Fristensky, B., Wilkins, J. A., Levin, D. B., Sparling, R. 2014. Thermoanaerobacter thermohydrosulfuricus WC1 shows protein complement stability during fermentation of key lignocellulose-derived substrates. Applied and Environmental Microbiology 80: 1602-1615.

Verhoef, S., Gao, N., Ruijssenaars, H. J., De Winde, J. H. 2013. Crude glycerol as feedstock for the sustainable production of p-hydroxybenzoate by *Pseudomonas putida* S12. New Biotechnology 31: 114-119.

Victor, M. Markowitz1., I-Min, A. C., Krishna, P., Ken, C., Ernest, S., Yuri, G., Anna, R., Biju, J., Jinghua, H., Peter, W., Marcel, H., Iain, A., Konstantinos, M., Natalia, N. I., Nikos, C. K. 2012. IMG: the integrated microbial genomes database and comparative analysis system. Nucleic Acid Reseach. 40: D115-D122.

Vogel, C and Marcotte, E. M. 2012. Insights into the regulation of protein abundance from proteomic and transcriptomic analyses. Nature Reviews Genetics 13: 227-232.

Wang, F and Lee, S. Y. 1997. Poly (3-hydroxybutyrate) production with high productivity and high polymer content by a fed-batch culture of *Alcaligenes latus*

under nitrogen limitation. Applied and Environmental Microbiology 63: 3703-3706.

Wang, P., Lv, C., Zhu, G. 2015. Novel type II and monomeric NAD^+ specific isocitrate dehydrogenases: phylogenetic affinity, enzymatic characterization, and evolutionary implication. Scientific Reports 5: 9150-9161.

Wang, Q and Nomura, C. T. 2010. Monitoring differences in gene expression levels and polyhydroxyalkanoate (PHA) production in *Pseudomonas putida* KT2440 grown on different carbon sources. Journal of Bioscience and Bioengineering 110: 653- 659.

Wang, Q., Tappel, R. C., Zhu, C., Nomura, C. T. 2011. Development of a new strategy for production of medium-chain-length polyhydroxyalkanoates (MCL-PHA) from inexpensive non-fatty acid feedstocks in recombinant *Escherichia coli*. Applied and Environmental Microbiology AEM. 07020-11.

Wang, T., Jia, S., Dai, K., Liu, H., Wang, R. 2014. Cloning and expression of a trehalose synthase from *Pseudomonas putida* KT2440 for the scale-up production of trehalose from maltose. Canadian Journal of Microbiology 60: 599-604.

Wang, Z., Gerstein, M., Snyder, M. 2009. RNA-Seq: a revolutionary tool for transcriptomics. Nature Reviews Genetics 10: 57-63.

Wargo, M. J., Szwergold, B. S., Hogan, D. A. 2008. Identification of two gene clusters and a transcriptional regulator required for *Pseudomonas aeruginosa* glycine betaine catabolism. Journal of Bacteriology 190: 2690-2699.

Weber, F. J., Ooijkaas, L. P., Schemen, R., Hartmans, S., De Bont, J. 1993. Adaptation of *Pseudomonas putida* S12 to high concentrations of styrene and other organic solvents. Applied and Environmental Microbiology 59: 3502-3504.

Witholt, B and Kessler, B. 1999. Perspectives of medium chain length poly (hydroxyalkanoates), a versatile set of bacterial bioplastics. Current Opinion in Biotechnology 10: 279-285.

Wu, X., Monchy, S., Taghavi, S., Zhu, W., Ramos, J., Van Der Lelie, D. 2011. Comparative genomics and functional analysis of niche-specific adaptation in *Pseudomonas putida*. FEMS Microbiology Reviews 35: 299-323.

Yang, S. F., Tay, J. H., Liu, Y. 2003. A novel granular sludge sequencing batch reactor for removal of organic and nitrogen from wastewater. Journal of Biotechnology 106: 77-86.

Yang, F., Hanna, M. A., Sun, R. 2012. Value-added uses for crude glycerol a byproduct of biodiesel production. Biotechnol Biofuels 5: 1-10.

Yazdani, S. S and Gonzalez, R. 2007. Anaerobic fermentation of glycerol: a path to economic viability for the biofuels industry. Current Opinion in Biotechnology 18: 213-219.

Yuan, W., Jia, Y., Tian, J., Snell, K. D., Müh, U., Sinskey, A. J., Lambalot, R. H., Walsh, C. T., Stubbe, J. 2001. Class I and III Polyhydroxyalkanoate synthases from *Ralstonia eutropha* and *Allochromatium vinosum*: characterization and substrate specificity studies. Archives of Biochemistry and Biophysics 394: 87-98.

Zhang, W., Chen, L., Liu, D. 2012. Characterization of a marine-isolated mercury-resistant *Pseudomonas putida* strain SP1 and its potential application in marine mercury reduction. Applied Microbiology and Biotechnology 93: 1305-1314.

Zuckerkandl, E and Pauling, L. 1965. Evolutionary divergence and convergence in proteins. Evolving genes and proteins 97: 97-166.

Appendix (Supplementary Materials)

S1 Table. Gene expression abundance and differential gene expression values derived from RNAseq analysis under all the experimental conditions of the current study. This file was uploaded separately from the Thesis due to the size of the files, and can be found online with following link (with DropBox):

https://www.dropbox.com/s/y5p8qlmrxagxcis/S1_Tables_A_RNAseq.pdf?dl=0

S2 Tables. Protein expression abundance and differential gene expression values derived from Proteomics analysis under the specific experimental comparing conditions: **A**), Pure glycerol vs Waste glycerol exponential culture; **B**), Waste glycerol stationary culture and Waste fatty acids exponential culture vs Waste glycerol exponential culture, respectively. These files were uploaded separately from the Thesis due to the size of the files, and can be found online with following links (with DropBox):

Table S2A:

https://www.dropbox.com/s/mxxlg0d3spiawr8/S2%20Tables%20A%20Proteomics.pdf?dl=0

Table S2B:

https://www.dropbox.com/s/15kp7drpi6ng9hb/S2%20Tables%20B%20Proteomics.pdf?dl=0

S3 Table. Summary of Protein and RNA scores of the RNAseq and 1D-LS-MS/MS Proteomics analysis under the studied experimental conditions [a].

Protein scores							**RNA scores**
Growth Condition	**MS/MS collected**	**Total peptides**	**Non-redundant peptides**	**Proteins log(e)<-1**	**Proteins log(e)<-3**	**Proteins log(e)<-10**	**Genes**
WG_Exp_Rep1	33864	19928	8315	1947	1830	1377	5193
WG_Exp_Rep2	34996	17941	7431	1836	1714	1285	5189
PG_Exp_Rep1	34905	20138	8387	1914	1807	1382	5195
PG_Exp_Rep2	34996	17941	7431	1836	1714	1285	5200
WG_Sta_Rep1	36092	21644	9787	1997	1906	1500	5204
WG_Sta_Rep2	35168	20533	9503	1975	1873	1456	5198
WFA_Exp_Rep1	36081	20922	8817	1829	1718	1333	5199
WFA_Exp_Rep1	36587	20982	8844	1825	1713	1330	5195
			Average (proteins)				**Average (RNA)**
			WG_Exp	1892	1772	1331	5191
			PG_Exp	1875	1761	1333	5198
			WG_Sta	1916	1810	1478	5201
			WFA_Exp	1827	1715	1331	5197

[a:] WG: Waste glycerol; PG: Pure glycerol; WFA: Waste free fatty acids; Rep1/2: Biological replicates; Exp: Exponential phase; Sta: Stationary phase.

S4 Tables. Standard deviations of overall gene expression cross-state and intra-replicate population of RNAseq and 1D- LS-MS/MS Proteomic expression data associated in Chapter 3 (**A**) and Chapter 4 (**B**).

A	**Comparisons** [a]	**Standard Deviation**	
		RNA	Protein
Biological signal	WG_Exp_Rep1 vs PG_Exp_Rep1	0.66	1
	WG_Exp_Rep2 vs PG_Exp_Rep2	0.64	1.01
System noise	WG_Exp_Rep1 vs WG_Exp_Rep2	0.27	1
	PG_Exp_Rep1 vs PG_Exp_Rep2	0.25	1.04
Average ratio		2.5	1.01

B	**Comparisons** [a]	**Standard Deviation**	
		RNA	Protein
Biological signal	WG_Sta_Rep1 vs WG_Exp_Rep1	1.22	1.53
	WG_Sta_Rep2 vs WG_Exp_Rep2	1.1	1.52
	WFA_Exp_Rep1 vs WG_Exp_Rep1	1.01	1.59
	WFA_Exp_Rep2 vs WG_Exp_Rep2	1.01	1.53
System noise	WG_Exp_Rep1 vs WG_Exp_Rep2	0.27	1.1
	WG_Sta_Rep1 vs WG_Sta_Rep2	0.51	0.81
	WFA_Exp_Rep1 vs WFA_Exp_Rep2	0.28	1.03
Average ratio		3.32	1.53

[a:] WG: Waste glycerol; WFA: Waste fatty acids; PG: Pure glycerol; Exp: Exponential phase; Sta: Stationary phase; Rep1/2: Biological replicates.

S5 Table. Numbers of observed significantly up- and down-regulated genes and gene products in specific COG groups under the specific growth conditions [a].

COG Group	Description	Waste glycerol Sta vs Exp				WFA Vs WG Exp			
		RNA		Protein		RNA		Protein	
		Up	Down	Up	Down	Up	Down	Up	Down
K	Transcription	9	6	1	5	5	9	0	2
C	Energy production and conversion	12	36	6	10	14	19	8	8
O	Posttranslational modification, protein turnover, chaperones	2	6	0	3	4	2	0	0
H	Coenzyme transport and metabolism	5	4	0	2	3	5	0	0
J	Translation, ribosomal structure and biogenesis	3	0	0	2	6	0	1	4
R	General function prediction only	14	9	4	5	18	20	5	4
G	Carbohydrate transport and metabolism	3	10	5	3	4	17	1	7
M	Cell wall/membrane/envelope biogenesis	4	14	3	1	8	6	2	3
T	Signal transduction mechanisms	11	9	6	2	7	9	1	3
P	Inorganic ion transport and metabolism	14	33	6	2	10	13	0	1
S	Function unknown	17	9	8	2	12	11	4	3
E	Amino acid transport and metabolism	29	23	10	2	16	17	4	6
I	Lipid transport and metabolism	2	3	0	0	19	6	12	1
Q	Secondary metabolites biosynthesis, transport & catabolism	4	3	2	2	7	11	2	1
N	Cell motility	11	6	2	2	3	7	1	1
Total		144	175	50	45	141	159	31	30

[a:] WG, Waste glycerol cultures; WFA, Waste fatty acid cultures; Exp, Exponential phase; Sta, Stationary phase.

S6 Table. Monomer composition of mcl-PHA produced by *P. putida* LS46 grown on biodiesel derived waste glycerol and waste fatty acid culture (samples were harvested for mcl-PHA extraction and methylation at 48 hours post inoculation).

Conditions	**Monomer composition (mol%)** [a]							
	C6	C8	C9	C10	C12	C12:1	C14	C14:1
waste glycerol	2.69 ± 0.07	24.4 ± 0.53	nd	65.5 ± 0.41	2.42 ± 0.37	4.55 ± 0.32	0.39 ± 0.02	nd
waste fatty acids	4.38 ± 0.11	55.2 ± 0.61	1.02 ± 0.12	32.5 ± 0.30	5.1 ± 0.25	0.99 ± 0.01	0.71 ± 0.14	1.91 ± 0.11

[a]: Unsaturated monomers were determined via tandem GC/MS (See Method Chapter: 2.2.5) with 2 mass unit smaller than their saturated 3-hydroxyalkanoic acid standards.

S7 Table. Variation in expression values of putative fatty acid *de novo* synthesis genes and gene products in of *P. putida* LS46 under two growth conditions.

						WG Exp vs Sta		WFAvs WG Exp	
Locus Tag	**Gene Symbol**	**Gene Annotation**	**DNASeq Length (nt)**	**R[a]**	**P[a]**	**Rnet**	**Pnet**	**Rnet**	**Pnet**
PPUTLS46_000255	*fab*G 1	3-ketoacyl-(acyl-carrier-protein) reductase	741	12.6	20.1	0.23	0.01	-0.5	-0.06
PPUTLS46_002112	*fad*G	short-chain dehydrogenase/reductase SDR	741	6.25	nr	0.28	nc	0.06	nc
PPUTLS46_011825	*fad*G	short-chain dehydrogenase/reductase SDR	765	8.28	nr	0.25	nc	-0.19	nc
PPUTLS46_011830	*fad*G	3-oxoacyl-ACP reductase	762	7.16	nr	0.68	nc	0.02	nc
PPUTLS46_018726	*fad*G	short-chain dehydrogenase/reductase SDR	765	6.3	nr	-0.07	nc	-0.66	nc
PPUTLS46_018731	*fad*G	3-oxoacyl-ACP reductase	738	6.46	nr	-0.51	nc	-1.6	nc
PPUTLS46_023353	*fab*G 2	3-ketoacyl-(acyl-carrier-protein) reductase	1353	11.3	17.7	-1.39	1.82	-2.24	-0.3
PPUTLS46_015924	*fab*G 3	3-ketoacyl-(acyl-carrier-protein) reductase	750	10.1	19.5	-0.59	-0.43	-0.47	0.45
PPUTLS46_000265	*fab*F	3-oxoacyl-(acyl carrier protein) synthase II	1245	12.1	18.3	1.05	-0.14	0.83	0.23
PPUTLS46_012710	*fab*A	3-hydroxydecanoyl-(acyl carrier protein) dehydratase	516	11.7	17.4	1.13	1.42	1.44	0.07
PPUTLS46_012715	*fab*B	3-oxoacyl-(acyl carrier protein) synthase I	1221	13.5	20.3	0.46	-0.49	0.79	0.03
PPUTLS46_012998	*fab*V	trans-2-enoyl-CoA reductase	1212	12.1	21.2	0.44	-0.19	1.8	0.04
PPUTLS46_014589	*fab*Z	(3R)-hydroxymyristoyl-ACP dehydratase	441	11.1	19.6	-0.39	-0.8	nc	nc
PPUTLS46_020461	*fab*H	3-oxoacyl-ACP synthase	930	nr	nr	nc	nc	nc	nc
PPUTLS46 000250	*fab*D	malonyl CoA-acyl carrier protein	885	12	18.6	-0.02	1.37	-0.05	-0.87
PPUTLS46_023463		acetyl-CoA carboxylase biotin carboxyl	462	11.5	21.7	-0.3	-0.92	0.85	-1.22
PPUTLS46_023468		acetyl-CoA carboxylase biotin carboxylase	1356	13.9	22.3	-0.64	0.09	0.54	-0.02
PPUTLS46_000435		acetyl-CoA carboxylase subunit beta	894	nr	nr	nc	nc	nc	nc
PPUTLS46_014614		acetyl-CoA carboxylase carboxyltransferase	948	12.3	20.7	0.75	0	1.12	-0.24

[a]:The log2 value of RNA and Protein expression abundance of *P. putida* LS46 grown in waste glycerol culture at 8hrs post-inocula. RNA or Protein that were either not detected or only observed in one biological replicate were not reported for comparative analysis, and therefore no Rnet and Pnet value calculated. nr: not reported. nc: not calculated. Exp: Exponential culutre; Sta: Stationary culture; Green shading: significantly up-regulated; Red shading: significantly down-regulated; WG: waste glycerol; WFA: waste fatty acids.

S8 Table. Expression values of identified putative FadE homologs in *P. putida* LS46 grown in exponential stage of waste fatty acids (WFA) cultures during exponential phase, and variations in their expression levels under two comparing conditions.

					WFA vs WG Exp	
Locus Tag	**Gene Annotation**	**DNA Seq Length (nt)**	**R[a]**	**P**	**Rnet**	**Pnet**
PPUTLS46_000145	acyl-CoA dehydrogenase	2448	11.1	18	-0.7	0.15
PPUTLS46_000650	acyl-CoAdehydrogenasedomain-containing protein	1167	7	nr	0.02	nc
PPUTLS46_000700	acyl-CoAdehydrogenasedomain-containing protein	1776	8.5	nr	-0.16	0.08
PPUTLS46_002222	acyl-CoAdehydrogenasedomain-containing protein	1770	7.5	nr	1.26	nc
PPUTLS46_002522	AcdA	1152	9.6	17.6	0.46	0.52
PPUTLS46_005901	acyl-CoA dehydrogenase	1803	10.2	nr	1.89	nc
PPUTLS46_006756	acyl-CoA dehydrogenase	1653	10.8	18.7	-0.33	0.59
PPUTLS46_007429	acyl-CoAdehydrogenasedomain-containing protein	1128	nr	nr	nc	nc
PPUTLS46_008099	acyl-CoA dehydrogenase	1134	3.8	nr	0.06	nc
PPUTLS46_010244	acyl-CoA dehydrogenase	1230	nr	nr	nc	nc
PPUTLS46_012190	isovaleryl-CoA dehydrogenase	1164	9.2	17.2	0.15	-0.55
PPUTLS46_015999	glutaryl-CoA dehydrogenase	1182	11	17.6	0.24	0.09
PPUTLS46_018781	acyl-CoA dehydrogenase type 2	1188	6.3	nr	-0.84	nc
PPUTLS46_018861	type 2 acyl-CoA dehydrogenase	1233	5.1	nr	0.59	nc
PPUTLS46_024438	acyl-CoA dehydrogenase	1779	nr	nr	nc	nc
PPUTLS46_024448	acyl-CoA dehydrogenase	1806	16.6	24.3	3.25	3.54
PPUTLS46_025248	acyl-CoA dehydrogenase type 2	1182	4	nr	-0.66	nc
PPUTLS46_026101	acyl-CoAdehydrogenasedomain-containing protein	1161	6	nr	1.8	nc

[a]: The log2 value of RNA and Protein expression abundance of *P. putida* LS46 grown in waste fatty acid derived culture at 8hrs post-inocula. RNA or Protein that were either not detected or only observed in one biological replicate were not reported for comparative analysis, and therefore no Rnet and Pnet value calculated. nr: not reported. nc: not calculated. Exp: Exponential culture; Green shading: significantly up-regulated. WFA: waste fatty acids. WG: waste glycerol.

S9 Table. Expression values of putative fatty acid beta-oxidation genes and gene products in *P. putida* LS46 grown in waste fatty acids (WFA) cultures during exponential phase, and variations in their expression levels under two conditions.

						WG Exp vs Sta		WFA vs WG (Exp)	
Clusters	**Locus Tag**	**Gene symbol/annotation**	**DNA seq length (nt)**	**R[a]**	**P[a]**	**Rne**	**Pnet**	**Rnet**	**Pnet**
1	PPUTLS46_004399	*fad*B	2148	16.1	25.5	1.54	0.52	4.4	4.65
	PPUTLS46_004404	*fad*A	1176	15.6	24.7	0.46	-0.69	3.79	4.8
2	PPUTLS46_007434	*fad*B1X	774	9.7	20.2	0.06	0.02	-0.33	0.03
	PPUTLS46_007429	*fad*Ex	1128	nr	nr	nc	nc	nc	nc
	PPUTLS46_007424	*fad*Ax	1194	nr	nr	nc	nc	nc	nc
	PPUTLS46_007419	*fad*B2x	768	nr	nr	nc	nc	nc	nc
	PPUTLS46_007414	*fad*Dx	1674	7.7	nr	1.06	nc	-0.57	nc
3	PPUTLS46_000695	3-hydroxybutyryl-CoA epimerase	1239	10.4	nr	1.33	nc	0.23	nc
	PPUTLS46_000700	Acyl-CoA dehydrogenase putative	1776	8.5	nr	0.08	nc	-1.33	nc
	PPUTLS46_000705	Alcohol dehydrogenase iron-containing	1164	7.1	nr	nc	-1.68	-1.58	nc
	PPUTLS46_000710	Thioesterase superfamily protein	453	6	nr	-0.01	nc	-0.95	nc
	PPUTLS46_000715	Acetyl-CoA acetyltransferase	1185	8	nr	0.03	-1.86	-1.02	nc
4	PPUTLS46_026256	TetR family transcriptional regulator	582	9.6	nr	-0.04	nc	1.56	nc
	PPUTLS46_026251	3-hydroxybutyryl-CoA dehydrogenase	849	11.1	16.7	nc	nc	1.73	2.19
	PPUTLS46_026246	beta-ketothiolase	1185	11.7	20.8	0.06	0.47	1.66	1.76
Others	PPUTLS46_012993	acetyl-CoA acetyltransferase	1179	11.8	23.1	-0.6	0.53	7.51	6.7
	PPUTLS46_003422	3-hydroxybutyrate dehydrogenase	771	10.81	19.24	nc	nc	3.84	nc
	PPUTLS46_006916	acyl-CoA thioesterase II	870	10.05	14.51	-0.2	0.03	-0.2	-0.39
	PPUTLS46_009584	Acyl-CoA thioesterase-like protein	798	10.2	19.1	-0.64	0.79	0.16	3.71

a: The log2 value of RNA and Protein expression abundance of *P. putida* LS46 grown in waste fatty acid derived culture at 8hrs post-inocula. RNA or Protein that were either not detected or only observed in one biological replicate were not reported for comparative analysis, and therefore no Rnet and Pnet value calculated. nr: not reported. nc: not caluculated. Exp: Exponential culture; Sta: Stationary culture. Green shading: significantly up-regulated; Red shading: significantly down-regulated. WFA: waste fatty acids. WG: waste glycerol.

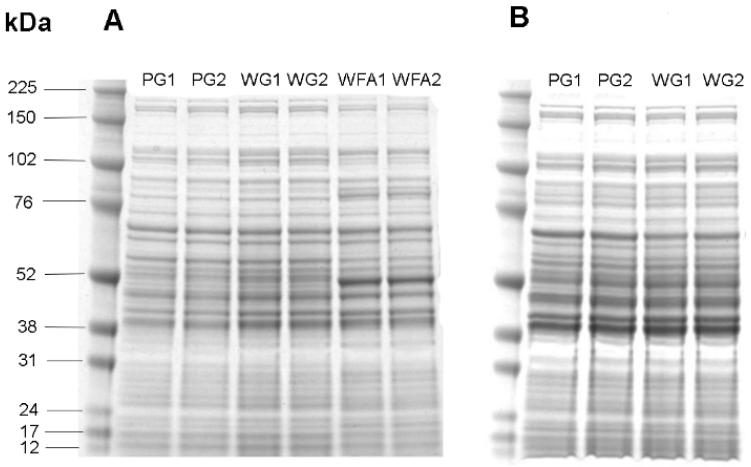

S1 Figures. SDS-PAGE of total protein of *P. putida* LS46 grown under exponential phase **(A)** of waste glycerol and waste fatty acids culture, and stationary phase **(B)** of waste glycerol culture. WG: waste glycerol; WFA: waste fatty acids; Numbers indicate two biological replicate. Protein samples from pure glycerol (PG) culture under exponential and stationary phase were ran as reference. 1/ 2 represent the two biological replicates. Protein ladder was also showed.

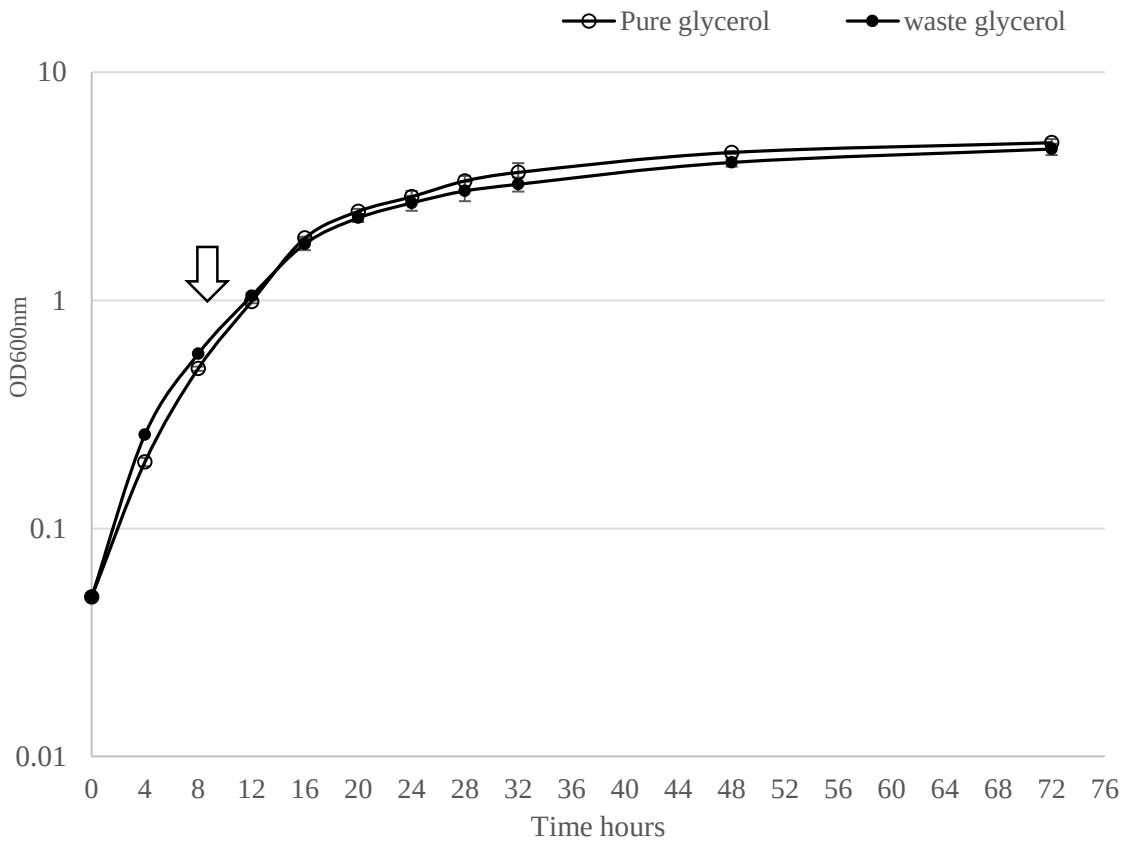

S2 Figure. Optical density at 600 nm of *P. putida* LS46 growing on pure glycerol (open circle) and waste biodiesel-derived glycerol (closed circle), respectively. Samples were collected at 8-hour post inoculation (arrow) for transcriptomic and proteomic analyses. OD_{600nm} measurement at 8 hours post inoculation were taken from pure glycerol and waste glycerol culture for statistical analysis, respectively (triplicate samples each), and recorded as 0.508/0.509/0.49 for pure glycerol culture; and 0.59/0.581/0.579 for waste glycerol culture. A two-tails t-test based on these two groups of number revealed a P value = 0.0003 (< 0.5) suggesting a statistically significant difference of the growth (based on OD_{600nm} measurement) under the sampling point (8-hour pi) between the two cultures.

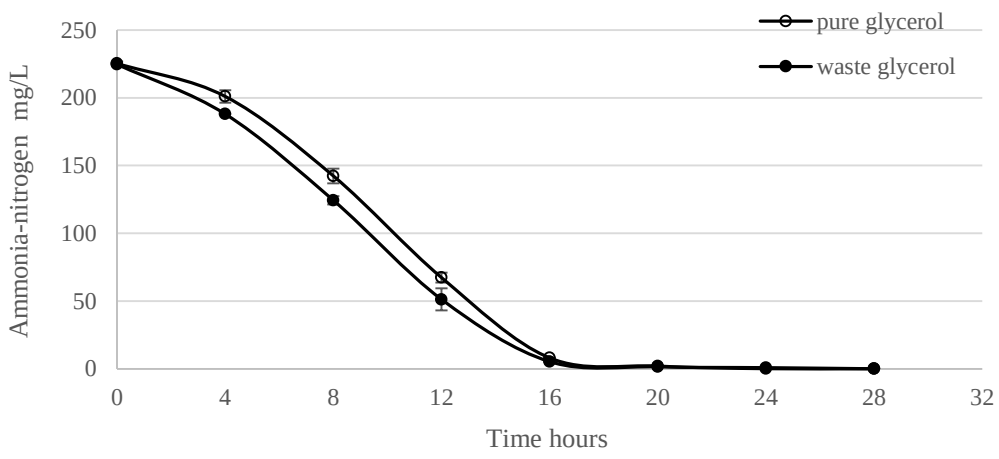

S3 Figure. Nitrogen consumption during the growth of *P. putida* LS46 under pure glycerol (open cycle) and waste glycerol culture (closed cycle).

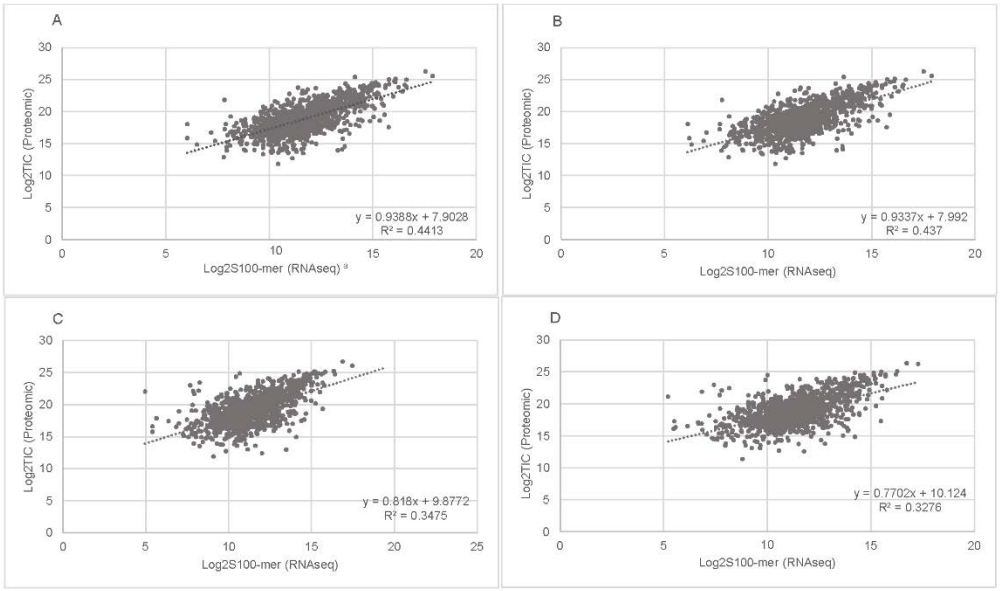

S4 Figures. Correlation of log2 expression values of transcriptomic and proteomic of two biological replicates under the waste glycerol mid-log and pure glycerol mid-log phases. Panel A/B: Pure glycerol exponential phase culture biological replicate 1 and 2; Panel C/D: Waste glycerol exponential phase culture biological replicate 1 and 2; [a:] Sum of total 100-mer alignment per gene.

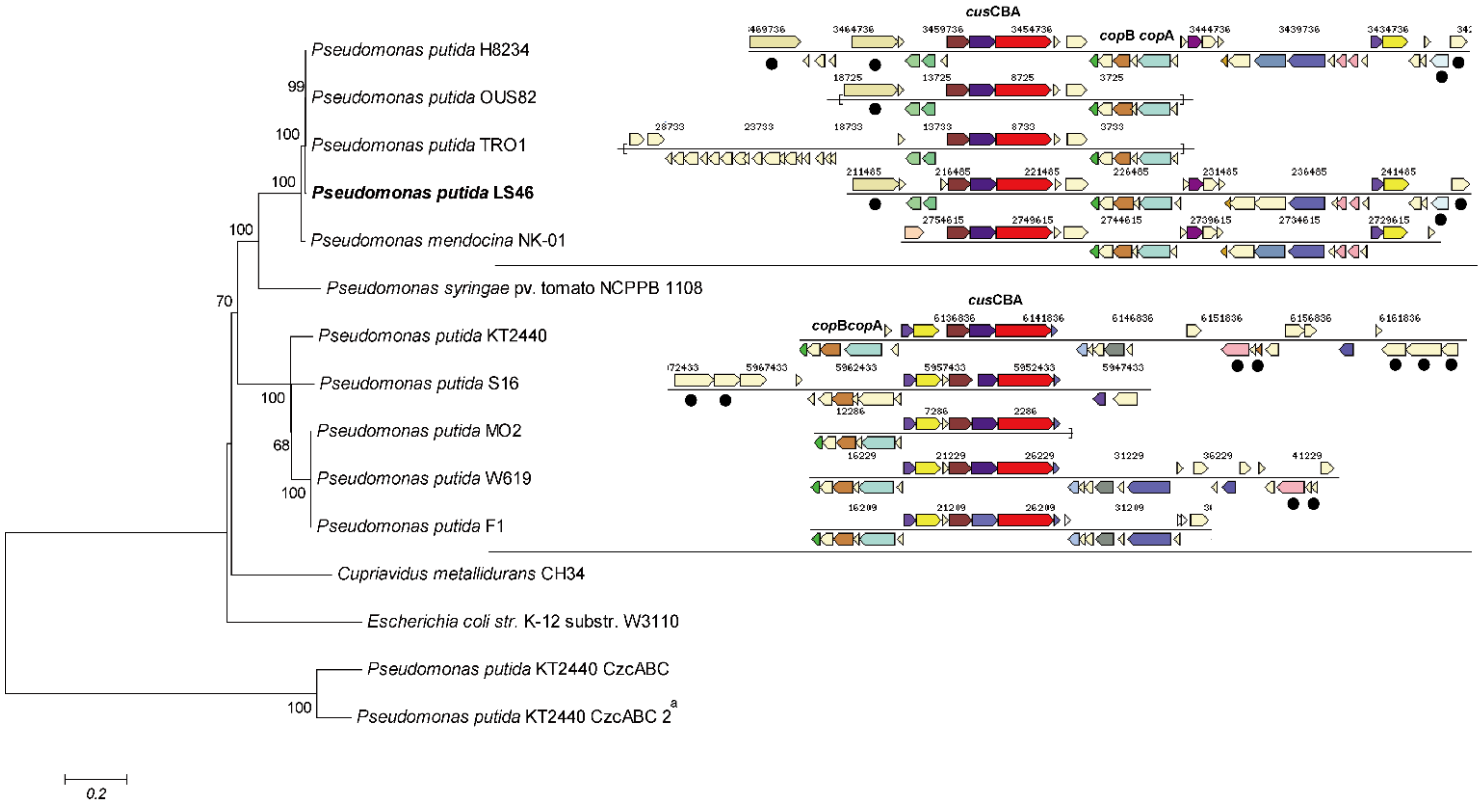
cusCBA
copB copA
Pseudomonas putida H8234
Pseudomonas putida OUS82
Pseudomonas putida TRO1
Pseudomonas putida LS46
Pseudomonas mendocina NK-01
Pseudomonas syringae pv. tomato NCPPB 1108
cusCBA
copBcopA
Pseudomonas putida KT2440
Pseudomonas putida S16
Pseudomonas putida MO2
Pseudomonas putida W619
Pseudomonas putida F1
Cupriavidus metallidurans CH34
Escherichia coli str. K-12 substr. W3110
Pseudomonas putida KT2440 CzcABC
Pseudomonas putida KT2440 CzcABC 2a
99
100
100
100
70
100
68
100
100
0.2

S5 Figure. Phylogenetic relationships between *P. putida LS46* (bolded) and other related Gram-negative bacteria based on the sequences of the *cus*ABC genes in Cluster 1. Alignments and phylogenetic analyses of sequences for gene cluster analyses was carried out by concatenating each protein sequence of the cluster prior to alignment, using MEGA 6. The bootstrapping neighbour-joining tree is drawn to scale, with branch lengths measured in the number of substitutions per site. The percentage of trees in which the associated taxa clustered together is shown above the branches. Gene Neighborhood orthology was showed on the right side of the tree colored according COG category. Each gene's neighborhood appears above and below a single line showing the genes reading in one direction on top and those reading in the opposite direction on the bottom; genes with the same color indicate association with the same COG group in each *P. putida* strain. Position of *cus*ABC and *cop*AB on the Cluster 1 were given as text on top of the neighbourhood of each group. Mobile elements, if present, were indicated by black dots under the gene. Previous studied CusABC ortholog from *P. syringae* pv tomato NCPPB 1108, *C. metallidurans* CH4, and *E. coli* K12 substrain W3110 were used as references for building the tree a: There are two copies to *czc*ABC gene cluster in the genome of *P. putida* KT2440.

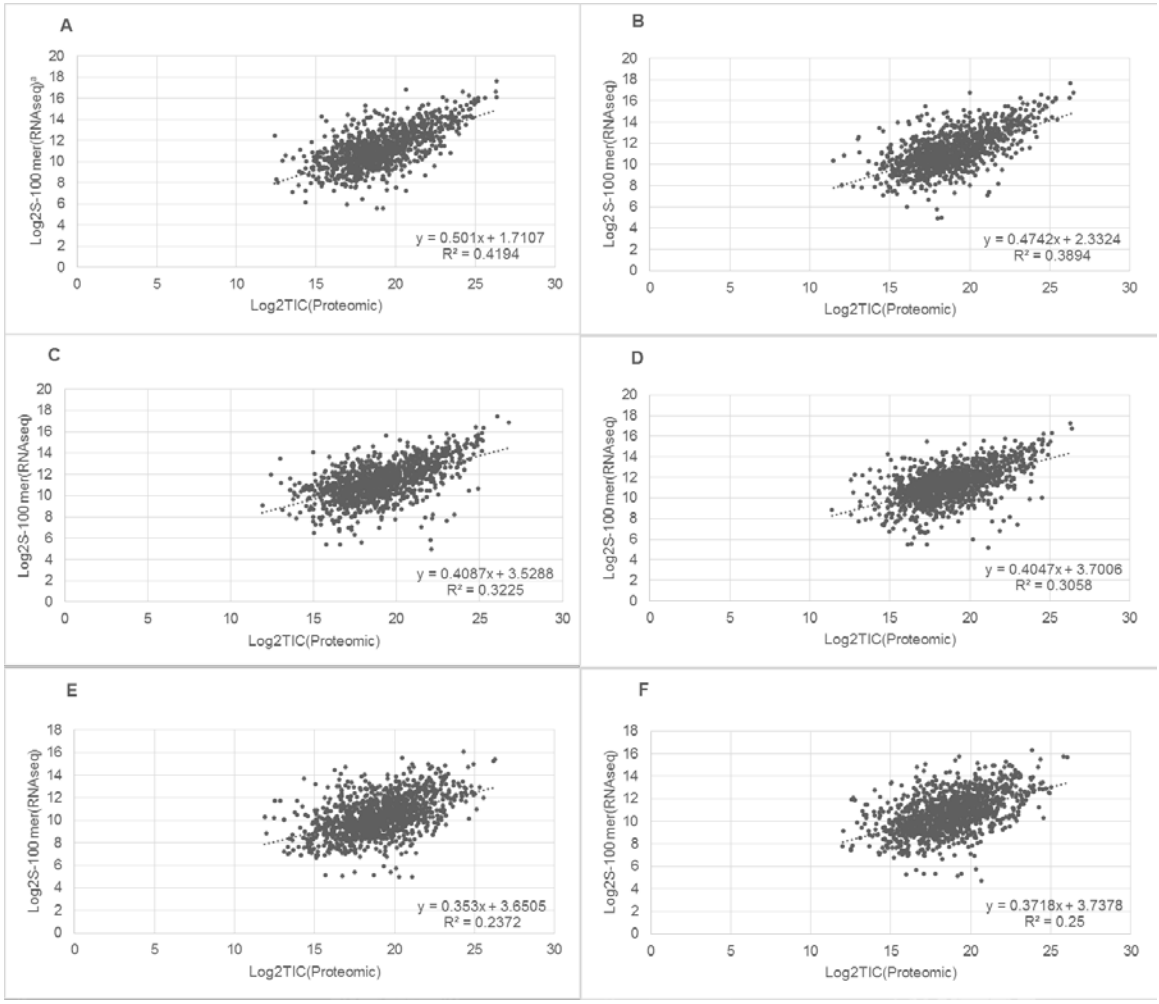

S6 Figures. Correlation of log2 expression values of transcriptomic and proteomic of two biological replicates under the three experimental conditions. [a:] Sum of total 100-mer alignment per gene; Panel A/B: Waste fatty acids exponential phase culture biological replicate 1 and 2; Panel C/D: Waste glycerol exponential phase culture biological replicate 1 and 2; Panel E/F: Waste glycerol stationary phase culture biological replicate 1 and 2.